Development and Validation of Crack Growth Models and Life Enhancement Methods for Rotorcraft Damage Tolerance

Center for Aerospace Research & Education

University of California Irvine

Summary

Simple & easy to use analytical results are produced in this project, for:

1. Residual stresses due to shot-peening (100% & 200%);

2. Residual stresses due to cold-working(first-order);

3. Plasticity-induced crack-closure in fatigue; analytical model for crack-opening stress-intensity factors

4. Effect of residual-plasticity on fatigue crack growth

Analytical model to model the shot-peening process with 200% coverage

- Elastic analysis of the loading process; Hertzian contact theory------Determine a_e.

- Elastic-plastic analysis of the loading process; Multilinear stress-strain relationship-----Determine a_p.

- Thus, a_e & a_p are determined for a given V & R of the shot.

- We assume that the ratio of ε_i^p to ε_i^e on the z-axis inside the target is equal to the ratio α, $\alpha = a_e / a_p$, of the deformation at the surface.

- The body is semi-infinite in depth: thus, only compressive stresses are predicted. For finite thickness objects, use simple equilibrium to predict tensile stresses.

Schematic diagram for calculating residual stress-200% Coverage

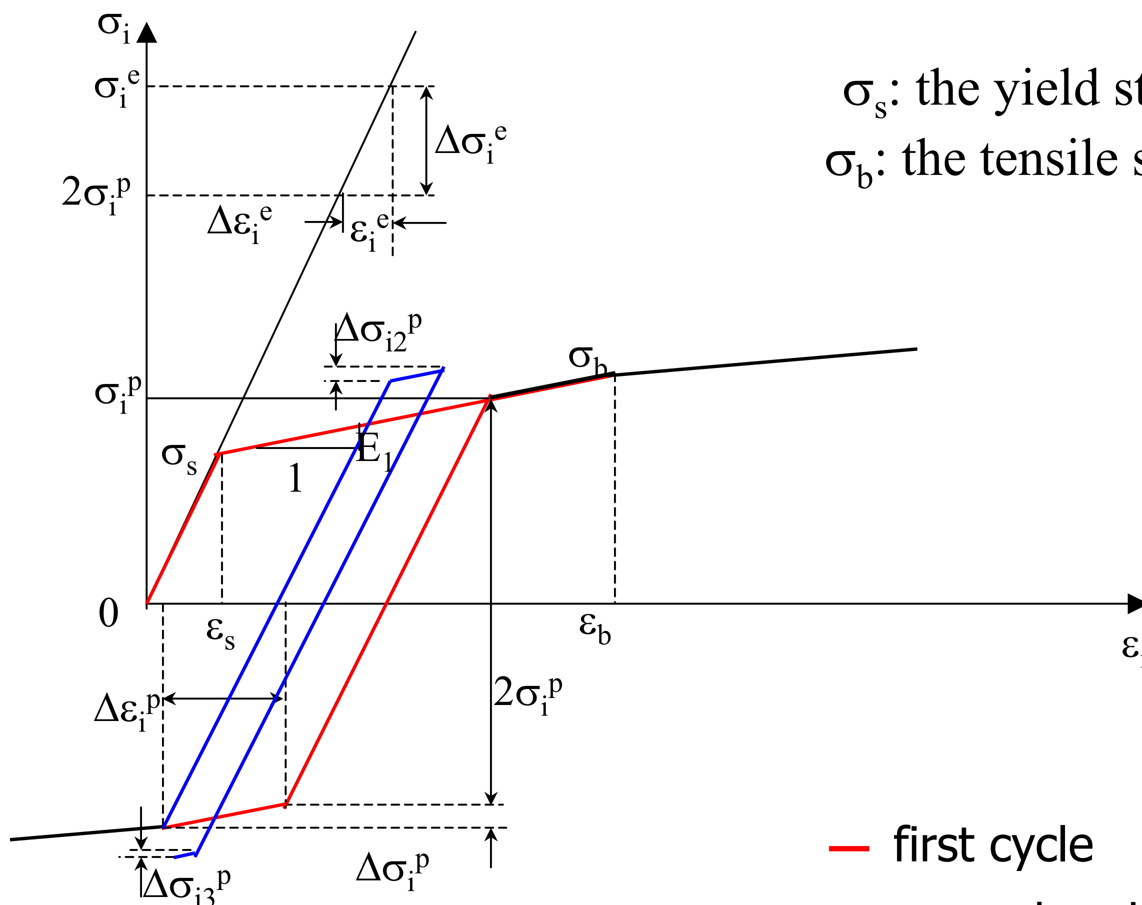

σ_s: the yield strength

σ_b: the tensile strength

first cycle

second cycle

Isotropic hardening

Elastic-plastic analysis

The strain deviations

$$e_x^p = e_y^p = \frac{1}{3}(1+\nu)\varepsilon_i^p$$

$$e_z^p = -\frac{2}{3}(1+\nu)\varepsilon_i^p = -2e_x^p$$

The stress deviations

$$s_x^p = s_y^p = \frac{1}{1+\nu}\frac{\sigma_i^p}{\varepsilon_i^p}e_x^p = \frac{1}{3}\sigma_i^p$$

$$s_z^p = -\frac{2}{3}\sigma_i^p = -2s_x^p$$

Loading Process –the first shot

Elastic-plastic equivalent strain

$$\varepsilon_i^p = \begin{cases} \varepsilon_i^e & \text{for } \varepsilon_i^e \le \varepsilon_s \\ \varepsilon_s + \alpha\left(\varepsilon_i^e - \varepsilon_s\right) & \text{for } \varepsilon_i^e > \varepsilon_s \end{cases}$$

Elastic-plastic equivalent stress

$$\sigma_i^p = \begin{cases} \sigma_i^e & \text{for } \varepsilon_i^p < \varepsilon_s \\ \sigma_s + E_1\left(\varepsilon_i^p - \varepsilon_s\right) & \text{for } \varepsilon_s \le \varepsilon_i^p < \varepsilon_b \\ \sigma_b & \text{for } \varepsilon_i^p \ge \varepsilon_b \end{cases}$$

Unloading process –the first shot

Elastic-plastic equivalent stress after unloading

$$\sigma_{i1}^{p} = \begin{cases} 0 & \text{for } \sigma_i^e \le \sigma_s \\ \sigma_i^p - \sigma_i^e & \text{for } \sigma_s \le \sigma_i^e < 2\sigma_i^p \\ \sigma_i^p - 2\sigma_i^p - \Delta\sigma_i^p & \text{for } \sigma_i^e > 2\sigma_i^p \end{cases}$$

$$\Delta\sigma_i^e = \sigma_i^e - 2\sigma_i^p \longrightarrow \Delta\varepsilon_i^e = \frac{\Delta\sigma_i^e}{E}$$

$$\Downarrow$$

$$\Delta\varepsilon_i^p = \alpha\Delta\varepsilon_i^e \longrightarrow \Delta\sigma_i^p$$

Reloading process –the second shot

Elastic-plastic equivalent stress after reloading

$$\sigma_{i2}^{p} = \begin{cases} \sigma_{i1}^{p} + \sigma_{i}^{e} & \text{for } 2\sigma_{i}^{p} < \sigma_{i}^{e} \le -2\sigma_{i1}^{p} \\ -\sigma_{i1}^{p} + \Delta\sigma_{i2}^{p} & \text{for } -2\sigma_{i1}^{p} \le \sigma_{i}^{e} \end{cases}$$

$$\Delta\sigma_{i2}^{e} = \sigma_{i}^{e} + 2\sigma_{i1}^{p} \Rightarrow \Delta\varepsilon_{i2}^{e} = \frac{\Delta\sigma_{i2}^{e}}{E}$$

$$\Downarrow$$

$$\Delta\varepsilon_{i2}^{p} = \alpha\Delta\varepsilon_{i2}^{e} \Rightarrow \Delta\sigma_{i2}^{p}$$

Unloading process –the second shot

Elastic-plastic equivalent stress after unloading

$$\sigma_{i3}^{p} = \begin{cases} \sigma_{i1}^{p} & \text{for } 2\sigma_{i}^{p} < \sigma_{i}^{e} \le -2\sigma_{i1}^{p} \\ \sigma_{i2}^{p} - \sigma_{i}^{e} & \text{for } -2\sigma_{i1}^{p} \le \sigma_{i}^{e} < 2\sigma_{i2}^{p} \\ \sigma_{i2}^{p} - 2\sigma_{i2}^{p} - \Delta\sigma_{i3}^{p} & \text{for } \sigma_{i}^{e} > 2\sigma_{i2}^{p} \end{cases}$$

$$\Delta\sigma_{i3}^{e} = \sigma_{i}^{e} - 2\sigma_{i2}^{p} \Longrightarrow \Delta\varepsilon_{i3}^{e} = \frac{\Delta\sigma_{i3}^{e}}{E}$$

$$\Big\Downarrow$$

$$\Delta\varepsilon_{i3}^{p} = \alpha\Delta\varepsilon_{i3}^{e} \Longrightarrow \Delta\sigma_{i3}^{p}$$

Residual stress after two shots

The residual stresses after two shots

$$\sigma_{ij}^{r} = \begin{cases} 0 & \text{for } \sigma_i^e \le \sigma_s \\ s_{ij}^p - s_{ij}^e & \text{for } \sigma_s \le \sigma_i^e < 2\sigma_i^p \end{cases}$$

$$\sigma_x^r = \sigma_y^r = \frac{1}{3}\left(\sigma_i^p - \sigma_i^e\right) \text{ for } \sigma_s \le \sigma_i^e \le 2\sigma_i^p, \quad \sigma_z^r = -2\sigma_x^r$$

$$\sigma_{ij}^{r} = \begin{cases} \frac{1}{3}\sigma_{i1}^p & \text{for } 2\sigma_i^p < \sigma_i^e \le -2\sigma_{i1}^p \\ \frac{1}{3}\left(\sigma_{i2}^p - \sigma_i^e\right) & \text{for } -2\sigma_{i1}^p \le \sigma_i^e < 2\sigma_{i2}^p \\ \frac{1}{3}\left(\sigma_{i2}^p - 2\sigma_{i2}^p - \Delta\sigma_{i3}^p\right) & \text{for } \sigma_i^e > 2\sigma_{i2}^p \end{cases}$$

Residual stress field for 200% coverage

The residual stress and strain fields should satisfy

$$\sigma_x^R = \sigma_y^R = f(z), \qquad \sigma_z^R = 0$$

$$\varepsilon_x^R = \varepsilon_y^R = 0, \qquad \varepsilon_z^R = g(z)$$

The relaxation values of σ_{ij}^r can be calculated by Hooke's law as

$$\sigma_x' = \sigma_y' = \frac{v}{1-v}\sigma_z^r$$

The final residual stress field is

$$\sigma_x^R = \sigma_y^R = \sigma_x^r - \frac{v}{1-v}\sigma_z^r = \frac{1+v}{1-v}\sigma_x^r$$

The effect of the coverage

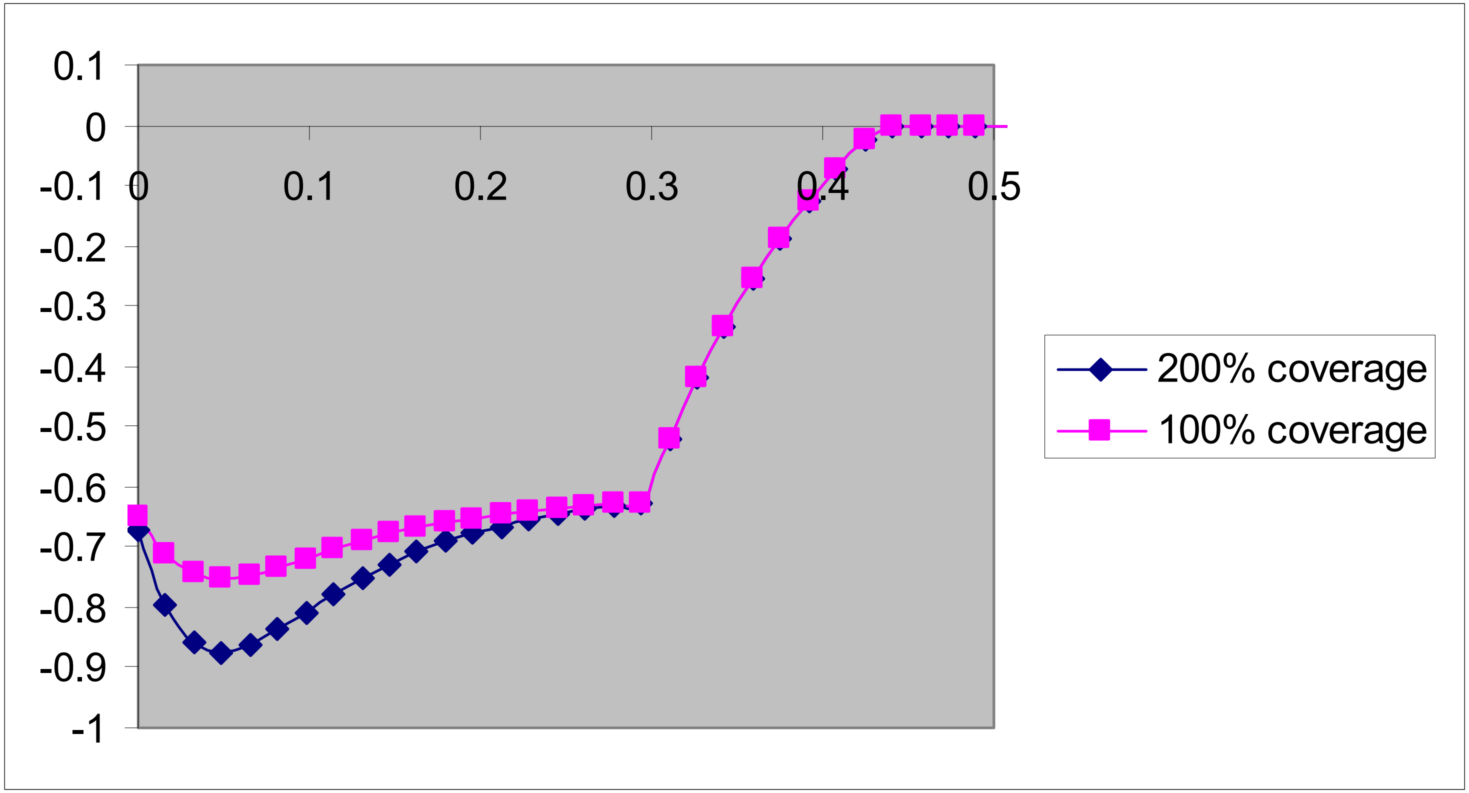

R=0.55mm, E=200GPa, ν=0.3, ρ=7800kg/m^3, V=30.65m/s

σ_s=0.70GPa, σ_b=0.885GPa, ε_b=0.140

40Cr Steel

The effect of the coverage

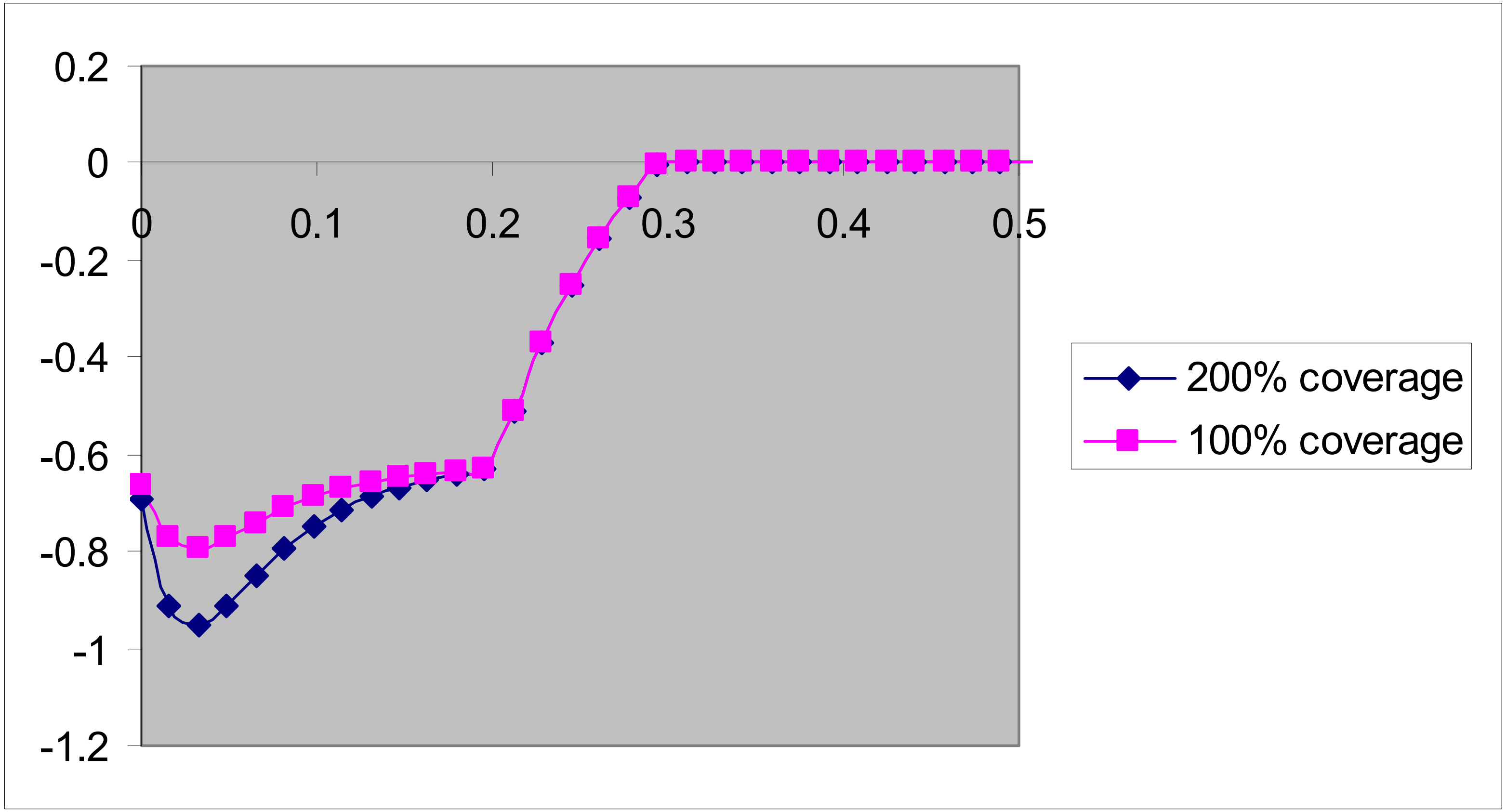

R=0.275mm, E=200GPa, v=0.3, ρ=7800kg/m^3, V=50.44m/s

σ_s=0.70GPa, σ_b=0.885GPa, ε_b=0.140

40Cr Steel

The effect of the coverage

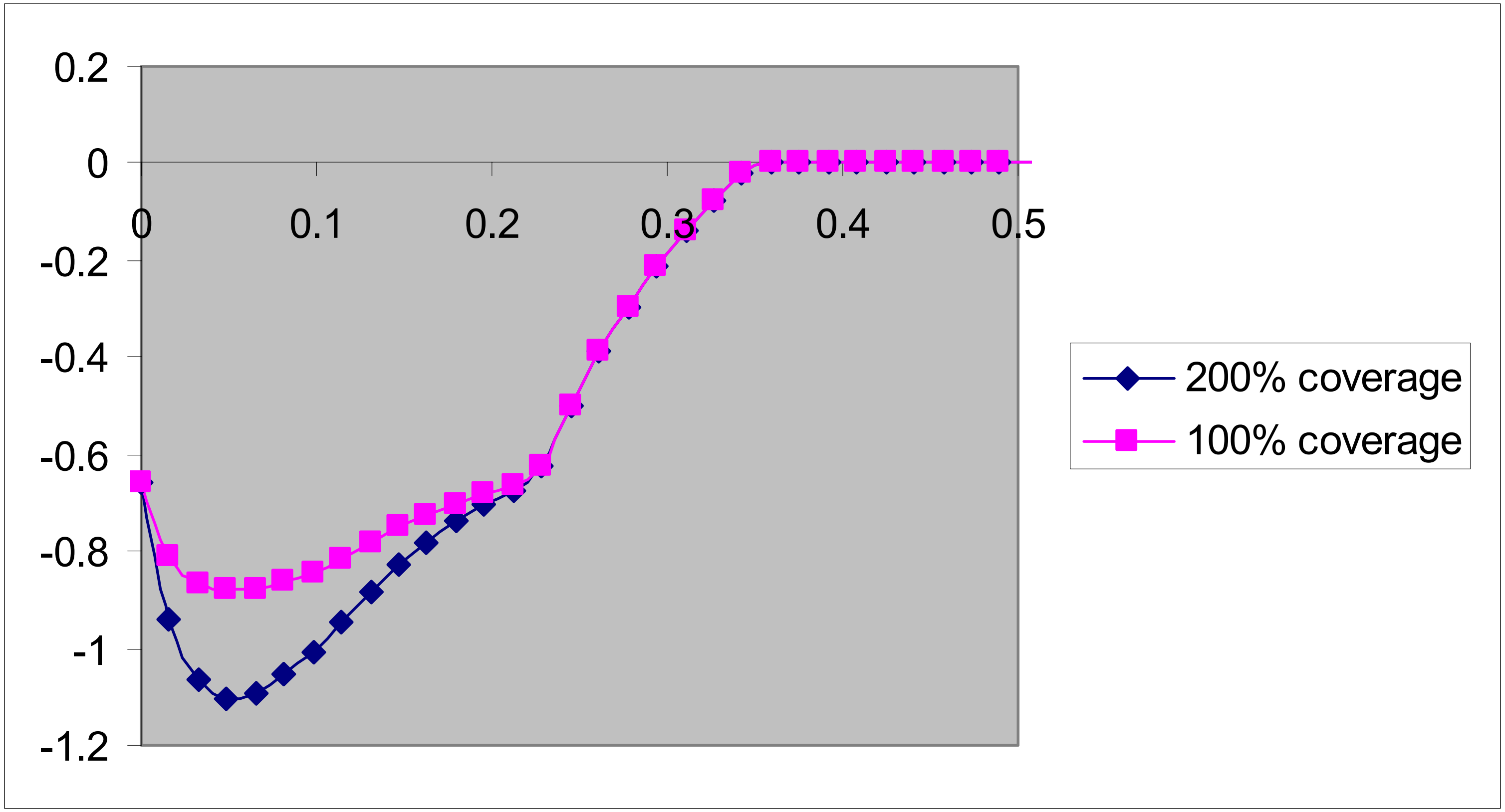

R=0.55mm, E=200GPa, v=0.3, ρ=7800kg/m^3 , V=36.58m/s

σ_s=1.27GPa, σ_b=1.54GPa, ε_b=0.045

The effect of the coverage

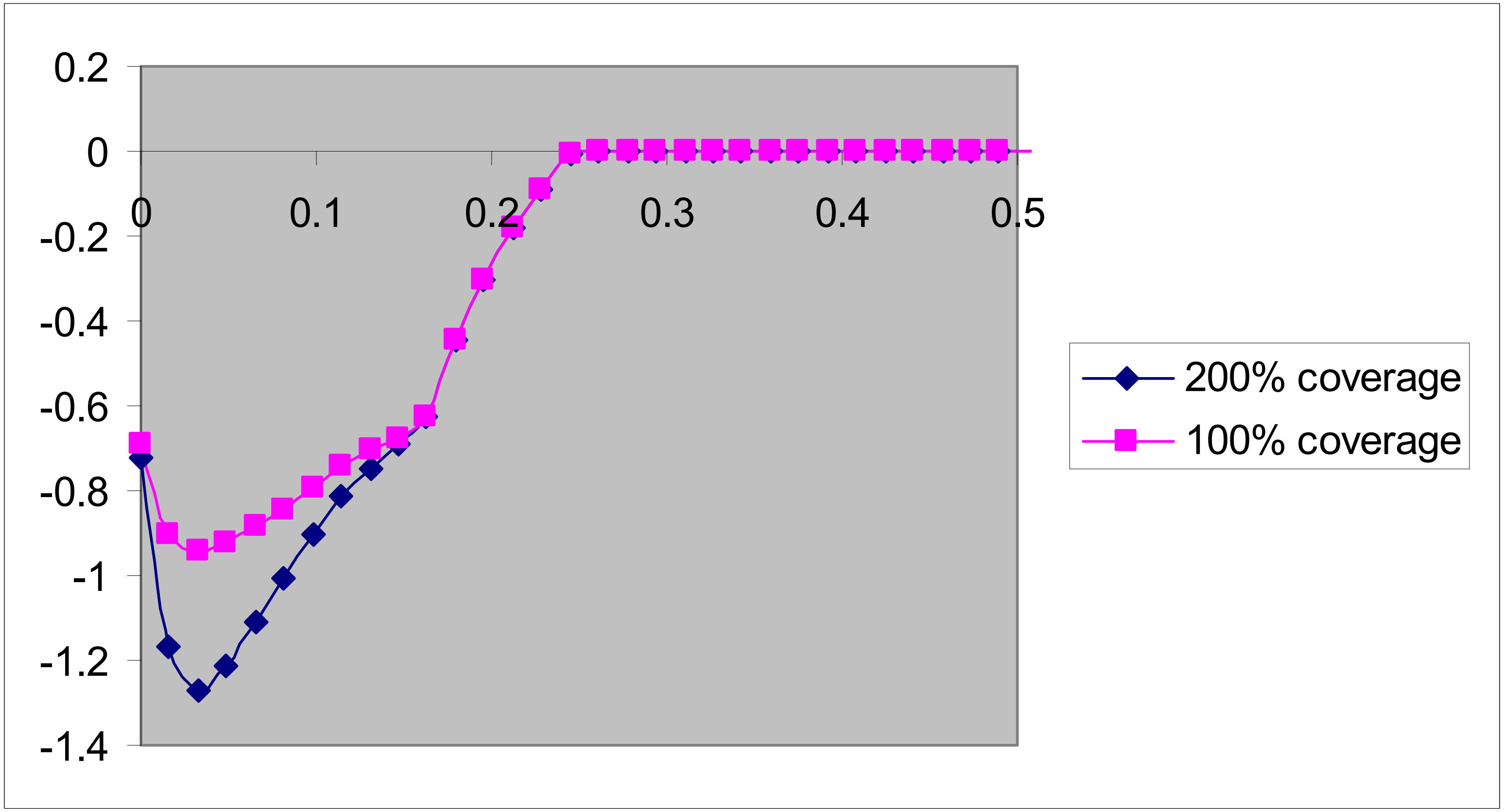

R=0.275mm, E=200GPa, v=0.3, ρ=7800kg/m^3 , V=63.58m/s

σ_s=1.27GPa, σ_b=1.54GPa, ε_b=0.045

The effect of the coverage

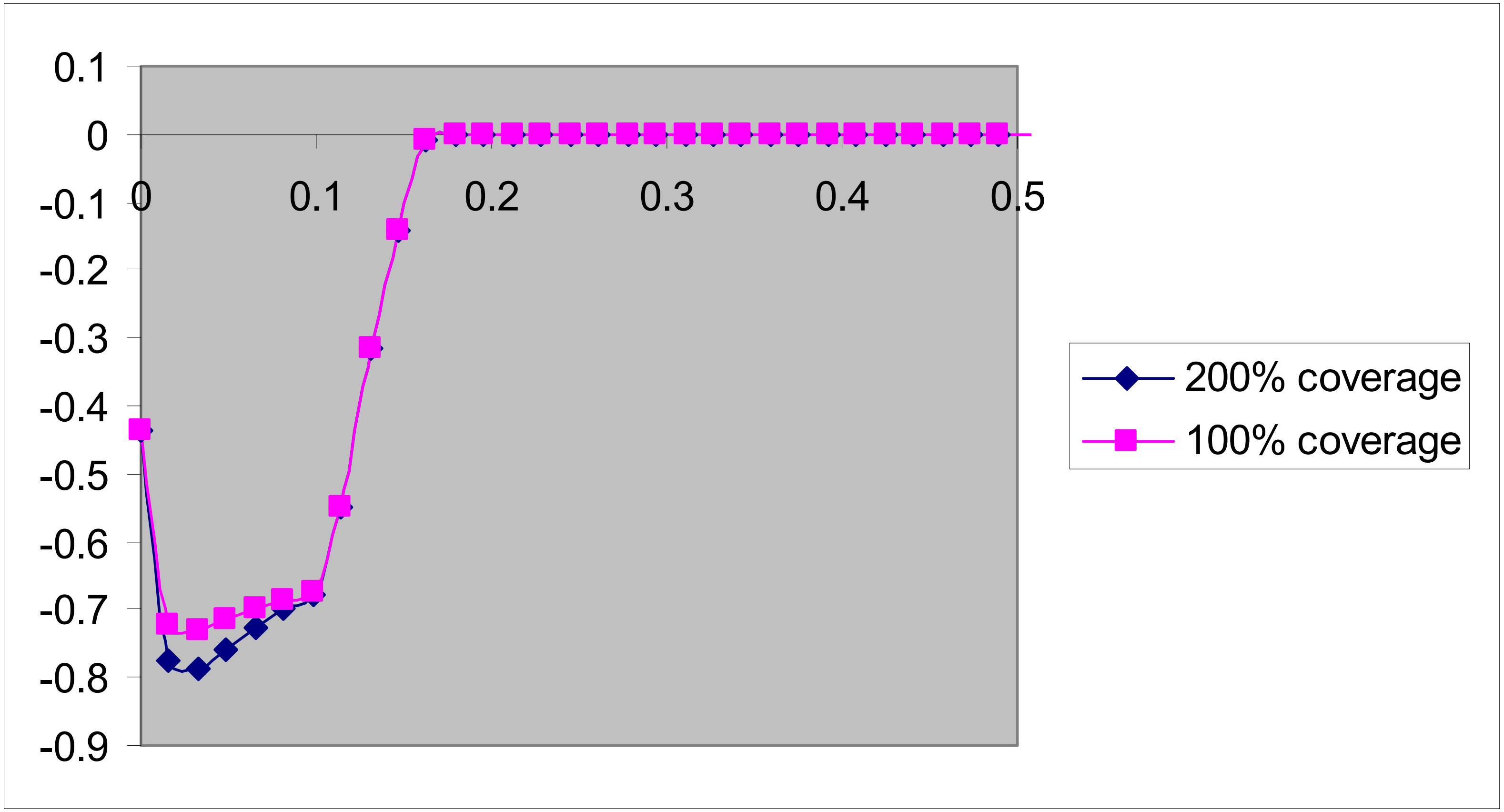

R=0.3mm, E=70GPa, v=0.33, V=30m/s, ρ=2700kg/m^3

σ_s=0.462GPa, σ_b=0.526GPa, ε_b=0.11

7075 Aluminium

Wichita state data

Tensile test properties

1. 7050 T7451 Al, 7 specimens
2. 7075 T7351 Al, 7 specimens

Residual stresses tests

Shot-peening

1. 7050 T7451 Al, 100% coverage, 1 specimen
2. 7075 T7351 Al, 200% coverage, 1 specimen

Average Tensile Properties

Aluminium 7050-T7451 (0.25" thick sheet) (Wichita state test data)

	$\sigma_{ultimate}$ Ksi	$\sigma_{Failure}$ Ksi	E Msi	υ	ε %	0.5% σ_{Yield} Ksi	1% σ_{Yield} Ksi
Average	75.07	61.56	10.10	0.336	13.697	68.29	69.17
Std. Dev	0.319	0.568	0.047	0.009	0.7440	0.258	0.300
CoV	0.425	0.923	0.461	2.605	5.432	0.377	0.434

The measured density is 2.76 g/cm^3

Stress- Strain Curve

Specimen 1 Al-7050-T7451 (Wichita state test)

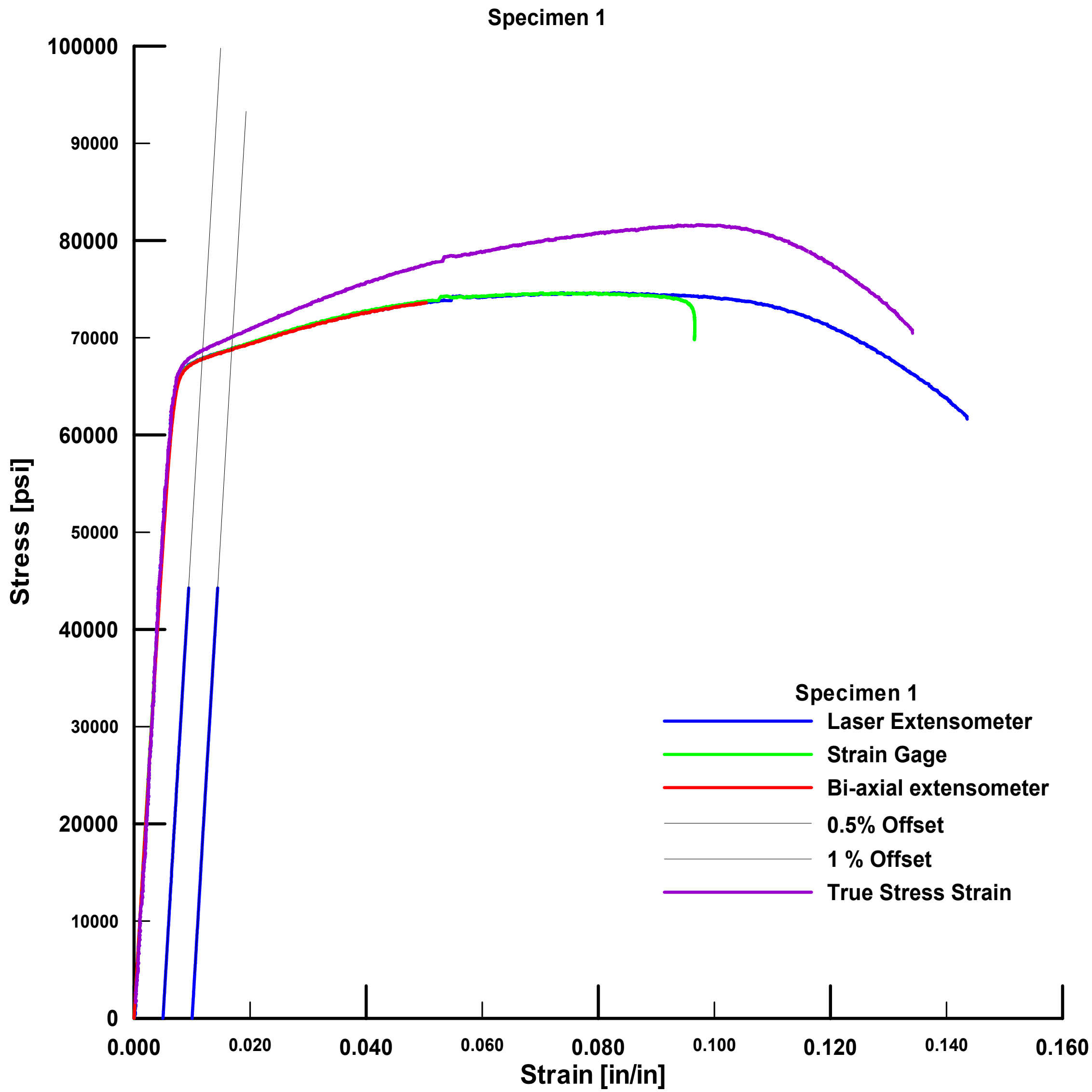

UCI
University of California, Irvine

Experiment (Wichita state)

7050 –T7451 alloys

Shot-peening parameters

Measured intensity – 0.077 ~ 0.078A
100% and 200% coverage's
Shot diameter- 230R (0.023in)
Cast Steel Shots

Comparison of the experimental and theoretical results

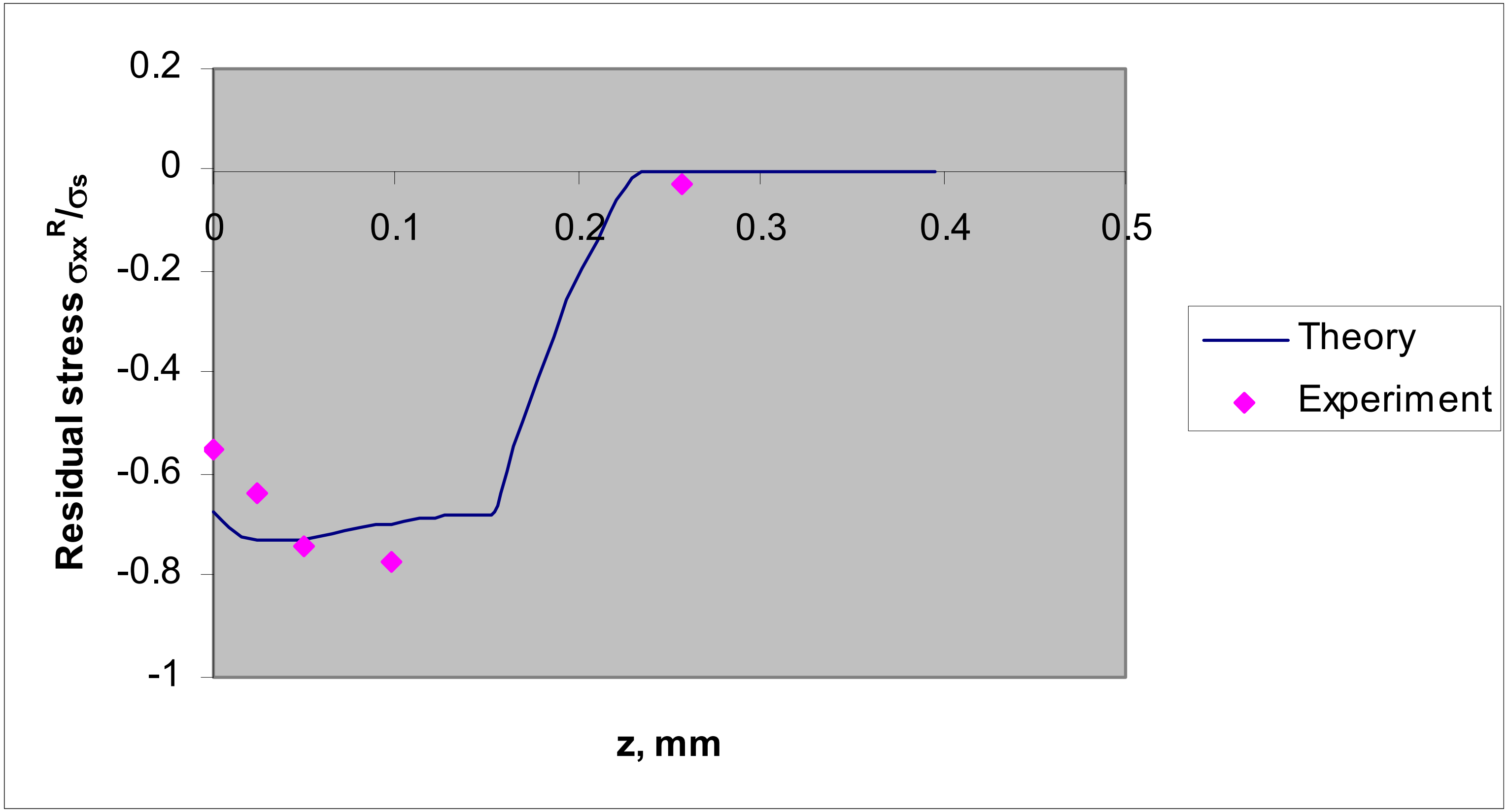

100% coverage 7050 –T7451 alloys

Comparison of the experimental and theoretical results

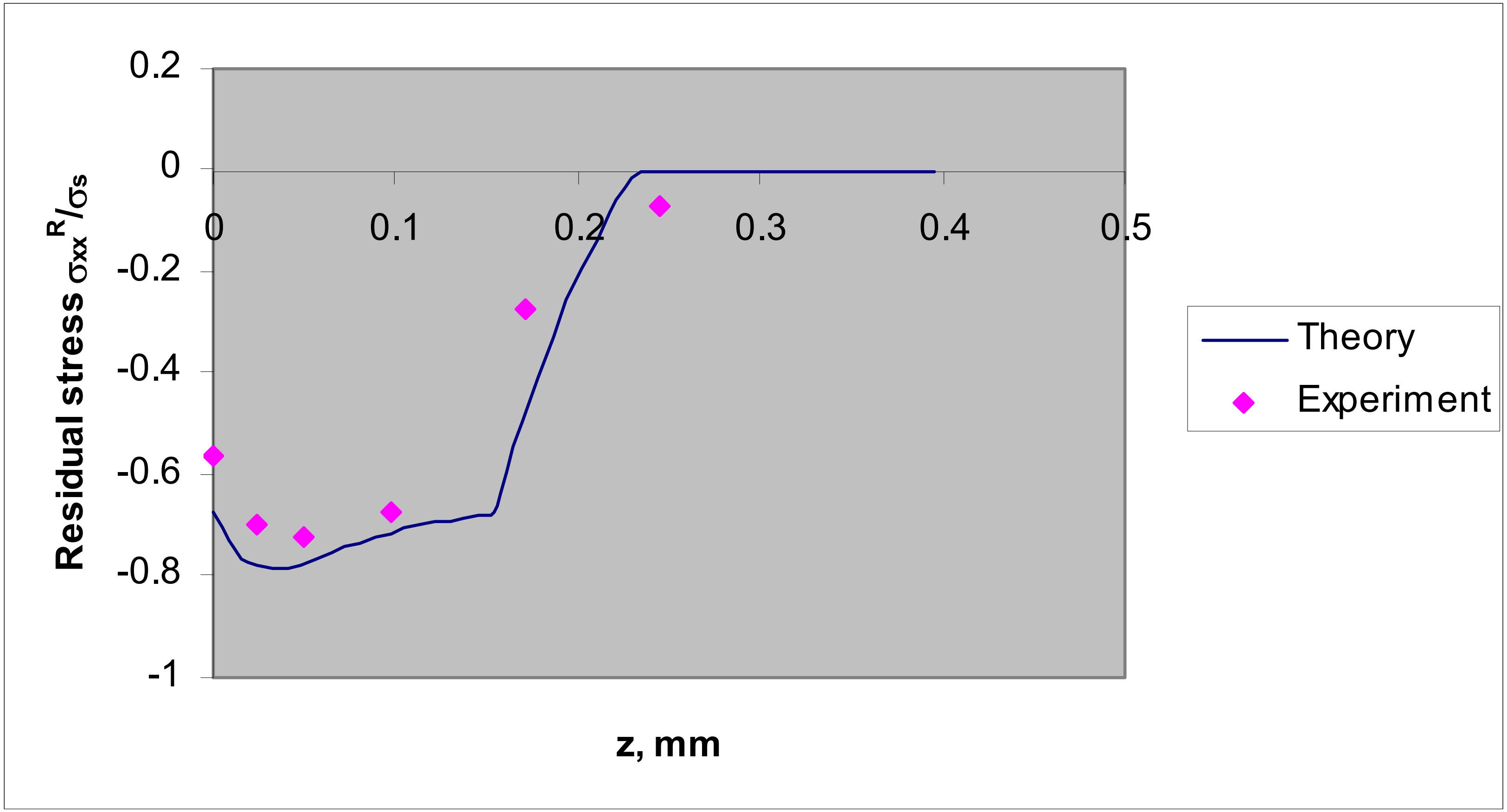

200% coverage 7050 –T7451 alloys

UCI
University of California, Irvine

Experimental data from Sikorsky

Al7075-T73, Ti-6Al-4V alpha-beta, & Ti-6Al-4V Beta-STOA

Material	Intensity	Shot Size	Shot Velocity
Al7075-T7351	0.009 –0.011N	S170 est.	TBD
	0.0016A	S170 est.	TBD
Ti-6Al-4V Beta-STOA	0.006 –0.008N	S170 est.	TBD
	0.008-0.012A	S170 est.	TBD
Ti-6Al-4V Alpha-Beta	0.011A	S170	TBD

For intensities below .004A the type "N" test strip should be used. For comparison of the nominal intensity designations, type "A" test strip deflection may be multiplied by three to obtain the approximate deflection of a type "N" test strip.

Material Properties

- Al7075-T73

$\sigma_b = 69$ ksi, $\sigma_s = 57$ ksi, E =10.5 msi

- Ti-6Al-4V Alpha-Beta

$\sigma_b = 145$ ksi, $\sigma_s = 135$ ksi, E =16.5 msi

- Ti-6Al-4V Beta-STOA

$\sigma_b = 150$ ksi, $\sigma_s = 140$ ksi, E =16.5 msi

Coverage is at least 100% and is normally 200%

Material Properties

- Aluminum:

  Poison's Ratio=0.33, Density=0.101 lb/in^3, Thickness=0.50 inches, elongation=9%

- Titanium:

  Poison's Ratio=0.33, Density=0.16 lb/in^3, Thickness=0.50 inches, elongation=11%

Shot sizes are S110, S170, and S230, their nominal diameters are 0.011 inches, 0.017 inches and 0.023 inches, respectively.

The relationship between the Almen intensity, shot velocity and shot size can be found in Guagliano (2001).

Comparison of the residual stress for Al7075 T73 Metal Improvement

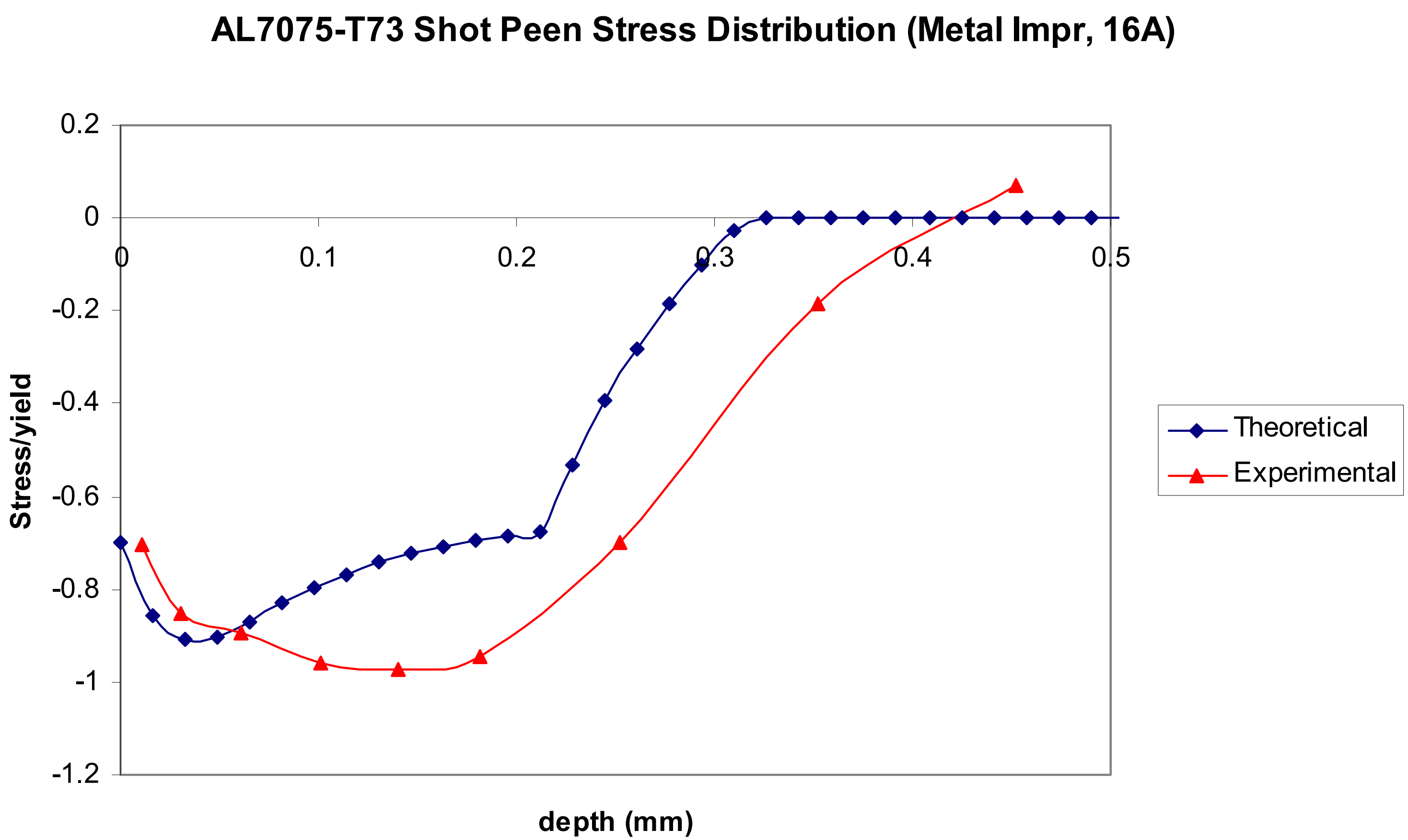

Experimental data from Sikorsky

Comparison of the residual stress for Al7075 T73 Metal Improvement

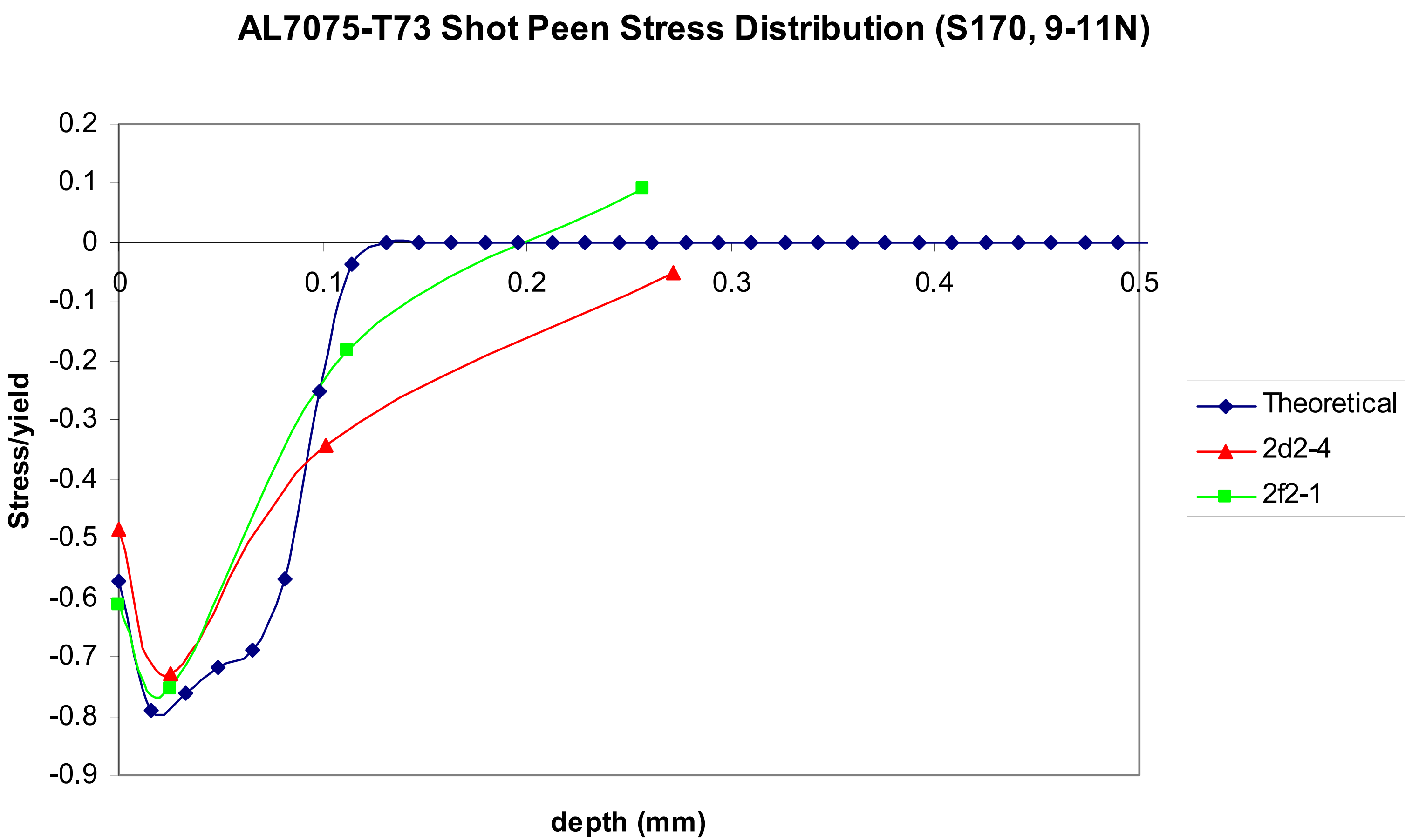

Experimental data from Sikorsky

UCI
University of California, Irvine

Comparison of the residual stress for Ti-6Al-4V Alpha-Beta

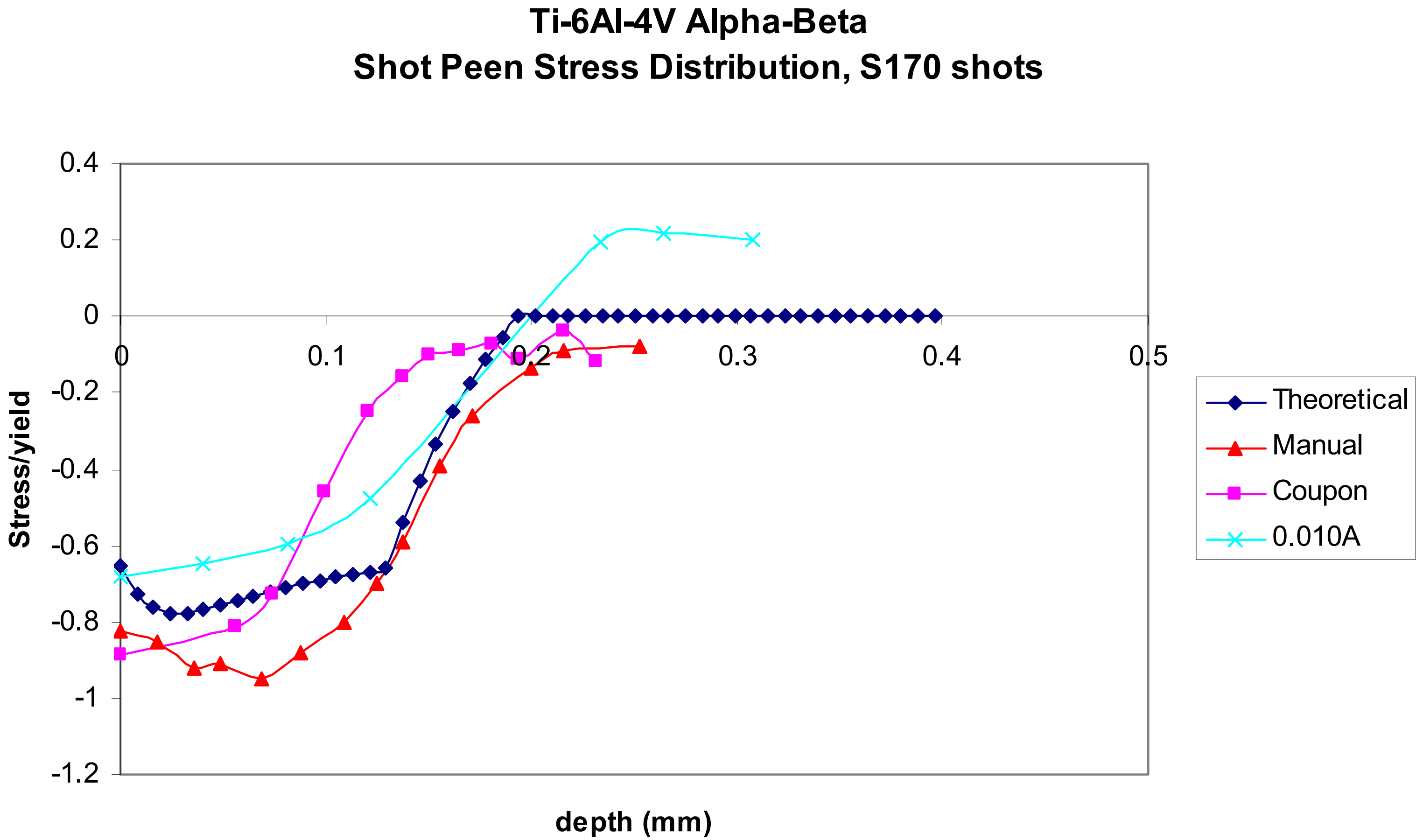

Experimental data from Sikorsky

UCI
University of California, Irvine

Comparison of the residual stress for Ti-6Al-4V Beta STOA

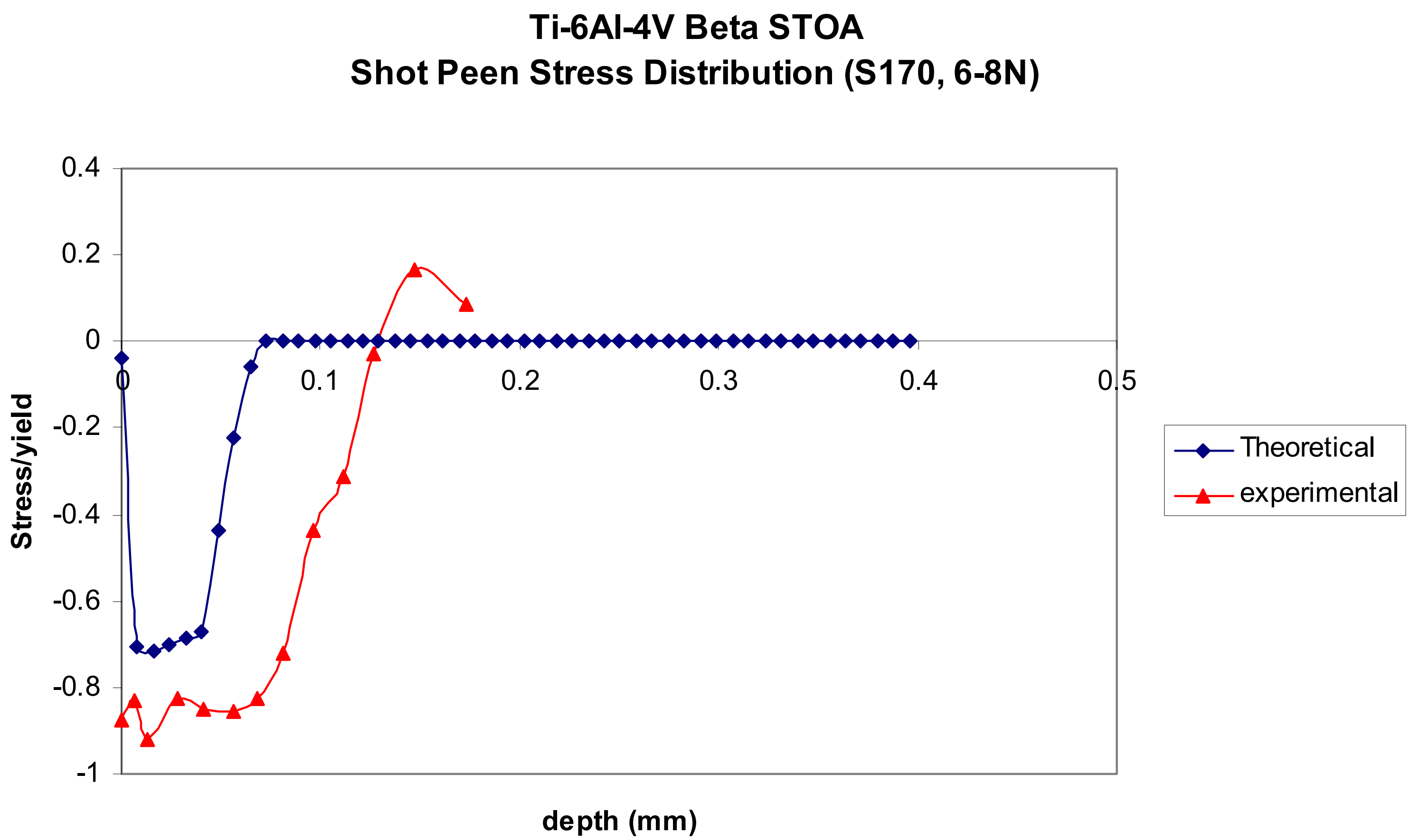

Experimental data from Sikorsky

Comparison of the residual stress for Ti-6Al-4V Beta STOA

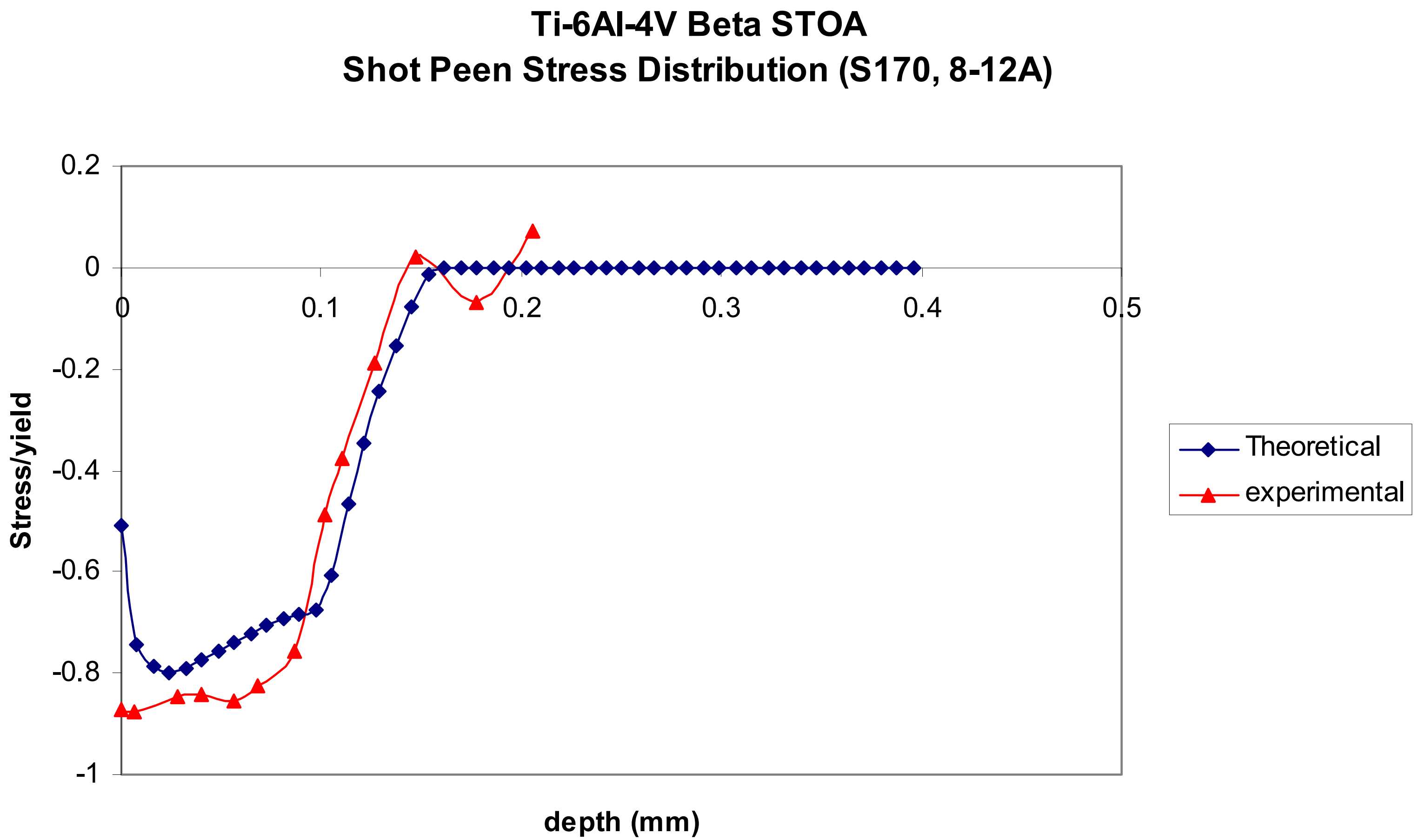

Experimental data from Sikorsky

Comparison of the residual stress for Ti-6Al-4V Beta STOA

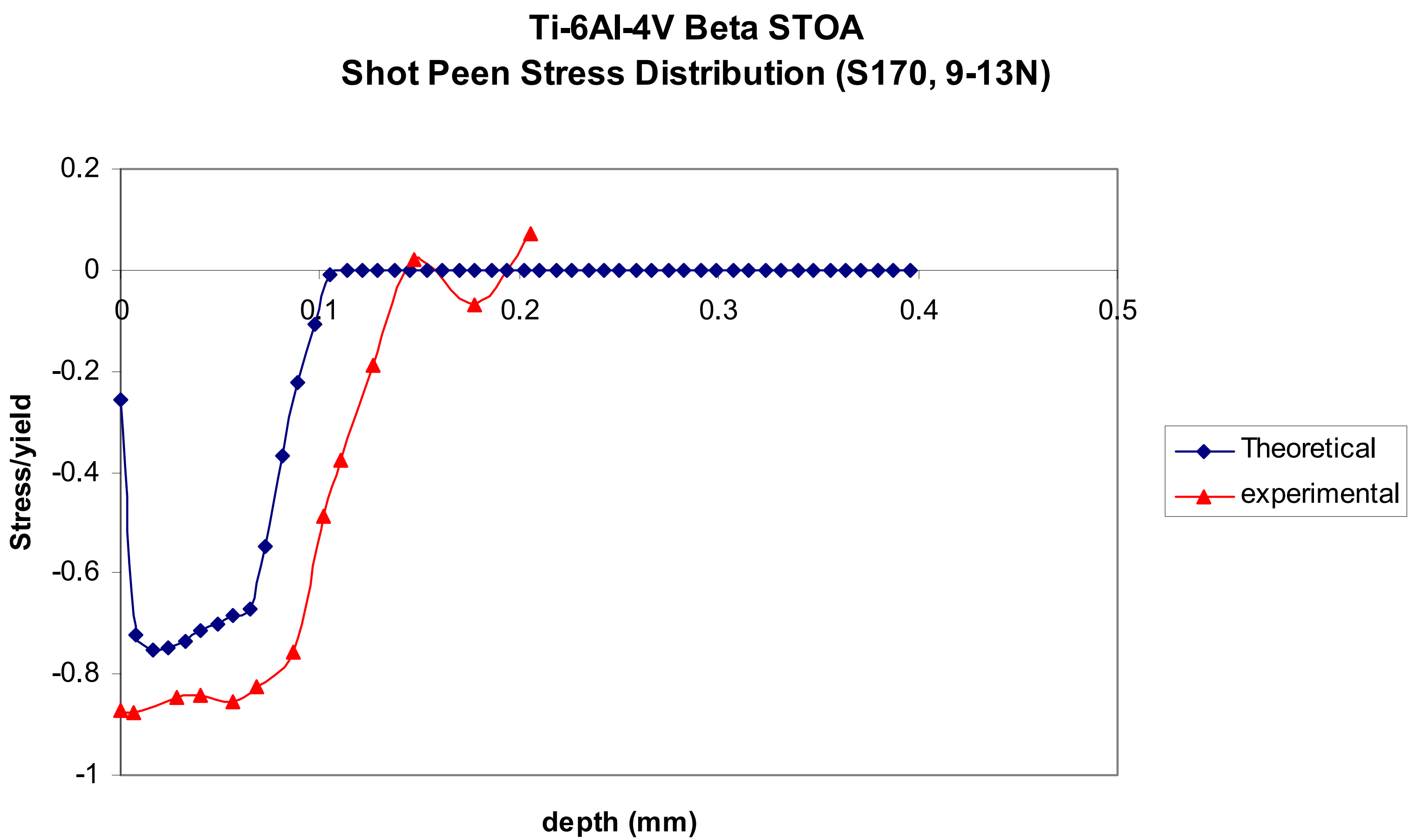

Experimental data from Sikorsky

Effect of plastic deformation due to cold-working

Assume that the plastic deformation is caused solely by cold-working of the fastener-hole; and that the applied far-field hoop stress does not produce any plastic deformation. The material is regarded to be elastic-perfectly-plastic.

For the elastic deformation, the stress-field near the hole

$$\sigma_{rr} = -p_0 \left(\frac{R}{r} \right)^2 \qquad \sigma_{\theta\theta} = p_0 \left(\frac{R}{r} \right)^2$$

r: the distance from the center of the hole.
R: the radius of the hole.
p_0: the radial pressure applied on the hole surface

Effect of plastic deformation due to cold-working

As the pressure p_0 is increased, the material near the hole begins to deform plastically.

In the plastic region $R \le r \le r_y$ the stresses are given by

$$\sigma_{rr} = -p_0 + \sigma_{ys} \ln\left(\frac{r}{R}\right) \qquad R \le r \le r_y$$

$$\sigma_{\theta\theta} = \sigma_{ys} - p_0 + \sigma_{ys} \ln\left(\frac{r}{R}\right) \qquad R \le r \le r_y$$

Tresca yield condition are used.

σ_{ys} is the yield-strength of the material and r_y is the radius of the plastic-region

Effect of plastic deformation due to cold-working

In the elastic region

$$\sigma_{rr} = -\frac{\sigma_{ys}}{2}\left(\frac{r_y}{r}\right)^2 \qquad r > r_y$$

$$\sigma_{\theta\theta} = \frac{\sigma_{ys}}{2}\left(\frac{r_y}{r}\right)^2 \qquad r > r_y$$

r_y is determined by

$$\frac{r_y}{R} = e^{\left(\frac{p_0}{\sigma_{ys}} - \frac{1}{2}\right)}$$

Effect of plastic deformation due to cold-working

The residual stress-field can be obtained by subtracting the elastic solution from the plastic solution

$$\sigma_{rr} = -p_0 + \sigma_{ys} \ln\left(\frac{r}{R}\right) + p_0\left(\frac{R}{r}\right)^2 \qquad R \le r \le r_y$$

$$\sigma_{\theta\theta} = \sigma_{ys} - p_0 + \sigma_{ys} \ln\left(\frac{r}{R}\right) - p_0\left(\frac{R}{r}\right)^2 \qquad R \le r \le r_y$$

$$\sigma_{rr} = -\frac{\sigma_{ys}}{2}\left(\frac{r_y}{r}\right)^2 + p_0\left(\frac{R}{r}\right)^2 \qquad r > r_y$$

$$\sigma_{\theta\theta} = \frac{\sigma_{ys}}{2}\left(\frac{r_y}{r}\right)^2 - p_0\left(\frac{R}{r}\right)^2 \qquad r > r_y$$

Effect of plastic deformation due to cold-working

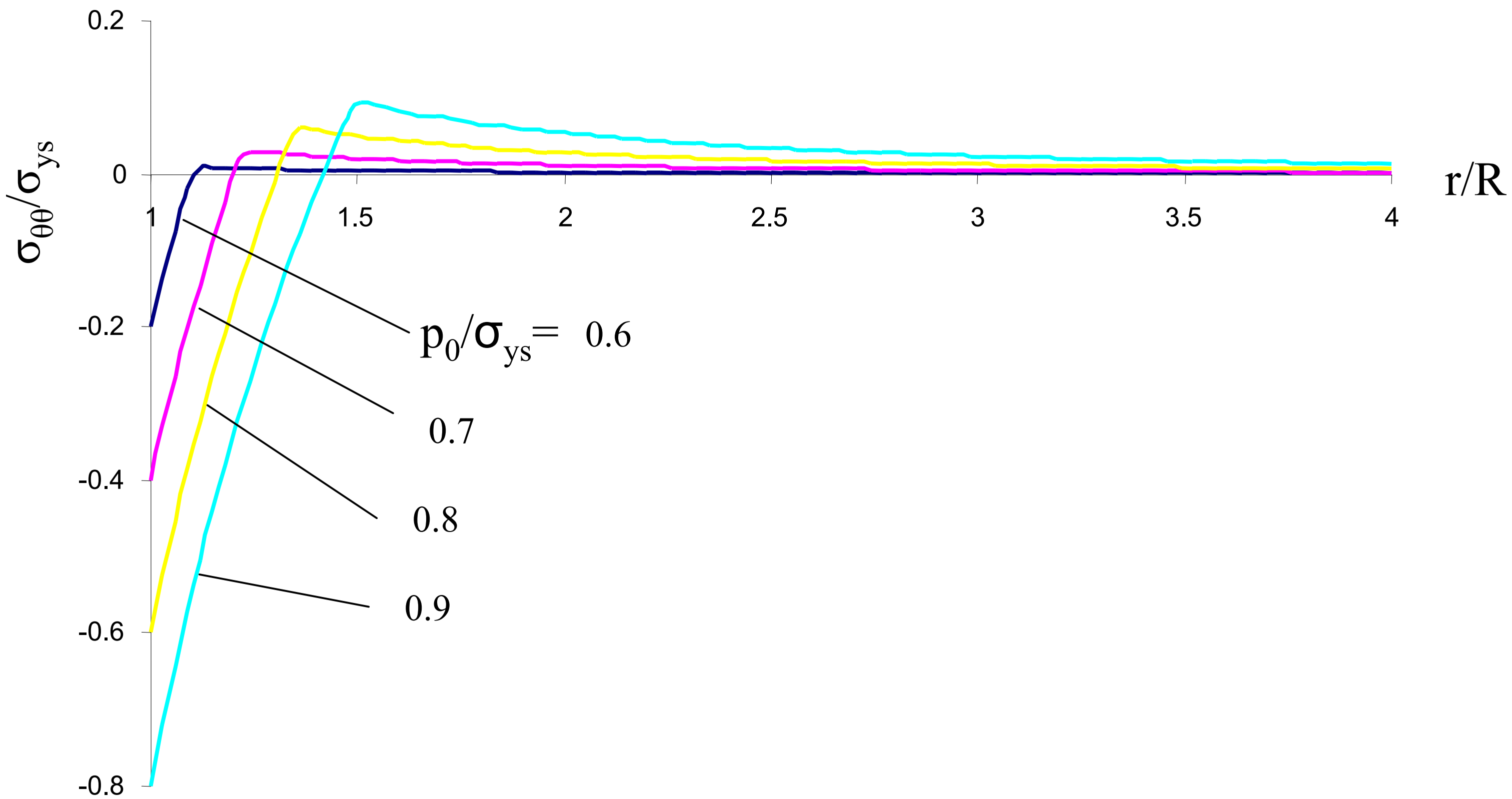

Residual stress $\sigma_{\theta\theta}$ along a radial line from the center of the hole, due to cold-working induced plasticity

Effect of plastic deformation due to cold-working

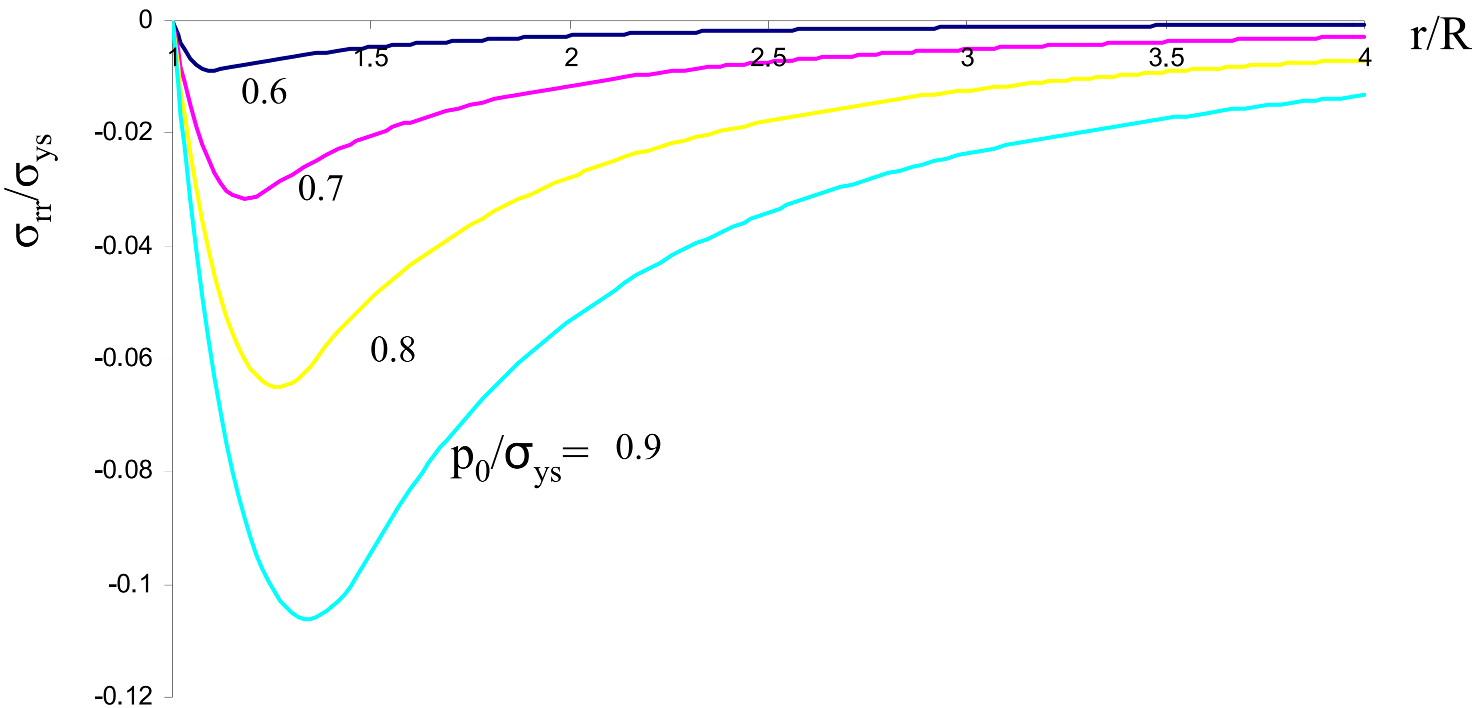

Residual stress σ_{rr} along a radial line from the center of the hole, due to cold-working induced plasticity

Effect of plastic deformation due to cold-working

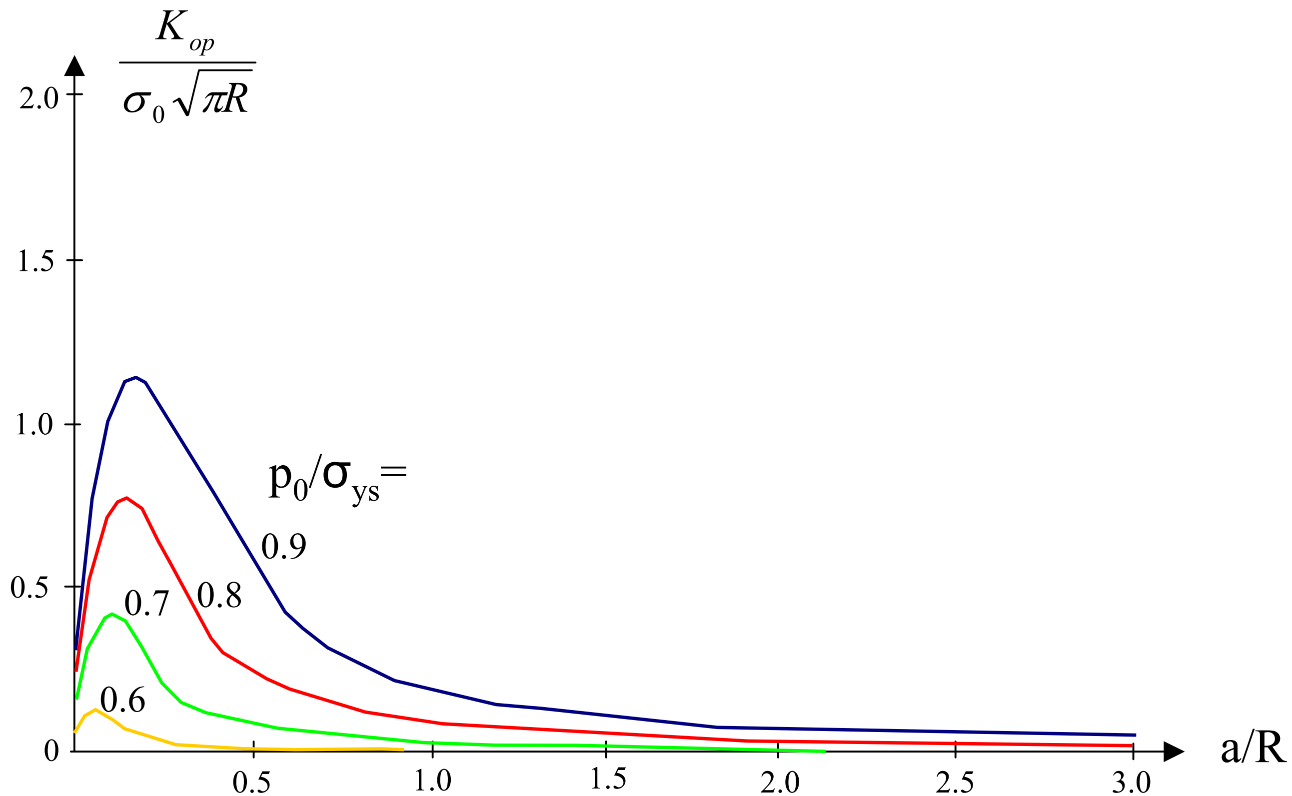

Variation of the open SIF K_{op} for cracks of various length as compared to the radius of the plastic zone due to cold-working

Analytical model for plasticity-induced crack-closure

The effects of the shot-peening, and cold-working on the crack growth: the residual stress field impedes the crack propagation. This model is based on the shape of the plastic zone.

Account for the 3-D effect by assuming that

$$\sigma_3 = T_Z\left(\sigma_2 + \sigma_1\right)$$

T_z is the 3D constraint factor. For plane stress $T_z = 0$

For plane strain $T_z = v$ v is the Poisson's ratio.

T_z should vary along the thickness, i.e. is a function of z. In the center of the specimen, $T_z = v$; on the surface, $T_z = 0$.

Modeling fatigue crack growth - Plastic Zone Model

The principal stresses for the Mode I crack can be written as

$$\sigma_1 = \frac{K_I}{\sqrt{2\pi r}} cos\left(\frac{\theta}{2}\right)\left[1 + sin\left(\frac{\theta}{2}\right)\right]$$

$$\sigma_2 = \frac{K_I}{\sqrt{2\pi r}} cos\left(\frac{\theta}{2}\right)\left[1 - sin\left(\frac{\theta}{2}\right)\right]$$

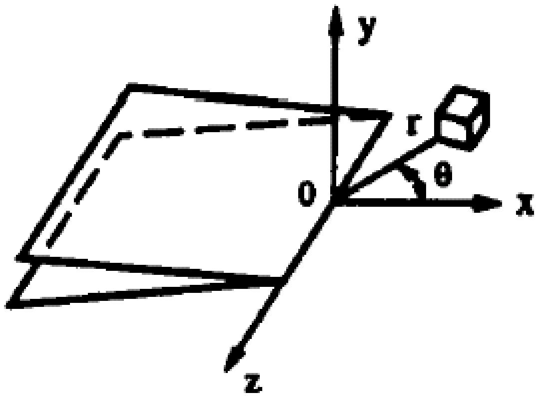

and

$$\sigma_3 = \frac{2T_Z K_I}{\sqrt{2\pi r}} \cos\left(\frac{\theta}{2}\right)$$

T_z can be approximately related to the plastic constrain factor α in NASGRO model (averaging T_z along the thickness)

$$T_z = \frac{v(\alpha - 1)}{2}$$

α =1 plane stress

α =3 plane strain

Modeling fatigue crack growth - Plastic Zone Model

Consider the von Mises equation the effective stress is

$$\sigma_e = \frac{1}{\sqrt{2}}\left[(\sigma_1 - \sigma_2)^2 + (\sigma_1 - \sigma_3)^2 + (\sigma_2 - \sigma_3)^2\right]^{\frac{1}{2}}$$

According to the von Mises criterion, yielding occurs when

$\sigma_e = \sigma_0$, the uniaxial yield strength

The Mode I plastic zone radius can be estimate as

$$r(\theta) = \frac{1}{4\pi}\left(\frac{K_I}{\sigma_0}\right)^2\left[(1 - 2T_z)^2(1 + \cos\theta) + \frac{3}{2}\sin^2\theta\right]$$

Crack tip plastic zone shapes

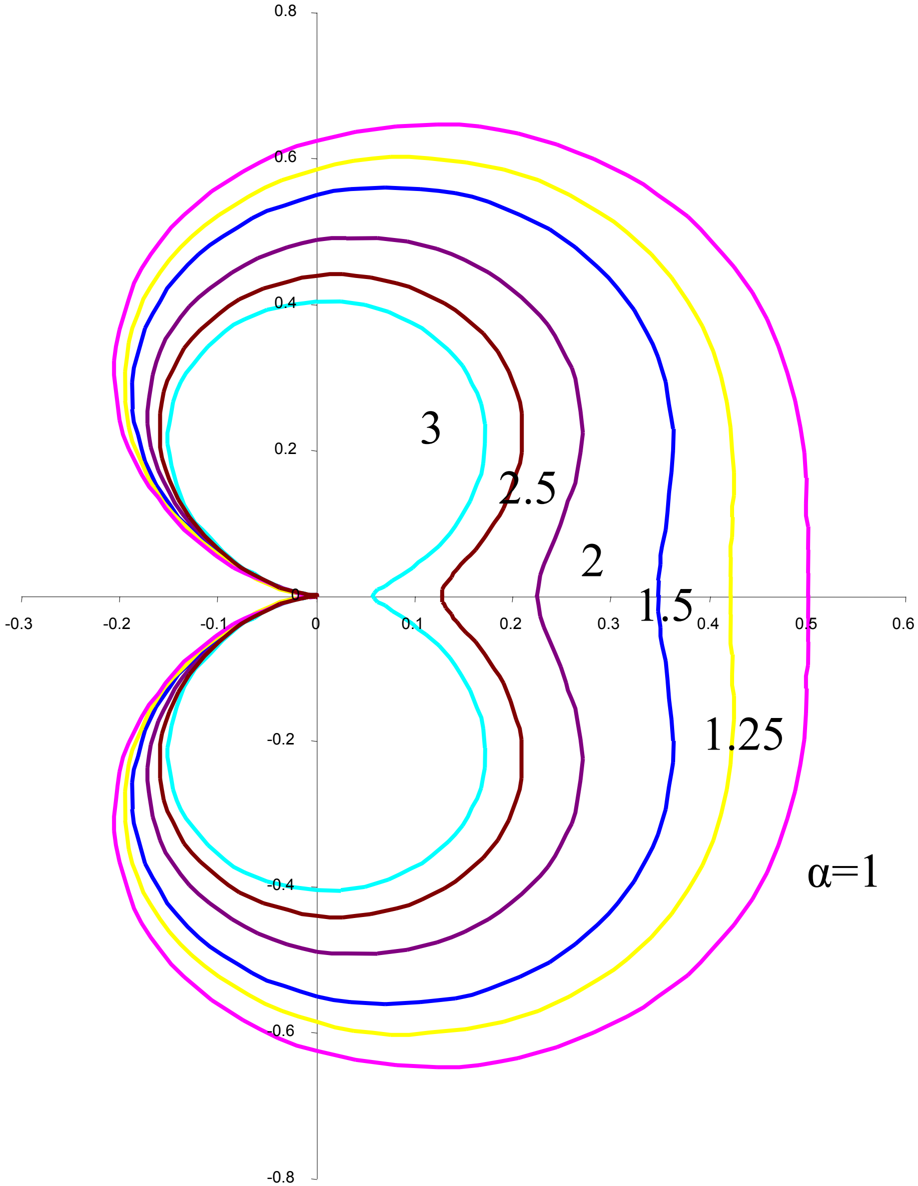

For plane stress $\alpha=1$

For plane strain $\alpha=3$

The crack tip plastic zone shapes under different 3D constraint

Plastic Zone model

Consider a structure subjected to a cyclic load with an overload.

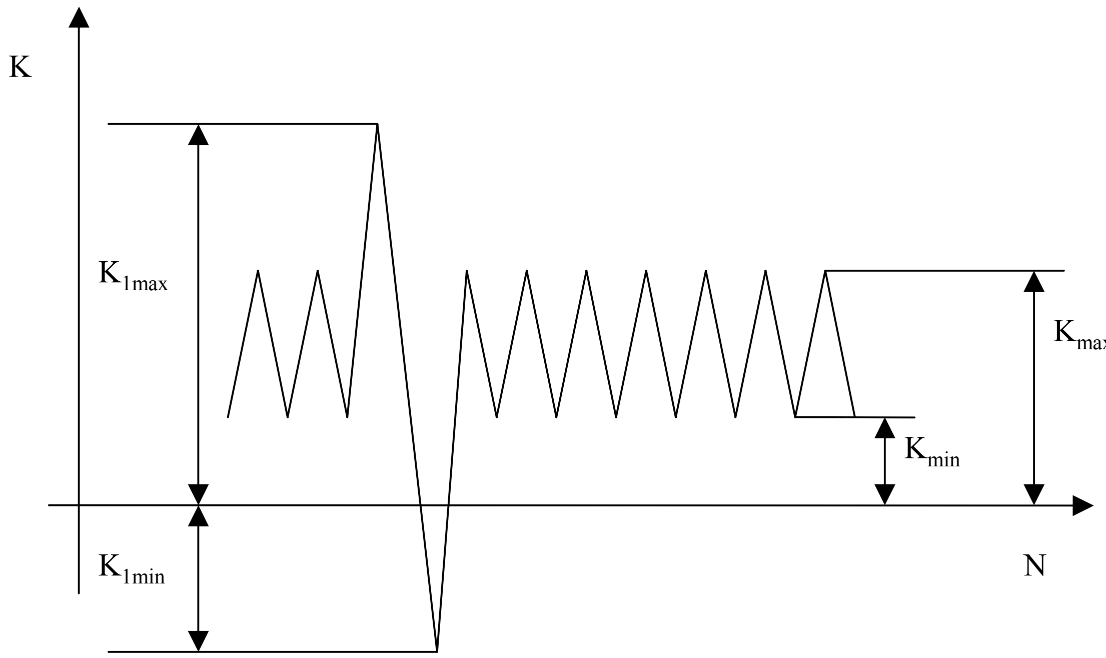

$$R_1 = \frac{K_{1min}}{K_{1max}} \qquad R = \frac{K_{min}}{K_{max}}$$

For the residual stress field due to the shot-peening or cold-working, R_1=0.

Plastic Zone model

After the application of the overload, the plastic zones formed at the crack tip are

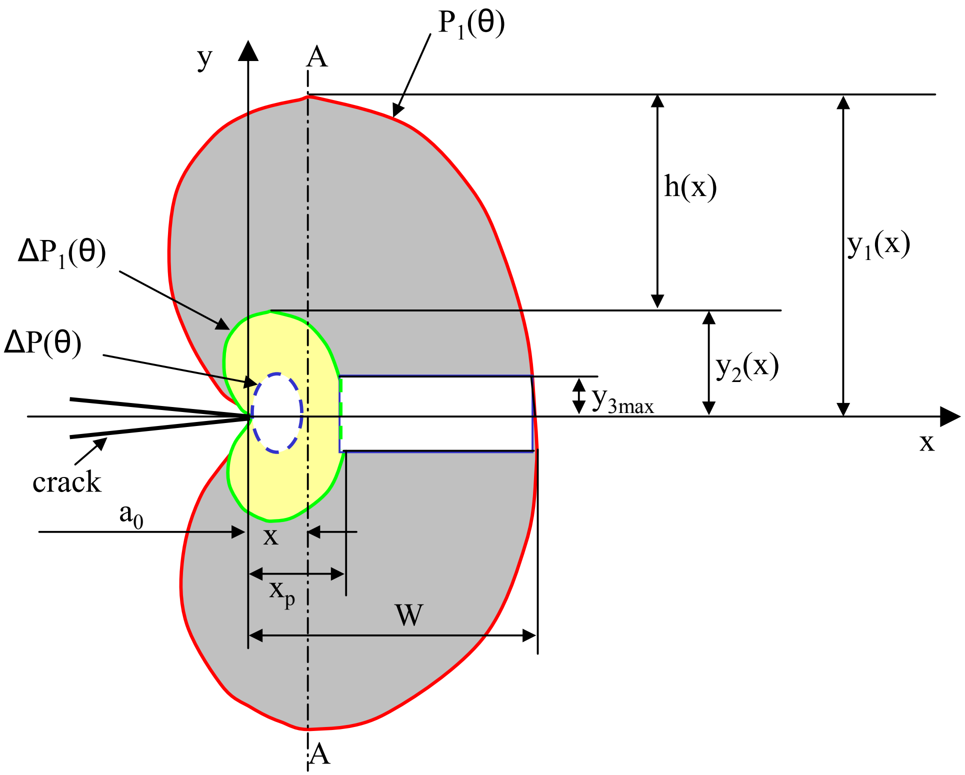

The plastic zone of overload

$$P_1(\theta) = \frac{1}{4\pi}\left(\frac{K_{1max}}{\sigma_0}\right)^2 f(\theta)$$

The cyclic plastic zone of overload

$$\Delta P_1(\theta) = \frac{\beta}{4\pi}\left(\frac{(1-R_1)K_{1max}}{2\sigma_0}\right)^2 f(\theta)$$

The baseline cyclic plastic zone

$$\Delta P(\theta) = \frac{\beta}{4\pi}\left(\frac{(1-R)K_{max}}{2\sigma_0}\right)^2 f(\theta)$$

β is the cyclic plastic zone size factor and depends on R

Plastic Zone model

During the loading half cycle, the crack will be opened from close only when the load is great enough to make the CTOD equal to the compressive deformation during the unloading half cycle

CTOD=2δ $\qquad$ $\delta = \lambda \Delta l$

Δl is the stretch of the material element. For an element just behind the crack tip, it can be calculated as

$$\Delta l = \int_{y_2}^{y_1} \varepsilon_p dy$$

Approximately

$$\varepsilon_p = m \frac{\sigma_0}{E}$$

m is a magnification factor depending on x, and is assumed to be proportional to the height $h(x)$ within the shade area,

$$m = m_0 \frac{h(x)}{w}$$

m_0 is a constant, w is the length of the overload affected zone

Plastic Zone model

From the figure,

$$h(x) = y_1(x) - y_2(x) \qquad \text{for } x < x_p$$

$$h(x) = y_1(x) - y_{3\max}(x) \qquad \text{for } x \geq x_p$$

Here

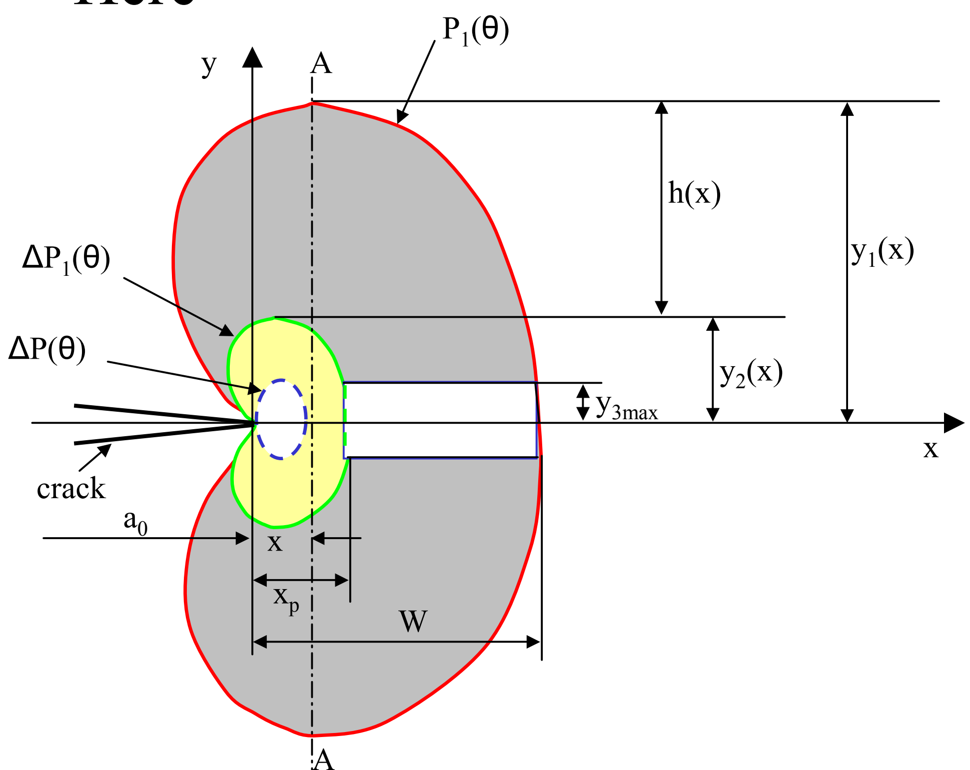

$$y_1(x) = \frac{1}{4\pi}\left(\frac{K_{1\max}}{\sigma_0}\right)^2 \bar{y}_1(x)$$

$$y_2(x) = \frac{\beta}{4\pi}\left(\frac{(1-R_1)K_{1\max}}{2\sigma_0}\right)^2 \bar{y}_2(x)$$

$$y_{3\max} = \frac{\beta}{4\pi}\left(\frac{(1-R)K_{\max}}{2\sigma_0}\right)^2 \bar{y}_{\max}$$

Plastic Zone model

The crack tip opening displacement can be expressed as

$$CTOD = k\frac{K_{1max}^2}{E\sigma_0}$$

and

$$\delta = \frac{\lambda m_0 \sigma_0}{Ew} h^2(x)$$

The crack opening SIF

$$K_{op}(x) = M_0\left[\bar{y}_1(x) - \frac{\beta(1-R_1)^2}{4}\bar{y}_2(x)\right]R_m K_{max} \quad \text{for } x < x_p$$

$$K_{op}(x) = M_0\left[\bar{y}_1(x) - \frac{\beta(1-R)^2}{4R_m^2}\bar{y}_{max}\right]R_m K_{max} \quad \text{for } x \geq x_p$$

M_0 is an empirical material constant.

$$R_m = \frac{K_{1max}}{K_{max}}$$

Plastic Zone model

M_0 can be determined from known test data, or by means of the NASGRO model, under constant amplitude cyclic load, i.e. R_m=1.

This model $$K_{op}(x) = M_0\left[\bar{y}_1(x) - \frac{\beta(1-R)^2}{4R_m^2}\bar{y}_{\max}\right]K_{\max}$$

NASGRO $$\frac{K_{op}}{K_{\max}} = \begin{cases} \max\left(R, A_0 + A_1R + A_2R^2 + A_3R^3\right), & R \geq 0 \\ A_0 + A_1R, & -2 \leq R < 0 \\ A_0 - 2A_1, & R < -2 \end{cases}$$

Equaling these two equations at R=0 $\longrightarrow$ M_0

Validation of the Fatigue Model

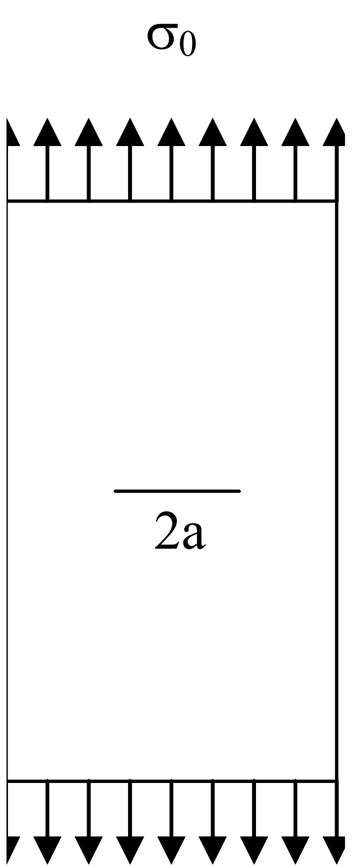

350WT steel center crack

Maximum stress (σ_{max})=114Mpa
Stress ratio R=0.1

C=1.02e-8
n=2.94

a=22.4mm

Yield strength =350 MPa

Plane stress, Tz/v=0

Validation of the Fatigue Model

Spectra

Constant Amplitude	Maximum stress (σ_{max})=114Mpa Stress ratio R=0.1
Case 1: R_m=1.25	2 overloads occur at 30 and 50 mm, respectively
Case 2: R_m=1.5	3 overloads occur at 30, 40, and 50 mm, respectively
Case 3: R_m=1.75	2 overloads occur at 30 and 50 mm, respectively

$$R_m = \frac{K_{1max}}{K_{max}}$$

Validation of the Fatigue Model

	Fatigue life: Experimental results (cycle)	Fatigue life: This model (cycle)
Case 1: Rm=1.25, 2 overloads	146,000	127,859
Case 2: Rm=1.5, 3 overloads	193,000	172,140
Case 3: Rm=1.75, 2 overloads	255,000	233,395

Comparing with experimental results [Taheri, et al. (2003), *Marine Structures*, 16: 69-91]

Validation of the Fatigue Model

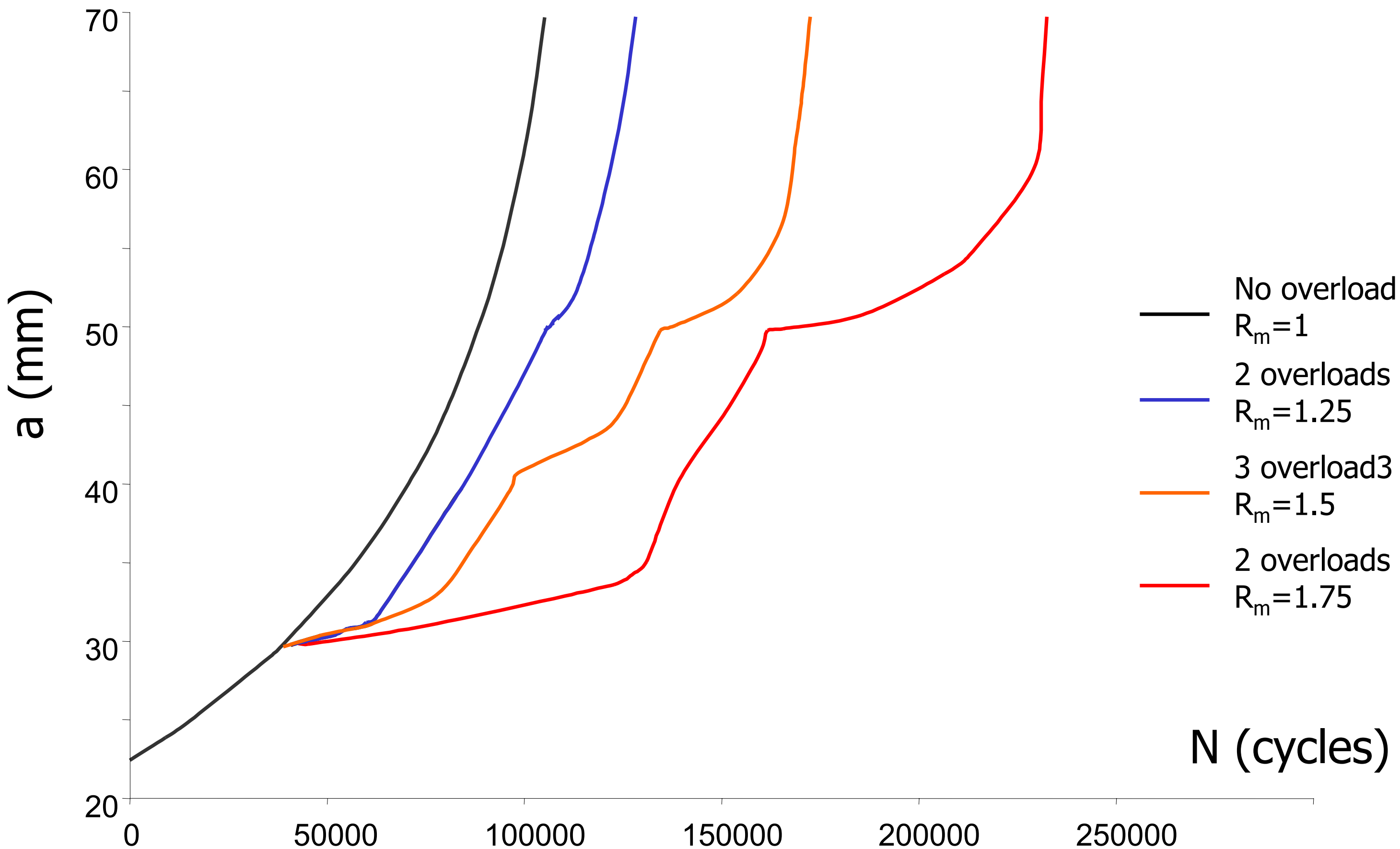

Tz/v=0

Numerical results

UCI
University of California, Irvine

Effect of Cold-working on Fatigue

2024-T3 AL

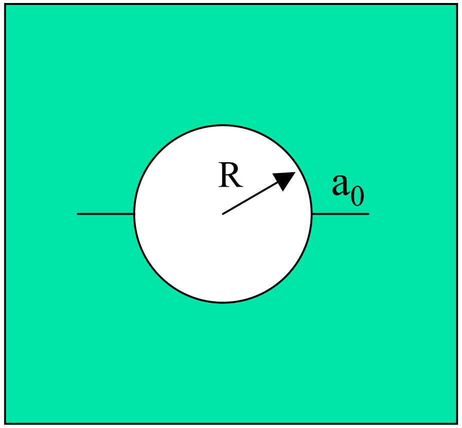

For a single hole in a sheet, for cold working
The radial pressure p_0 on the hole surface is $0.5\sigma_{ys}$

R=2 mm, a_0=4 mm, da=4 mm

C=2.383E-11
n=3.2

Effect of Cold-working on Fatigue

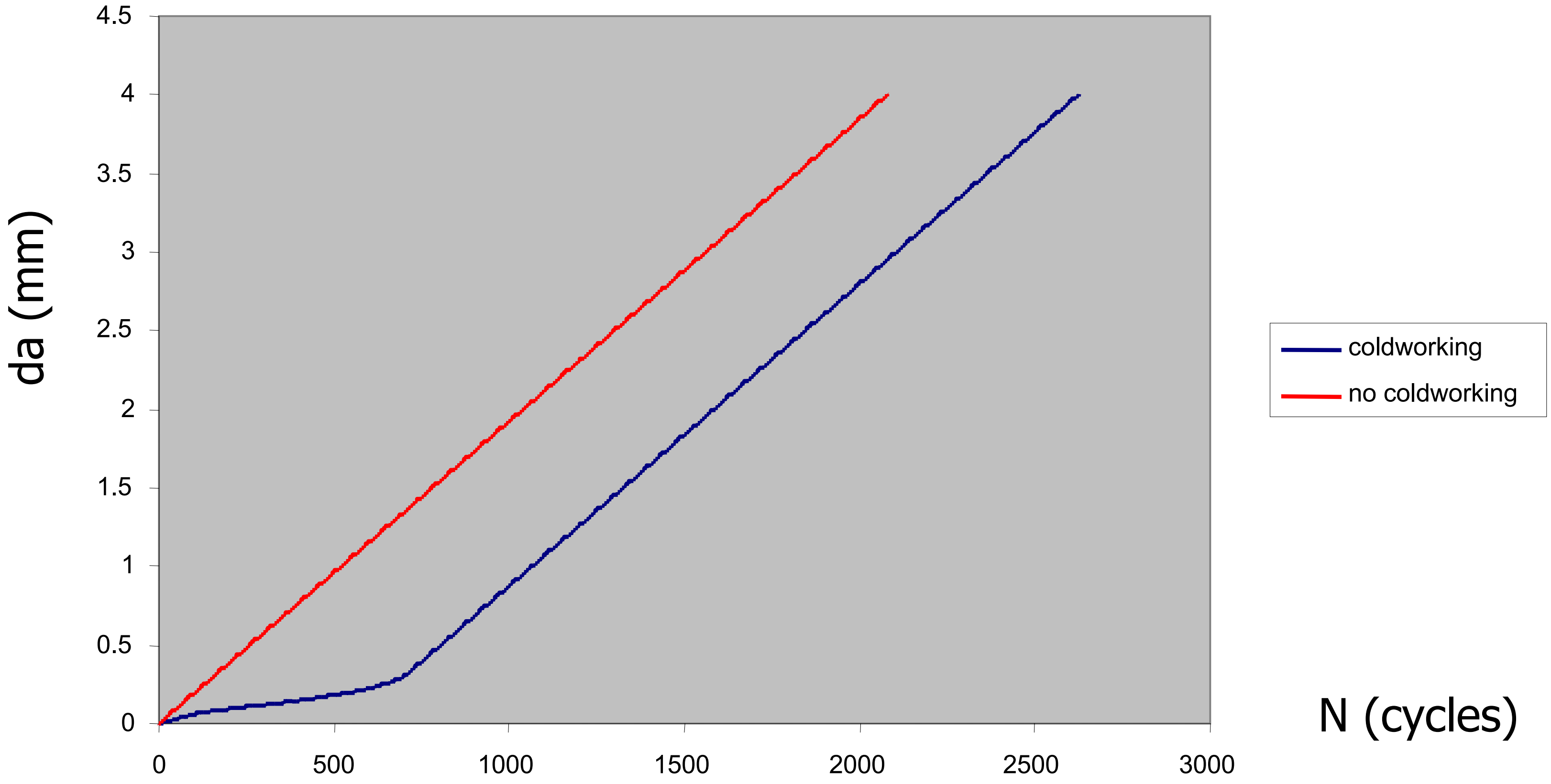

K_{max}=476.09 MPa mm$^{1/2}$

R=0

2,652 cycles

2,051 cycles

Tz/v=0.5

UCI
University of California, Irvine

Effect of Cold-working on Fatigue

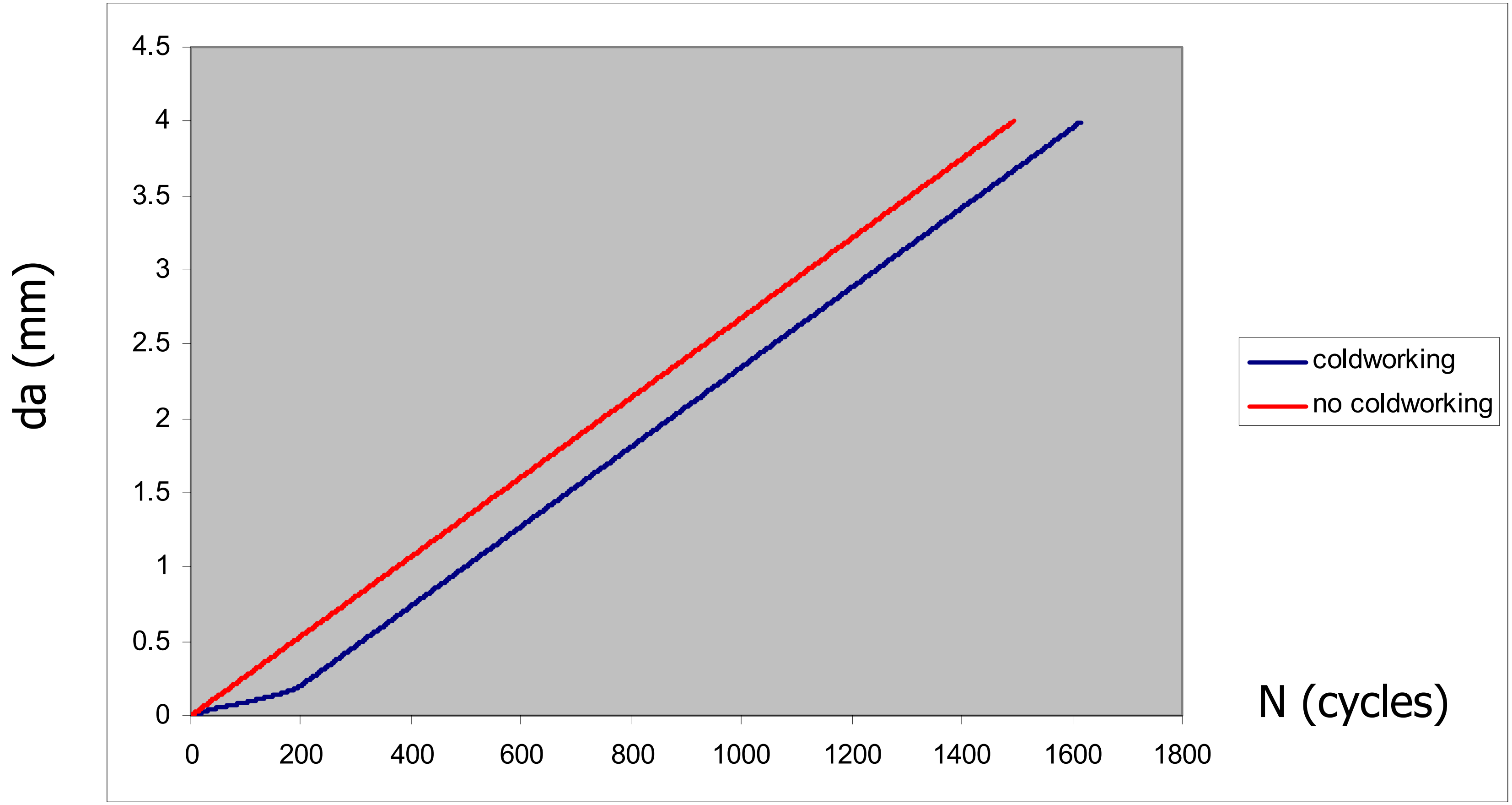

K_{max}=476.09 MPa mm$^{1/2}$ R=0 1,617 cycles

1,495 cycles

Tz/v=1

Effect of Cold-working on Fatigue

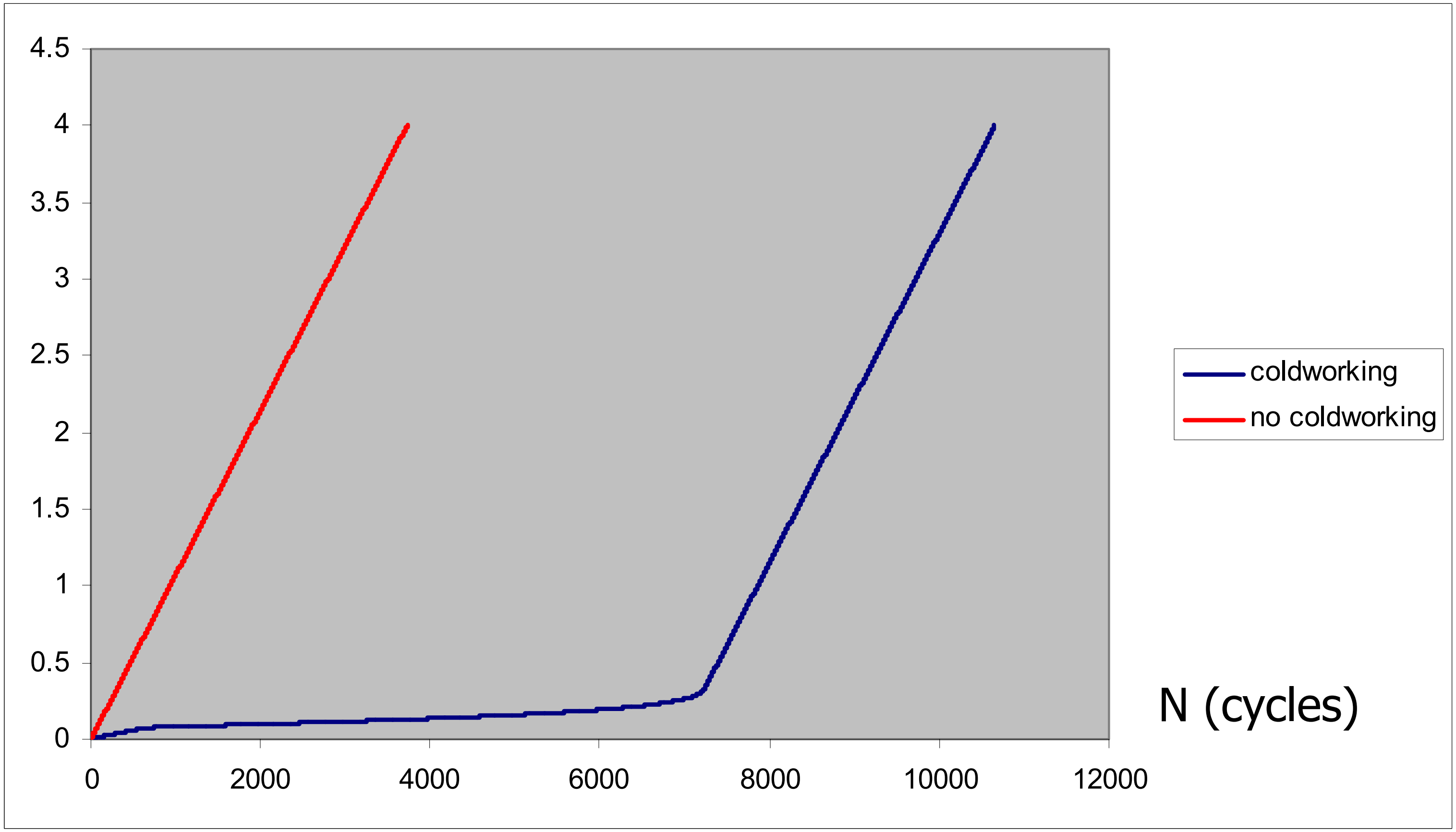

K_{max}=396.75 MPa mm$^{1/2}$ R=0 10,655 cycles

Tz/v=0.5 3,728 cycles

UCI
University of California, Irvine

Effect of Cold-working on Fatigue

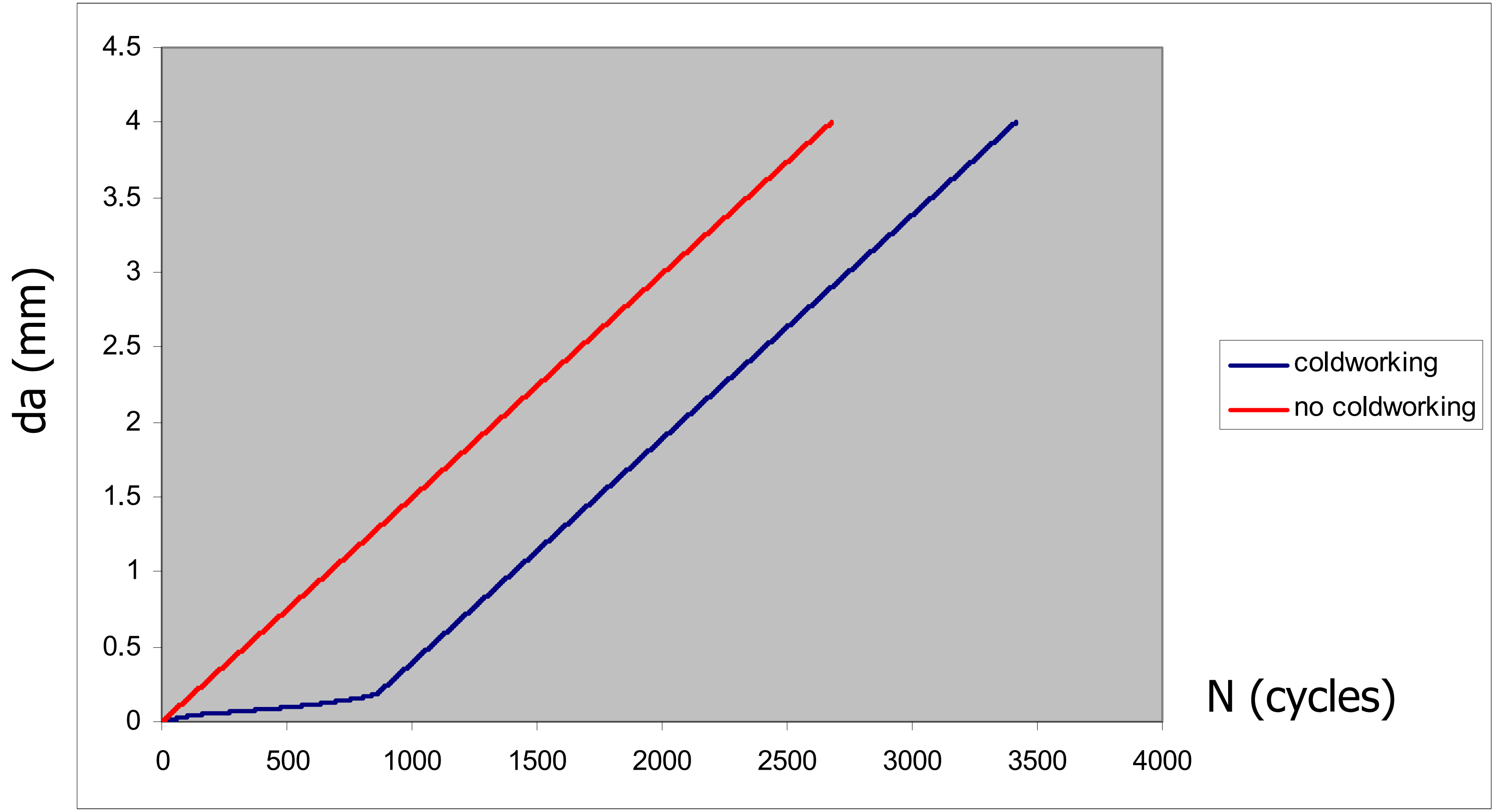

K_{max}=396.75 MPa mm$^{1/2}$ R=0

Tz/v=1

3,414 cycles

2,678 cycles

UCI
University of California, Irvine

Conclusions

- An analytical model to model the rivet misfit is developed.
- An analytical model to model the cold-working process is developed.
- An appropriate analytical model to model the shot-peening process with 200% coverage is developed.
- The effects of residual stresses on fatigue crack growth are considered.
- A plastic zone fatigue model, which accounts for the 3D effects and the residual stress is developed to

Conclusions

- The proposed analytical model for the shot-peening process with 200% coverage can simulate the experiment well.
- The effects of residual stresses on fatigue crack growth are considered.
- The developed plastic zone fatigue model, which accounts for the 3D effects and the residual stress, is verified by the existing experiment.

Workflow of proposed Analysis with effects of other residual stress fields

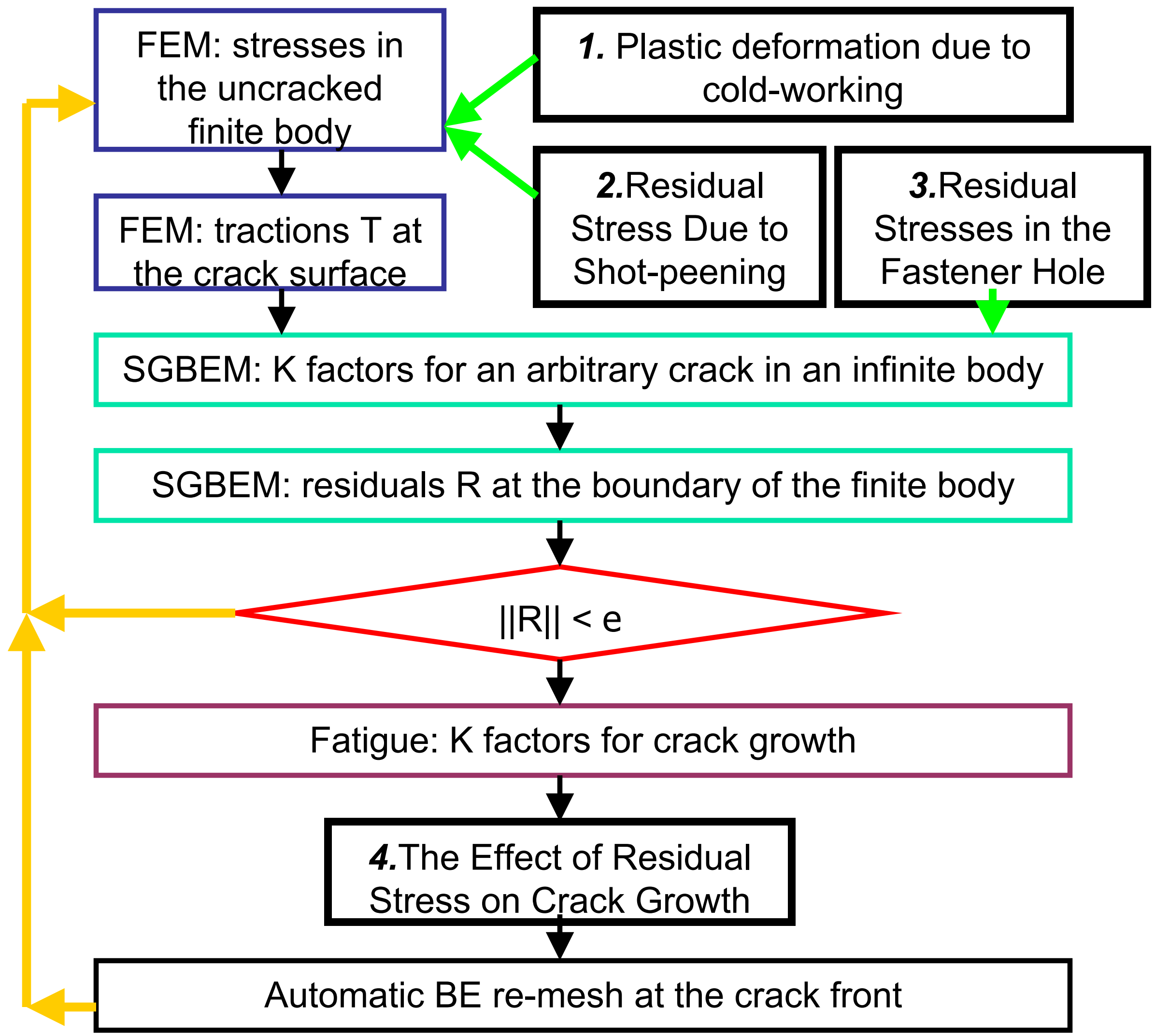

UCI
University of California, Irvine

Effect of Residual Stresses in the Fastener Hole

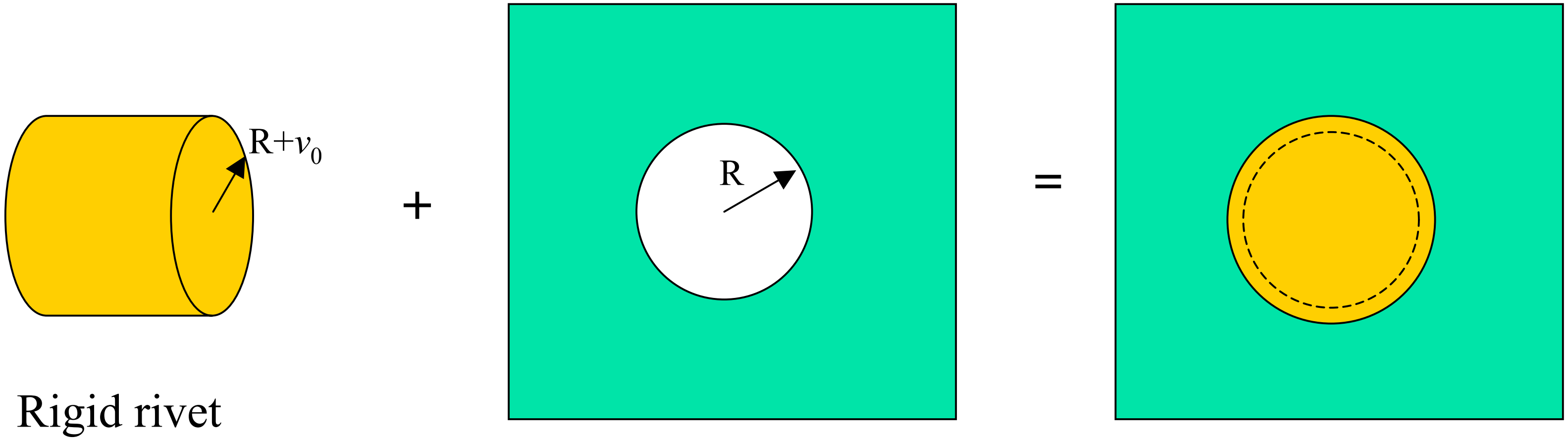

For a single hole in an infinite sheet:

The radial pressure p_0 on the hole surface

$$p_0 = (2\mu)\frac{v_0}{R} = k_0\frac{v_0}{R}$$

k_0 is the "stiffness" of the hole in an infinite sheet

Effect of Residual Stresses in the Fastener Hole

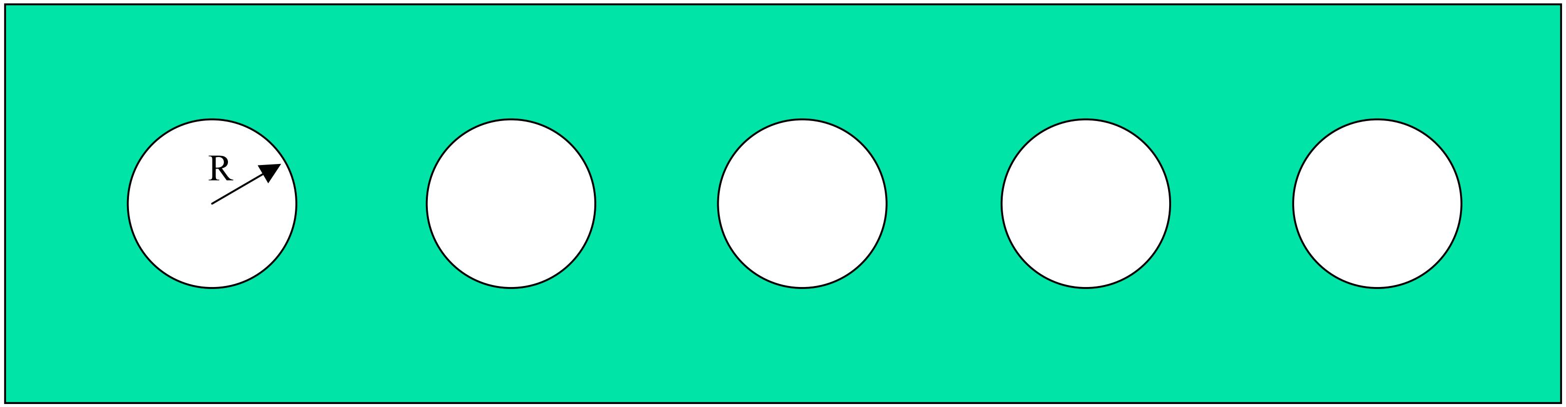

Assume that the rivet misfit is equal to v_0 for all the fastener holes in a row. Without any far field loading, the initial radial pressure p_0 on each hole is also

$$p_0 = (2\mu)\frac{v_0}{R} = k_0 \frac{v_0}{R}$$

Effect of Residual Stresses in the Fastener Hole

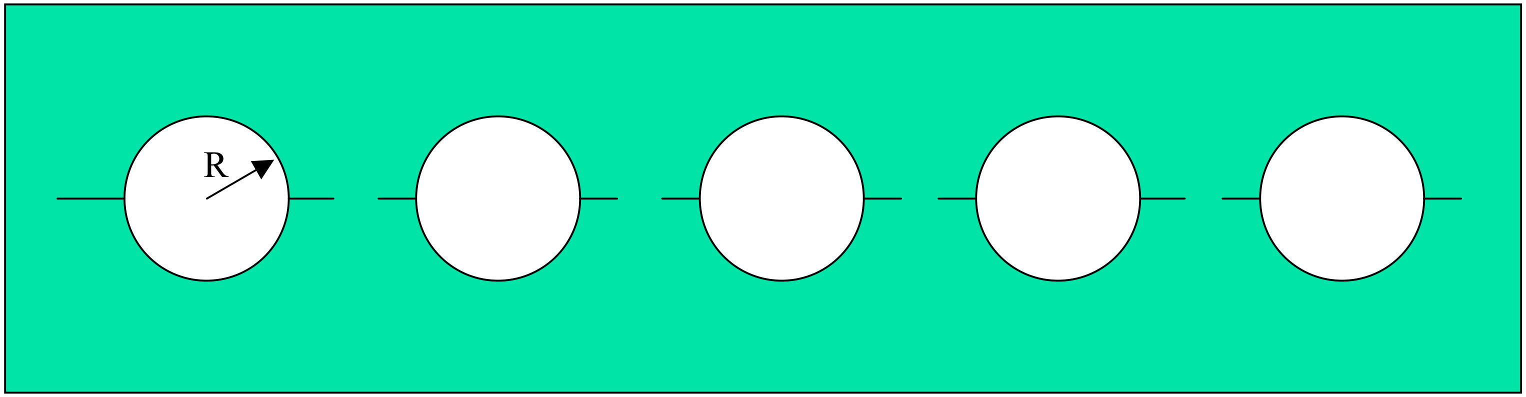

When cracks are present near the holes, the initial radial pressure on each hole will be a function of the crack length

$$p_i = k_i \frac{v_0}{R} \qquad \text{or} \qquad k_i = \frac{Rp_i}{v_0}$$

The initial radial pressure p_i is solved for, using the FEAM.

The stiffness k_i depends on the lengths of the cracks emanating from the ith hole.

Effect of Residual Stresses in the Fastener Hole

Let the applied far-field stress be σ_1, and the maximum v displacement at the ith hole due to σ_1 alone be designated as v_{i1}. v_{i1} is determined from the FEAM, and is a function of the lengths of the cracks emanating from the ith hole.

The radial pressure exerted due to initial fastener-misfit, is given during the course of far-field loading, by

$$p_{i1} = \begin{cases} k_i \left| v_{i1} - v_0 \right| / R & \text{when } v_{i1} < v_{i0} \\ 0 & \text{when } v_{i1} \geq v_{i0} \end{cases}$$

Effect of Residual Stresses in the Fastener Hole

A far-field zero-to tension cyclic load: 0 to σ_1 at the upper edge; and 0 to σ_0 at the lower edge

The maximum SIF at the crack at the ith hole is

$$K_{i\max} = K_i + K_{i1}$$

The minimum SIF at the crack at the ith hole is $K_{i\min} = K_{i0}$

K_i: the SIF due to far-field alone.

K_{i0}: the SIF due to the initial radial (at zero far-field tension) pressure due to fastener misfit.

K_{i1}: the SIF due to the residual pressure p_{i1} when applying far-field stress.

The residual stresses affect fatigue crack growth by two factors:

- Reducing the SIF rang ΔK;
- Increasing the stress-ratio.

Effect of Residual Stresses in the Fastener Hole

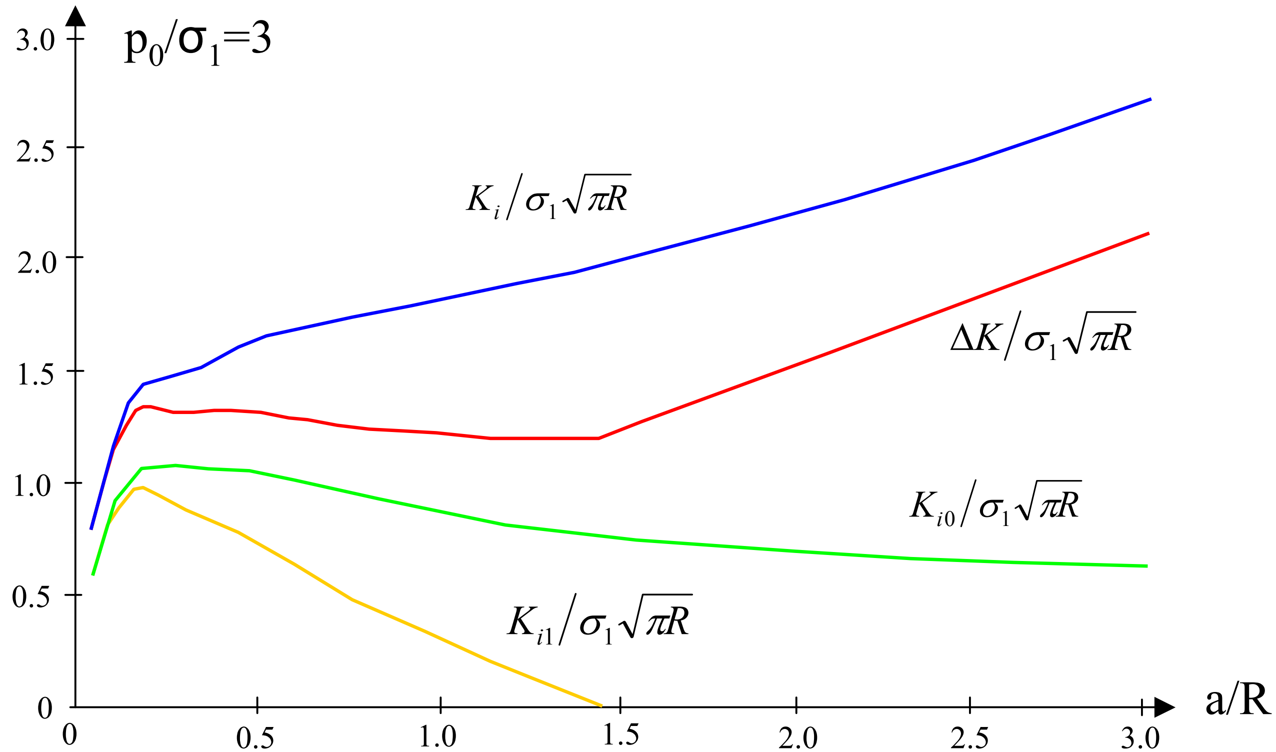

Variation of SIF and SIF rang as functions of (a/R), with the effect of residual stresses being considered ($p_0/\sigma_1=3$)

Effect of Residual Stresses in the Fastener Hole

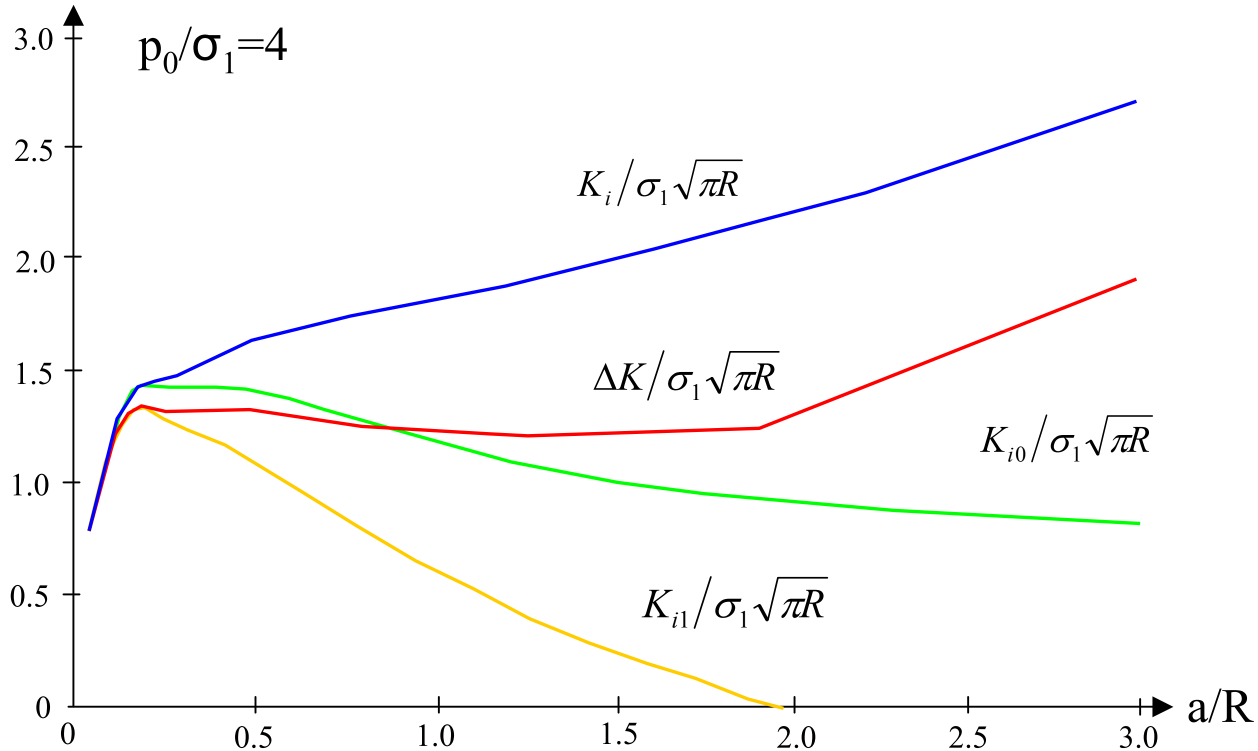

Variation of SIF and SIF rang as functions of (a/R), with the effect of residual stresses being considered (p_0/σ_1=4)

Effect of Residual Stresses in the Fastener Hole

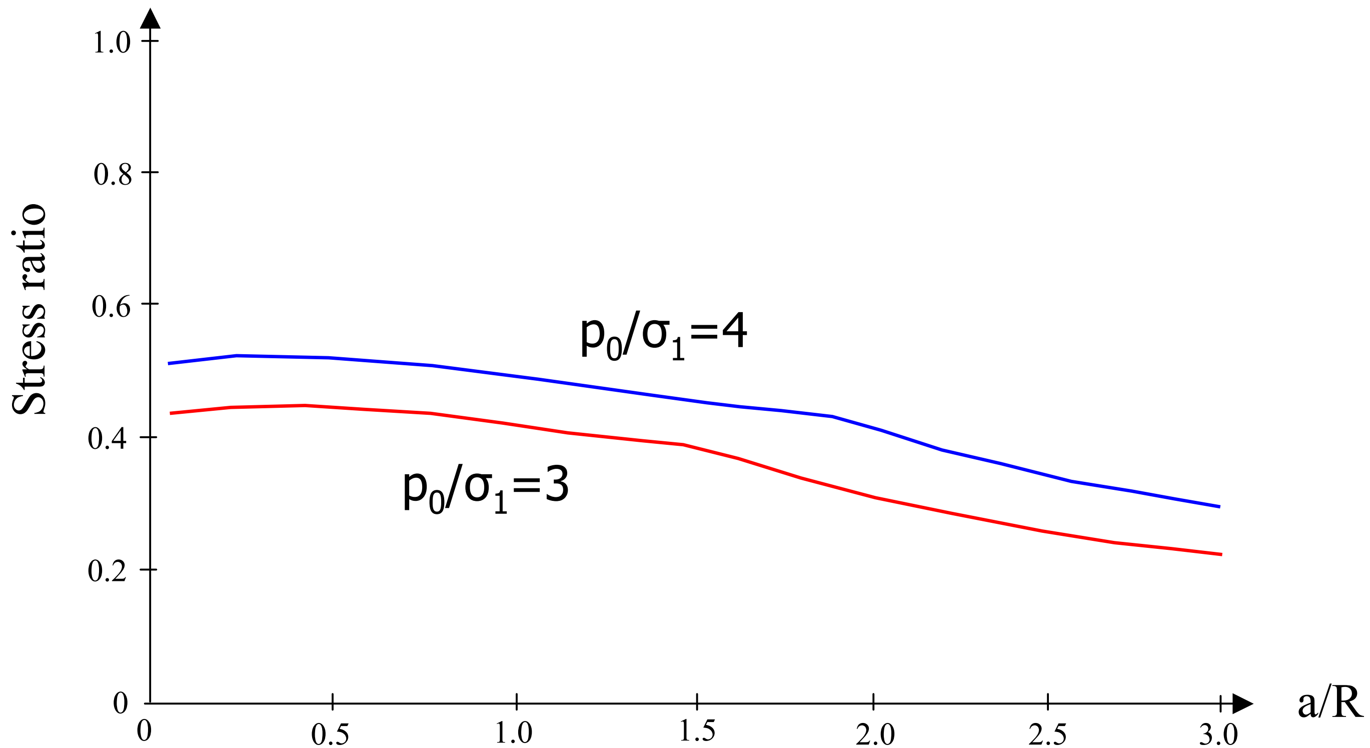

Variation of stress ratio as a function of a/R

Fatigue crack growth behavior of cracks emanating from fastener holes

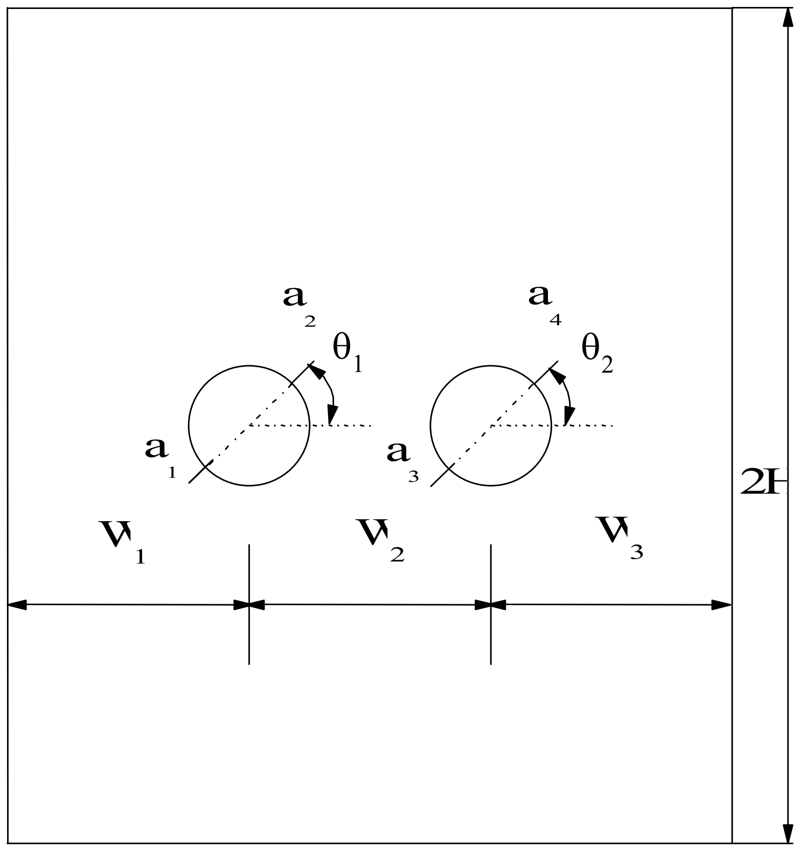

2024-T3 Aluminium alloy

The fastener-load is distributed along the periphery of the hole, by using the analytical solution for the contact problem between the rivet and the hole. In this example, for simplicity, the fastener load is distributed sinusoidally.

The initial crack configuration

Fatigue crack growth behavior of cracks emanating from fastener holes

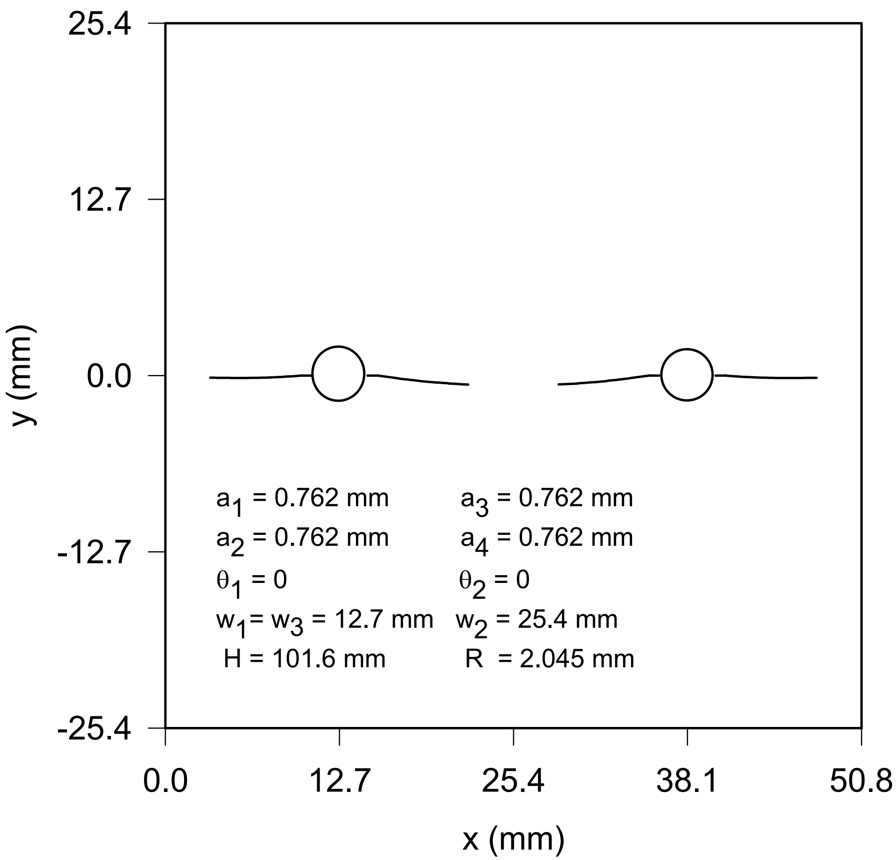

uniform stress σ_0 is applied on the upper horizontal edge, and an equilibrating sinusoidally distributed pin loading exists on the lower half of the hole periphery.

Stress σ_0=82.74 MPa

Stress ratio =0.1

The total applied loading cycles 19,800 cycles

Fatigue crack growth behavior of cracks emanating from fastener holes

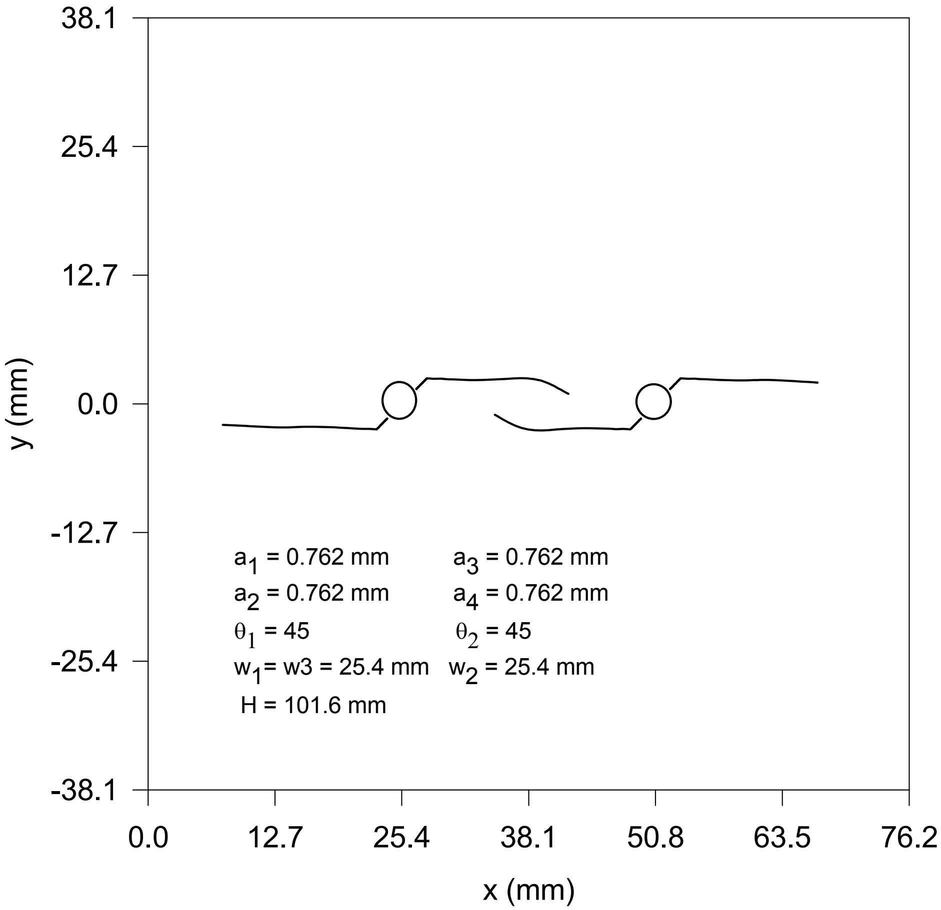

The loading consists of uniform stress σ_0 on the upper and lower edges of the sheet

Both the initial cracks emanating from the fastener holes are slanted at 45^o degrees

Crack growth direction is determined by using the maximum principal stress criterion

Fatigue crack growth behavior of cracks emanating from fastener holes

The variation of mode I and mode II stress intensity factors as the second crack is growing from its initial crack length a_2

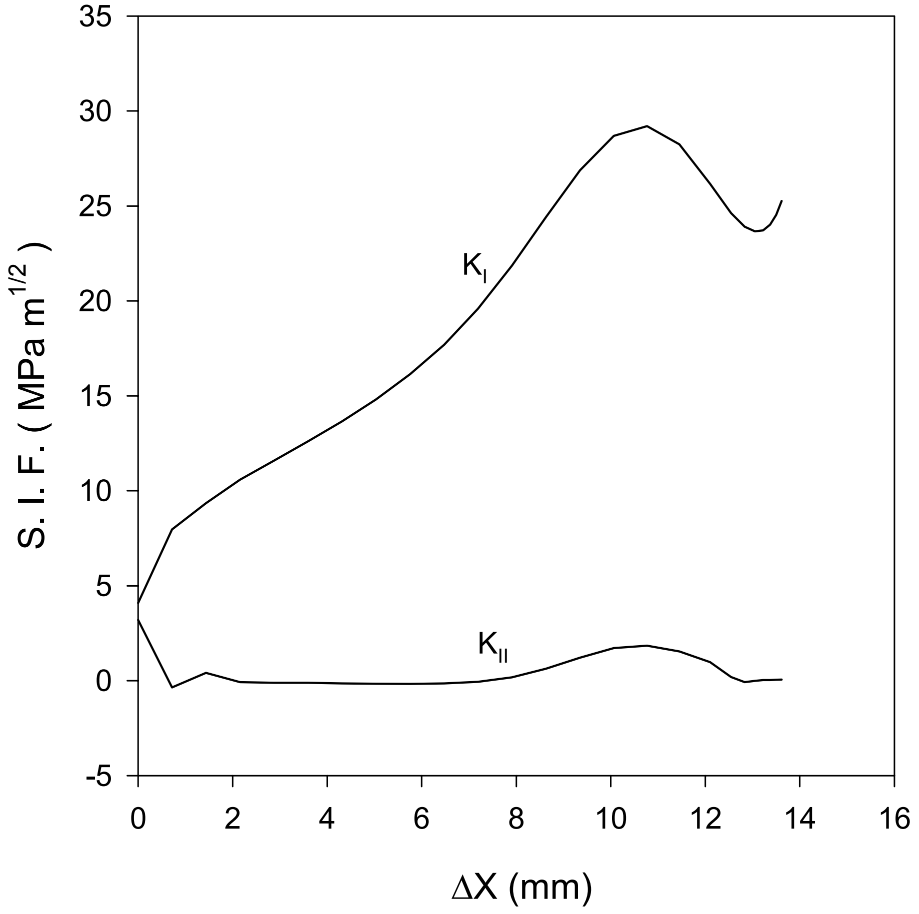

UCI
University of California, Irvine

Fatigue crack growth of an edge crack embedded in a beam with three rivet holes

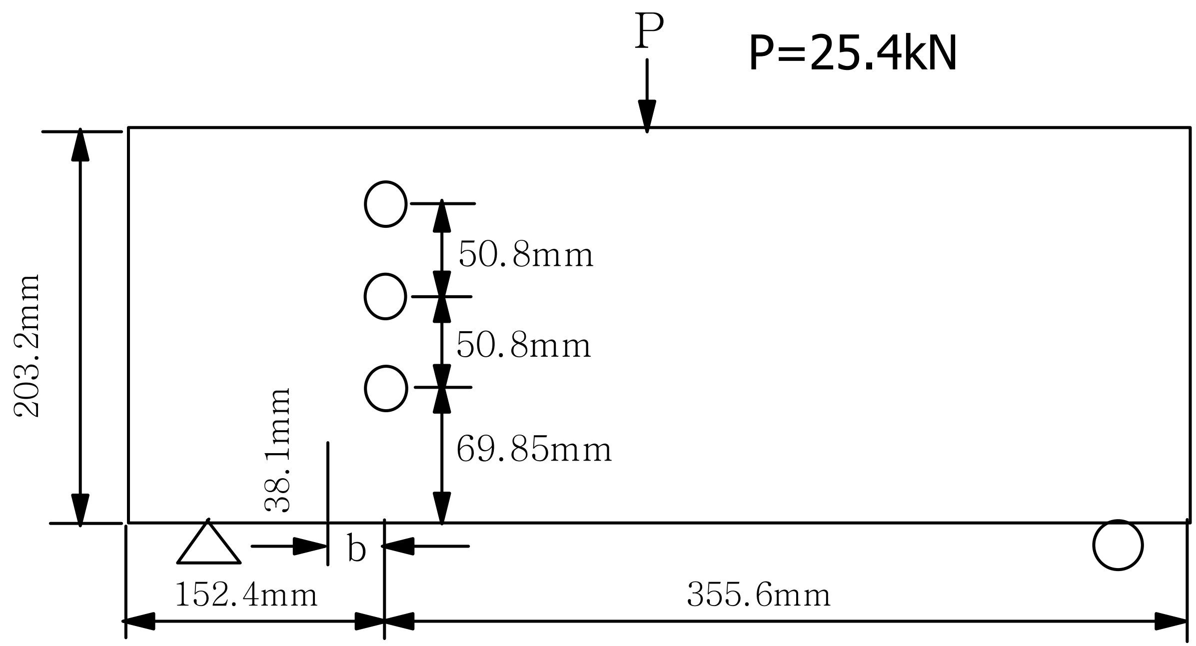

the thickness is 25.4mm

Schematic of cracked beam with rivet holes

PMMA

E=2.76GPa   Poisson's ratio is 0.38

Fatigue crack growth of an edge crack embedded in a beam with three rivet holes

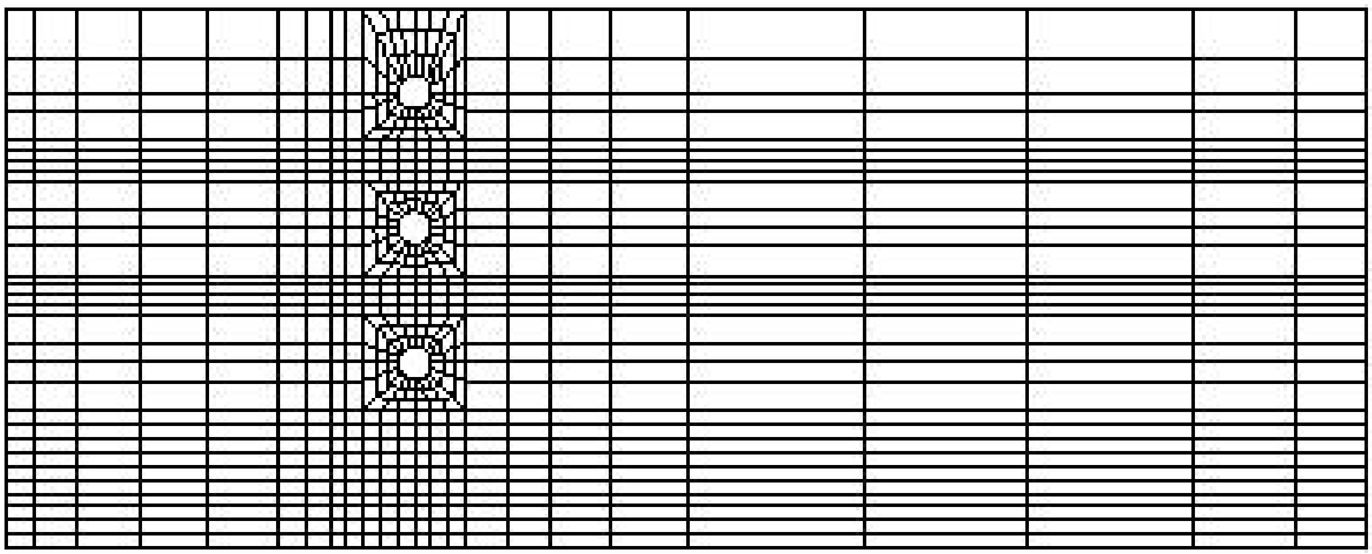

Finite element mesh for beam with rivet holes

Fatigue crack growth of an edge crack embedded in a beam with three rivet holes

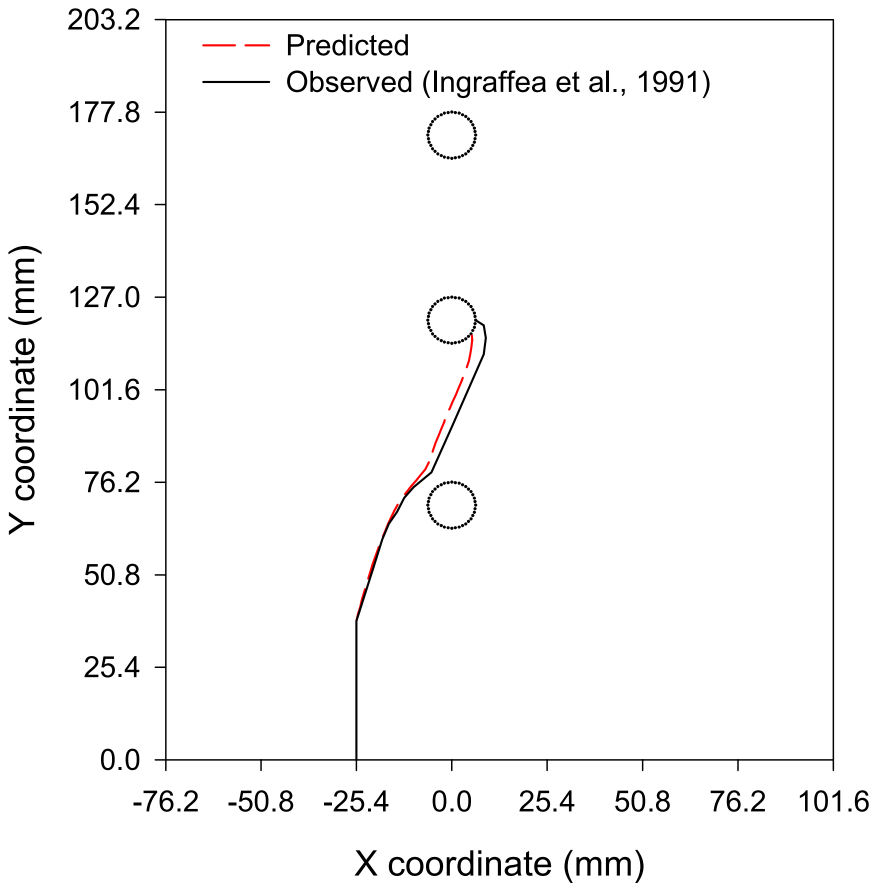

Simulated and experimental crack growth trajectories when b=25.4mm

Crack growth direction is determined by using the maximum principal stress criterion

Fatigue crack growth of an edge crack embedded in a beam with three rivet holes

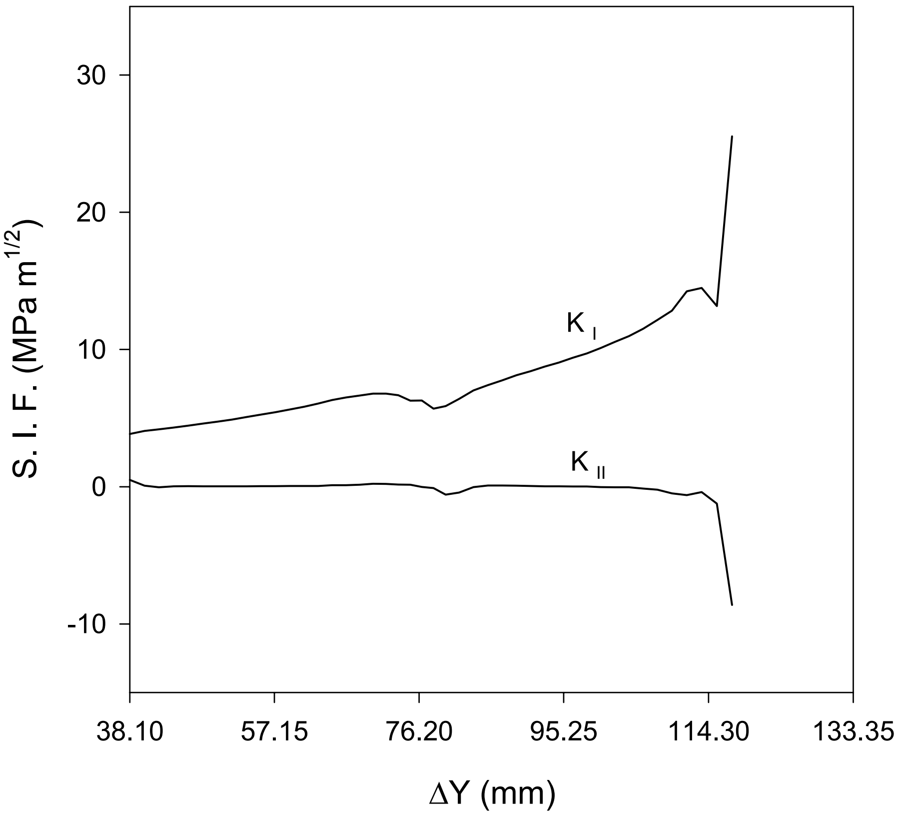

Variation of mode I and mode II stress intensity factors according to the increment of y coordinate of the crack tip when b=25.4mm

Fatigue crack growth of an edge crack embedded in a beam with three rivet holes

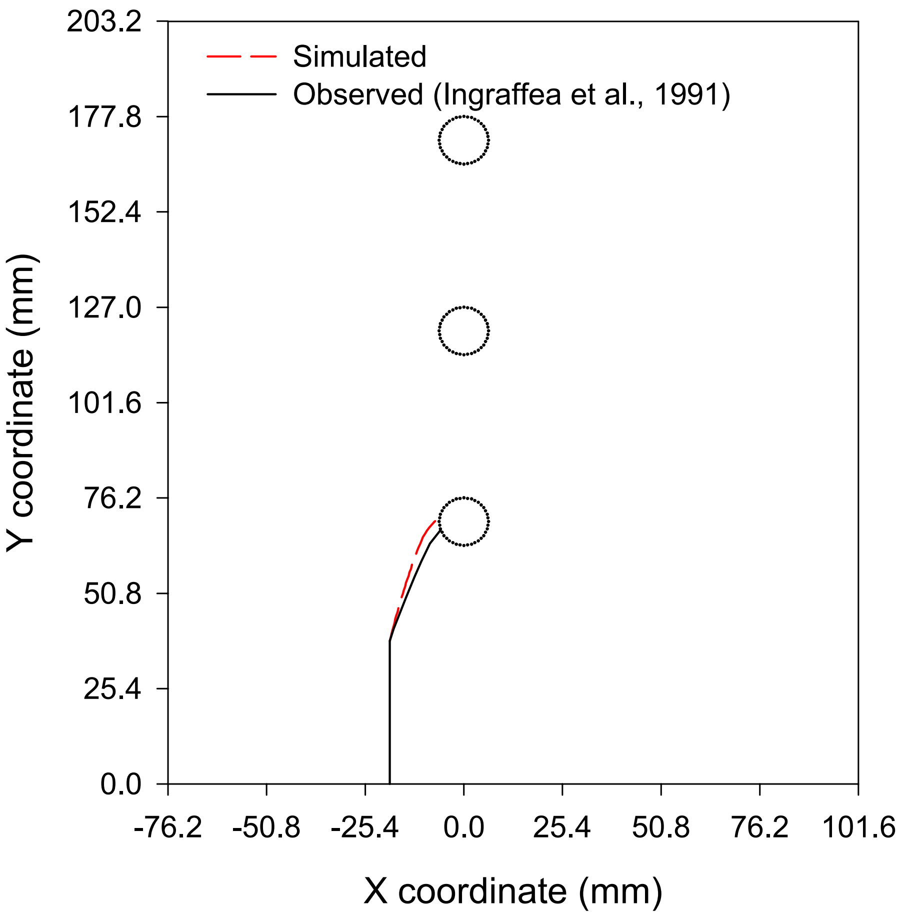

Simulated and experimental crack growth trajectories when b=19.05mm

Fatigue crack growth of an edge crack embedded in a beam with three rivet holes

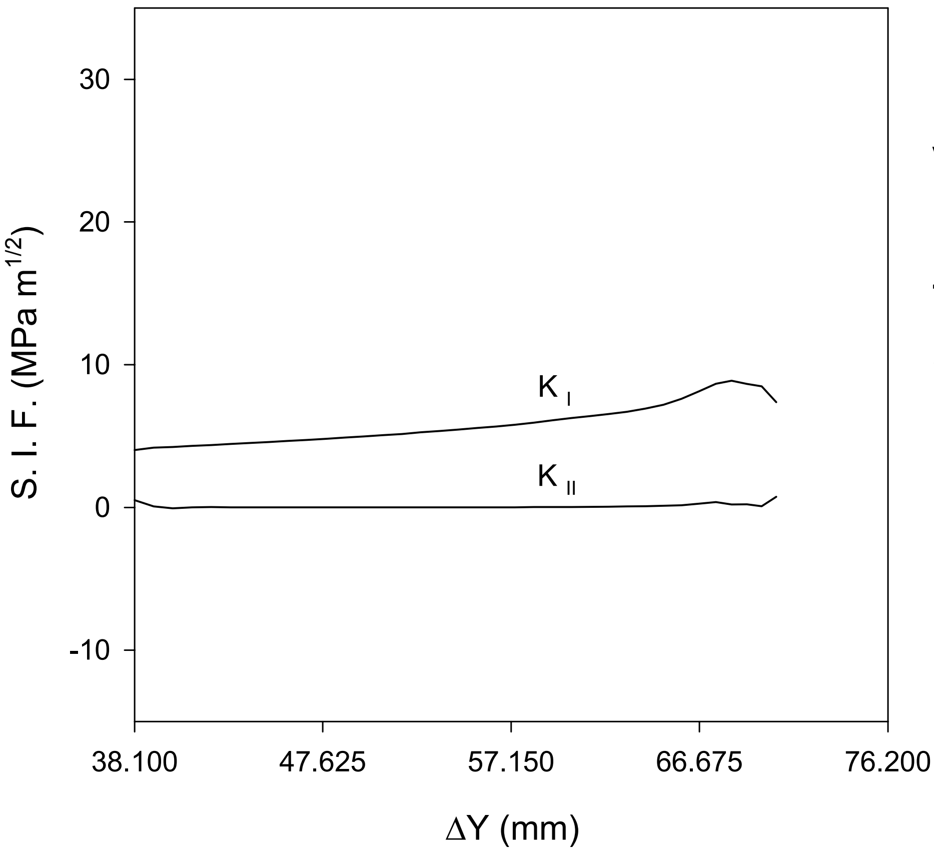

Variation of mode I and mode II stress intensity factors according to the increment in y coordinate of the crack tip when b=19.05mm

Conclusions on the analytical model for shot-peening with 200% coverage

- This theoretical model considers the influence of the main parameters of shot peening: velocity of the shot, diameter of the shot, and the material characteristics;
- This model can be easily extended to 300% or higher coverage;
- This model verifies that the residual stress field will reach a converged state after certain coverage;
- This model is very simple and fast; no additional empirical parameters are introduced.

Test Data

The following experimental data should be provided to UCI

- the residual stress levels, and material parameters;
- specimen types, and sizes;
- the distribution of the residual stresses due to rivet misfit;
- the distribution of the residual stresses due to cold working;
- the distribution of the residual stresses due to shot-peening with 200% coverage (including shot velocity, shot radius).

to validate the analytical models.

Fatigue Test Data

The following experimental data should be provided to UCI

- the residual stress levels, specimen types, crack sizes, and material parameters;
- load spectrum;
- fatigue life curves: $a \sim N$, and $da/dN \sim \Delta K$;
- fatigue crack profiles of the specimens.

for surface cracks subject to residual stresses due to rivet misfit, cold working, or shot-peening, for through thickness cracks at interference fit bushings, and for through thickness cracks at cold worked holes.

Fatigue Crack Growth for Through-thickness Crack

two examples, by considering the variation of the size of the plastic zone along the thickness of the specimen.

On the surface of the specimen, it is plane-stress status, which has large plastic zone. While in the center of the specimen, it is plane-strain, which has small plastic zone, about 1/3 of the size of the plastic zone on the surface. Thus, the crack open stress on the surface is greater than that in the center. Hence, the crack growth rate on the surface is less than that in the center.

Fatigue Crack Growth in Aluminum Three-Point Bend Specimens

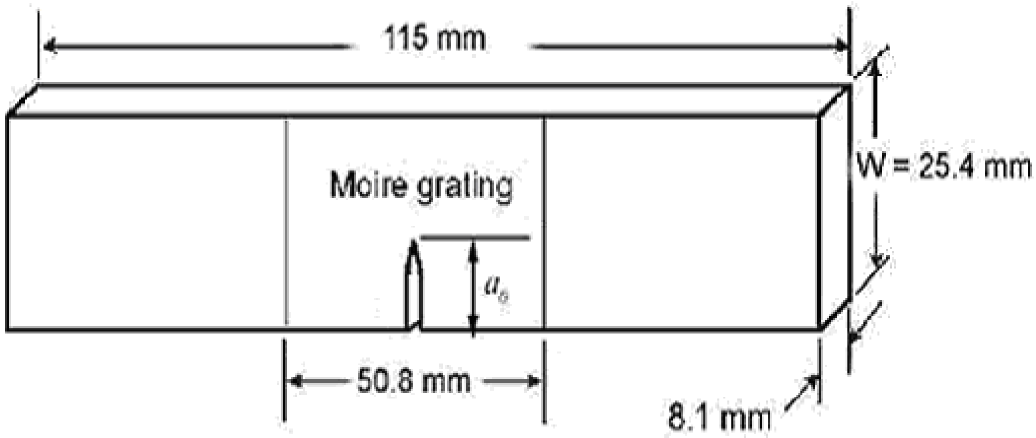

Single Edged Notch Bend (SENB) Specimen

Material 2024-T351 Al, a_0=13mm

Fatigue Crack Growth in Aluminum Three-Point Bend Specimens

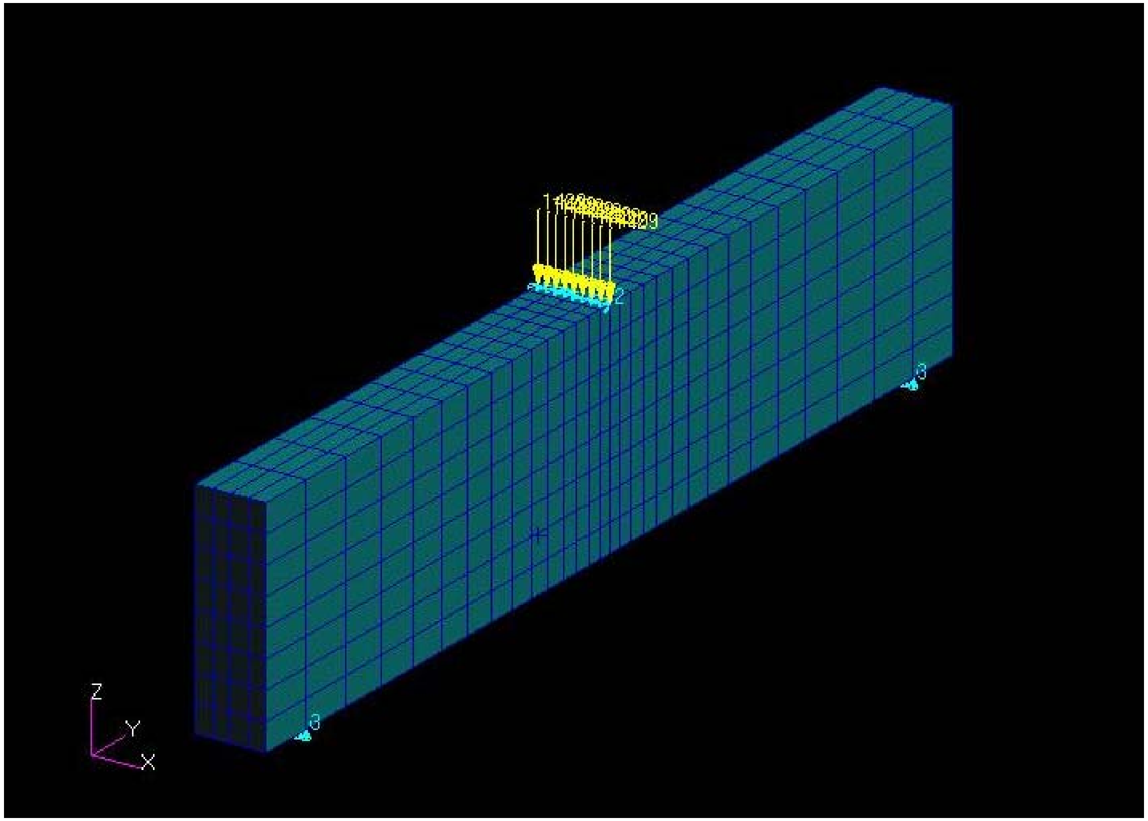

Global FEM model, 960 elements (Hexahedral 20)

Fatigue Crack Growth in Aluminum Three-Point Bend Specimens

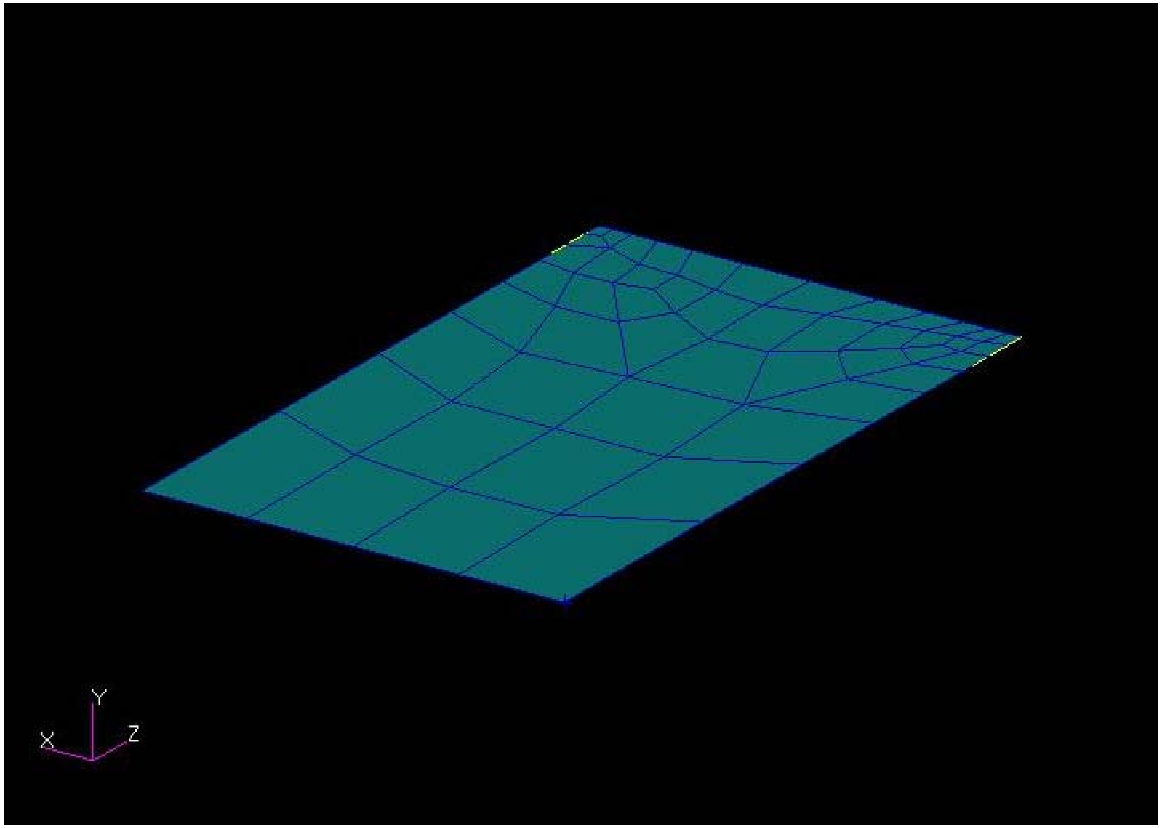

BEM model in the crack plane,
12 Elements along crack front (Quadrangular 8)

Fatigue Crack Growth in Aluminum Three-Point Bend Specimens

Test A2			
P_{max} (kN)	P_{min} (kN)	Cycles	
1.725	0.173	4963	
Top		Bottom	
X (mm)	Y (mm)	X (mm)	Y (mm)
0.84	0.09	0.51	0.27
2.10	2.10	2.05	2.10
2.10	4.20	2.05	4.20
2.10	6.30	2.15	6.30
1.45	8.08	0.62	8.01

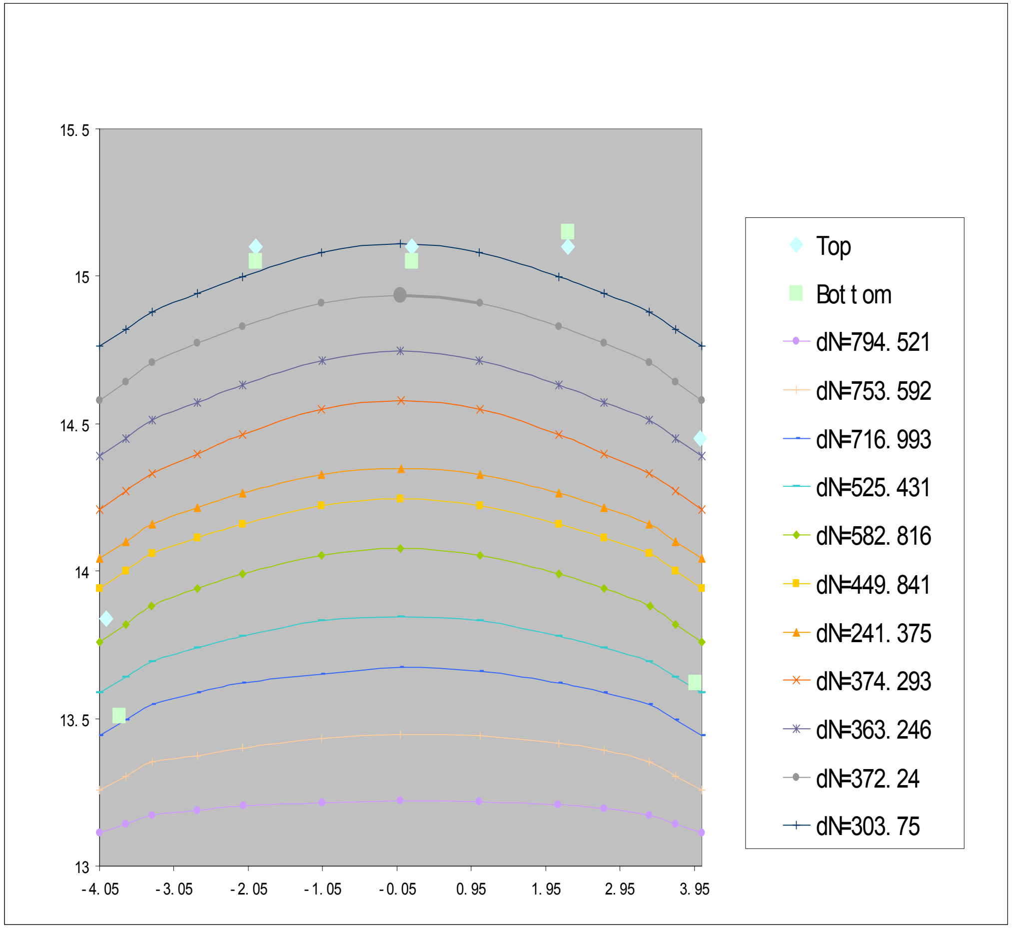

A2

Numerical N = 5480

Experimental N = 4963

FATIGUE CRACK GROWTH IN ALUMINUM double-edged crack (UW Test Data)

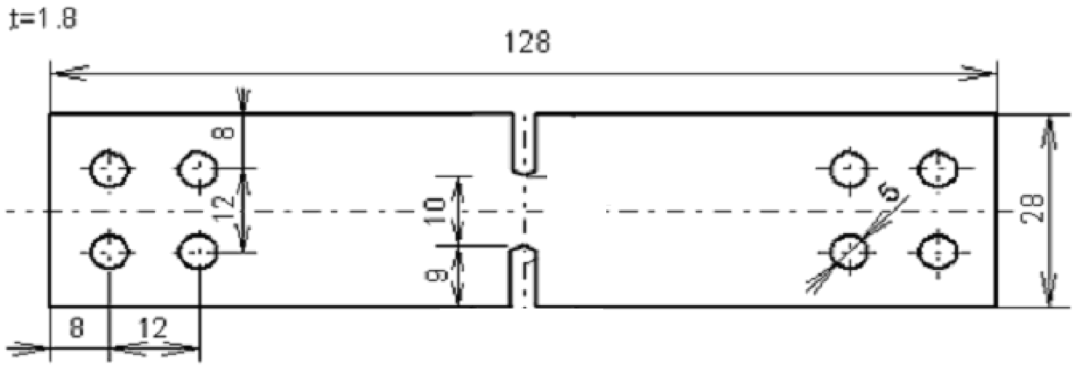

Tension, 400lb, Material 7075-T7351 Al

Shot Peening

Intensity 0.017, shot size 230-280, coverage 100%

Distribution of the residual stress due to shot-peeing

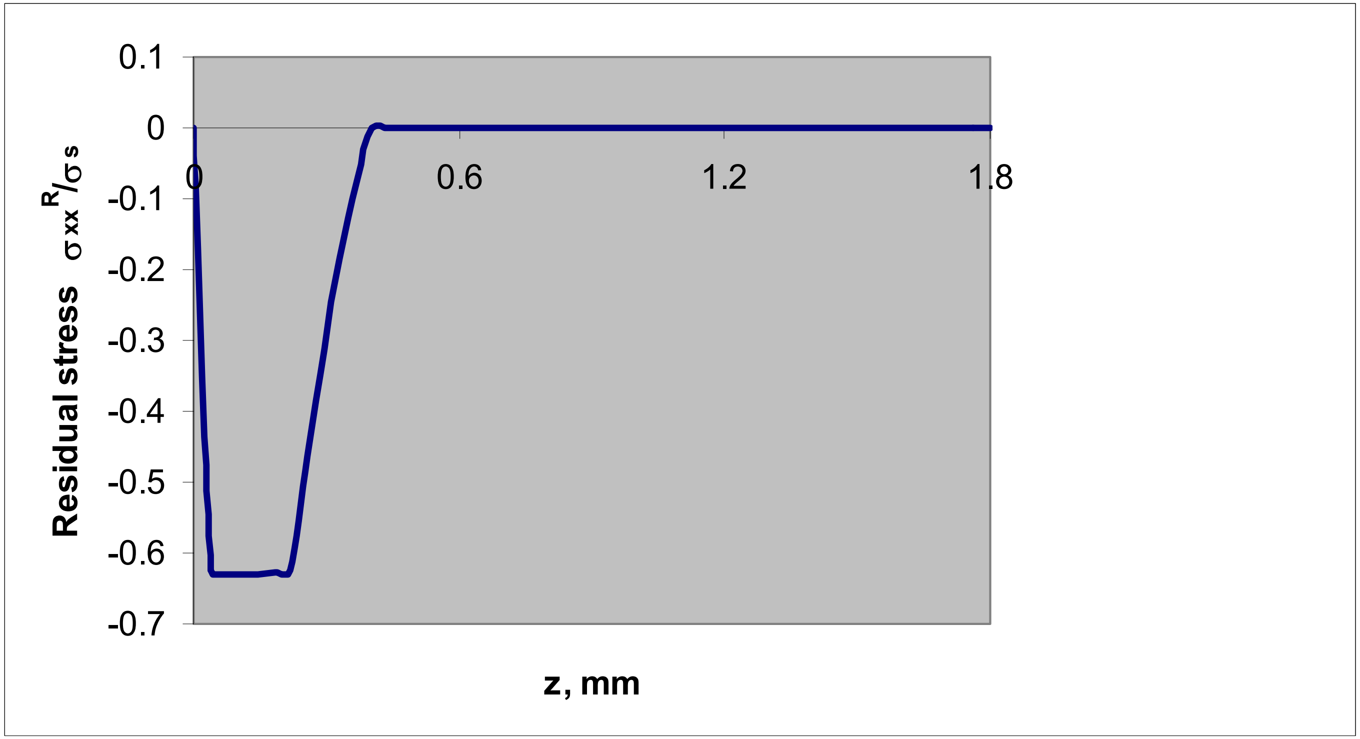

Shot Peening

Intensity 0.017, shot size 230-280, coverage 1.0

FATIGUE CRACK GROWTH IN ALUMINUM
double-edged crack

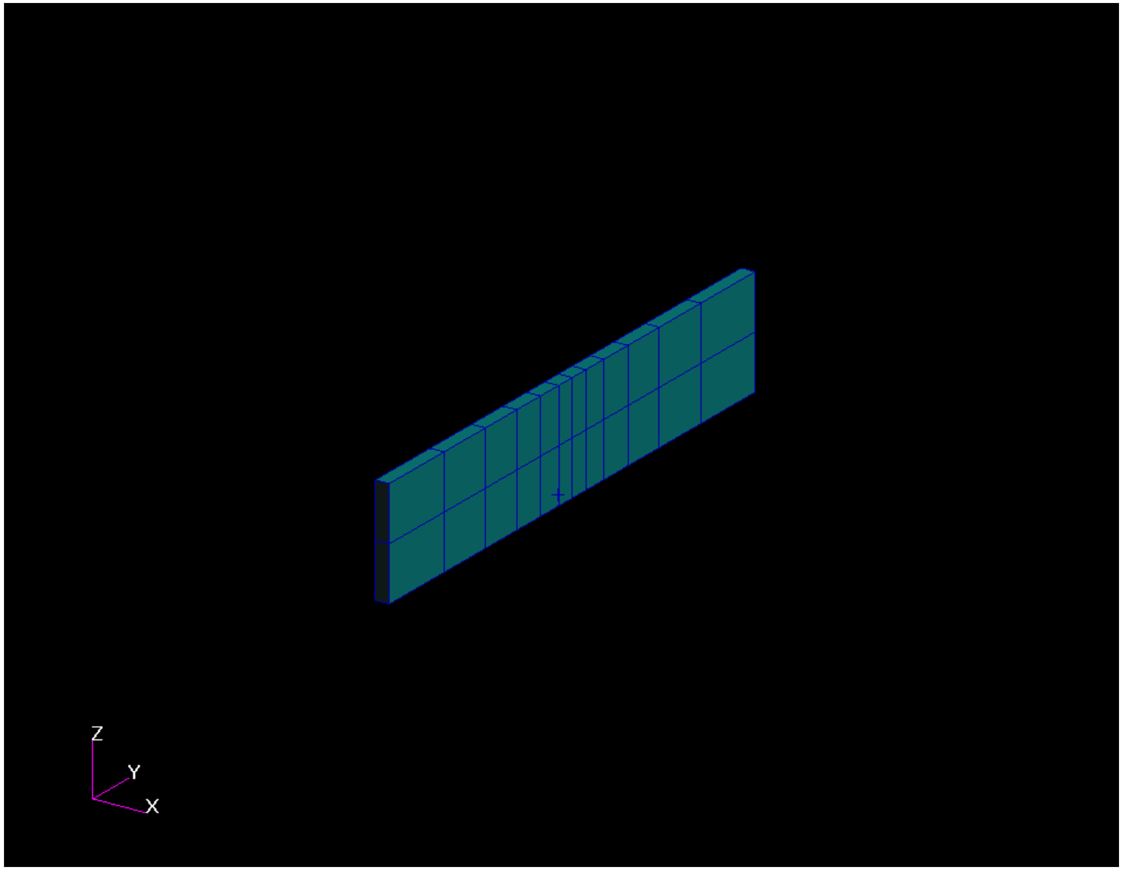

Global FEM model, 24 elements (Hexahedral 20)

FATIGUE CRACK GROWTH IN ALUMINUM
double-edged crack

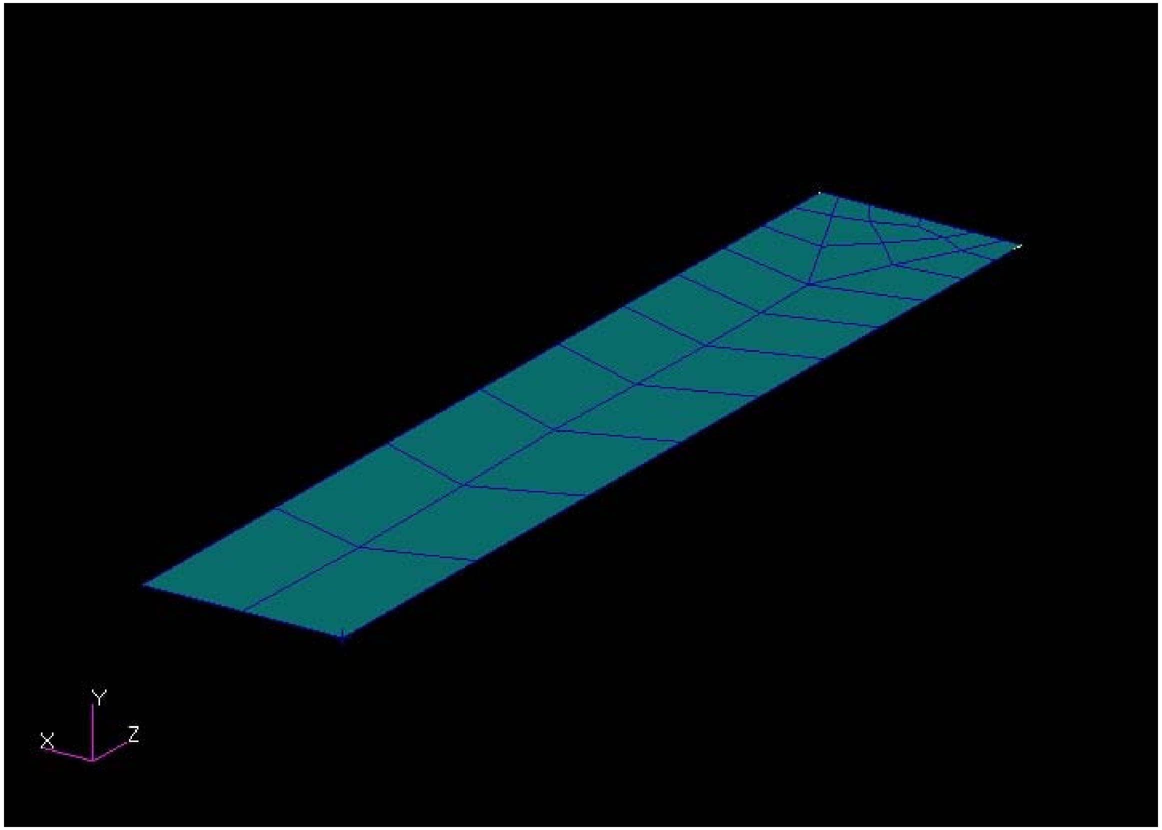

BEM model in the crack plane,
6 Elements along crack front (Quadrangular 8)

UCI
University of California, Irvine

Crack Profiles

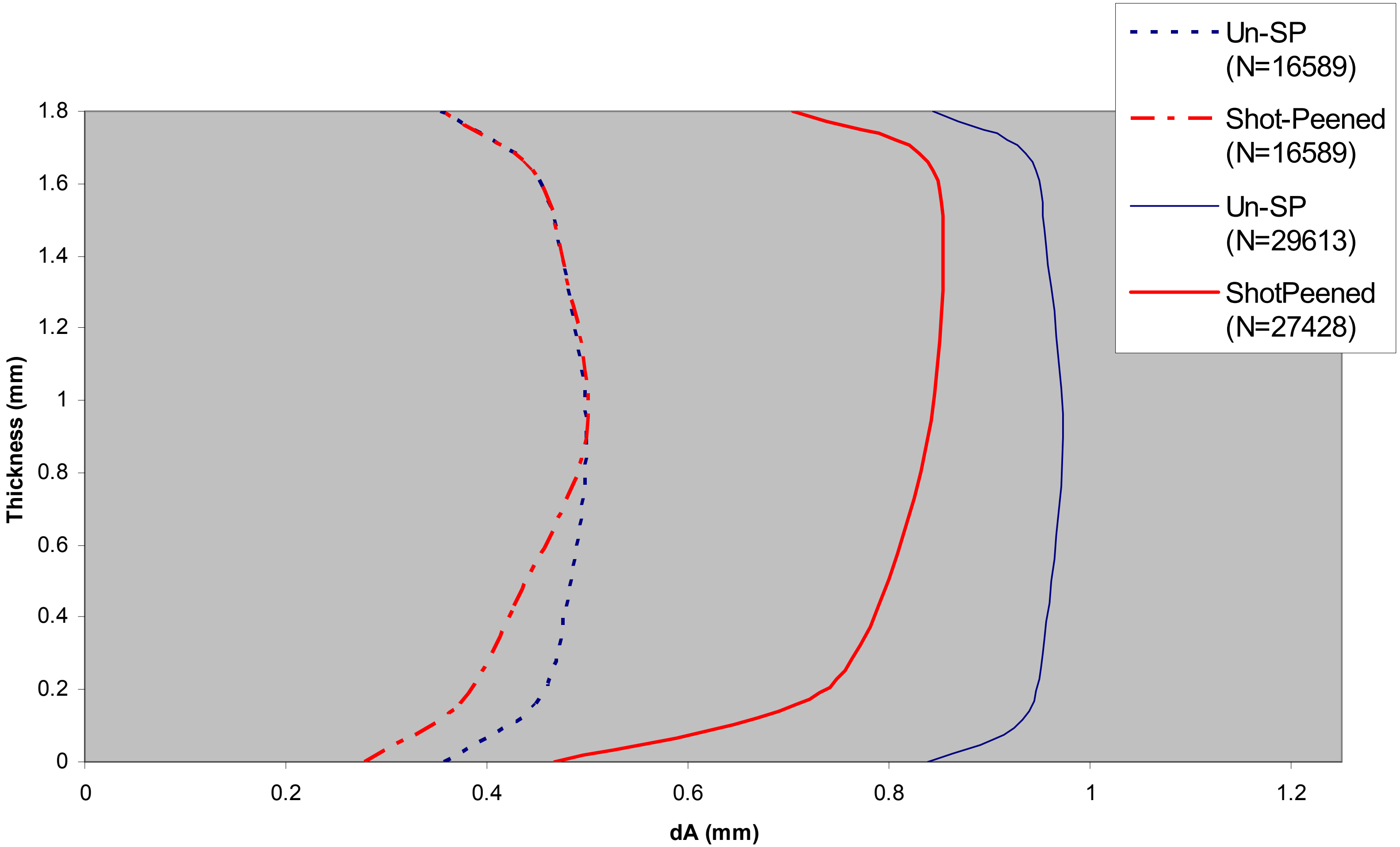

Numerical results

UCI
University of California, Irvine

The Effect of the Shot-Peening

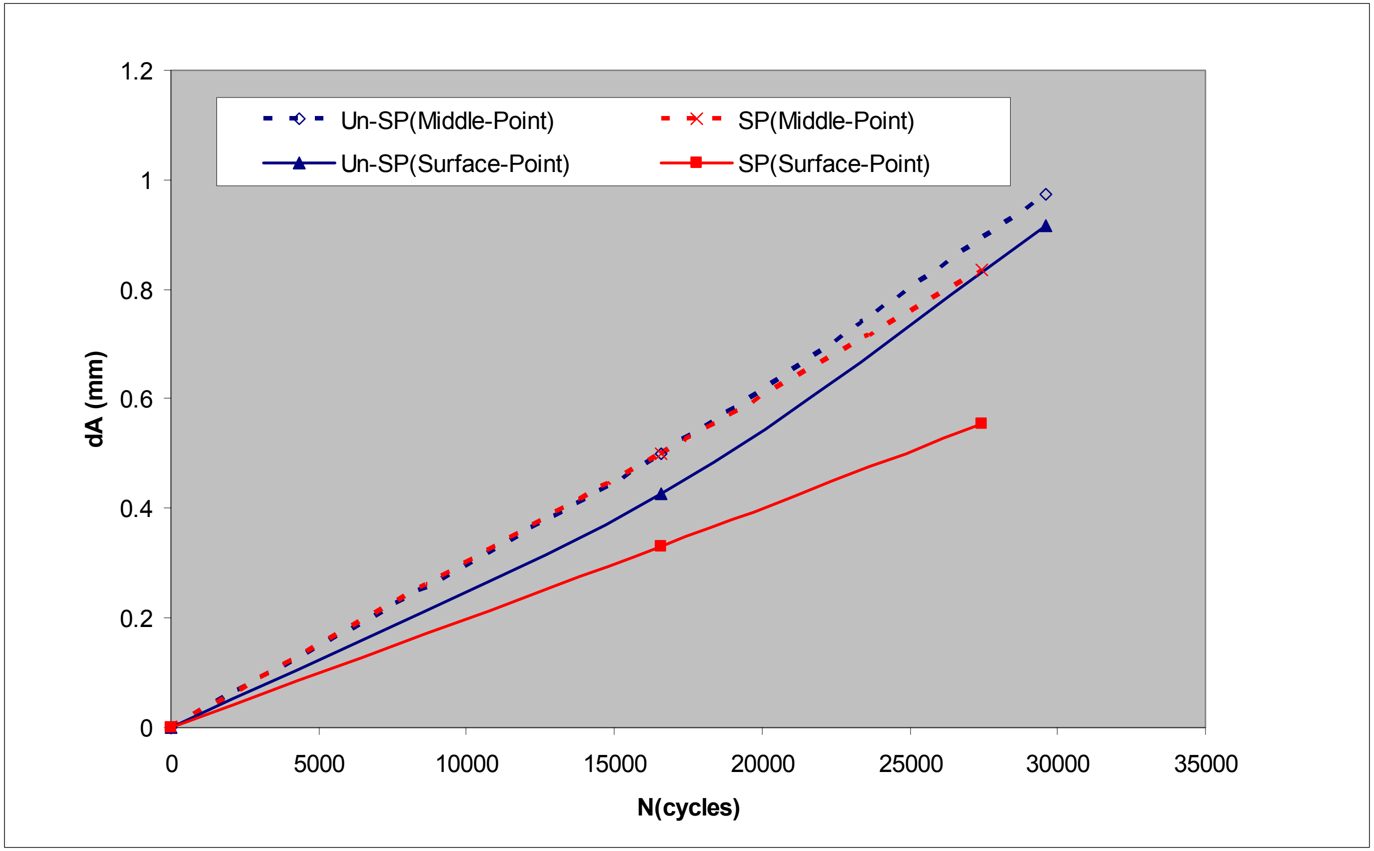

Numerical results

Plastic Zone model

Fatigue crack growth rate

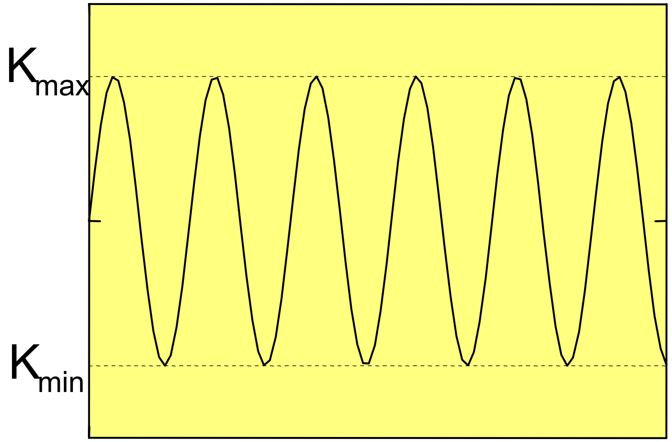

$$\frac{da}{dn} = C(\Delta K_{eff})^n$$

$$\Delta K = K_{\max} - K_{\min}$$

$$R = \frac{K_{\min}}{K_{\max}}$$

$$\Delta K_{eff} = K_{max} - K_{op}$$

$$\Delta K_{eff} = (1 - f)K_{max}$$

Plastic Zone model

2024-T3 AL

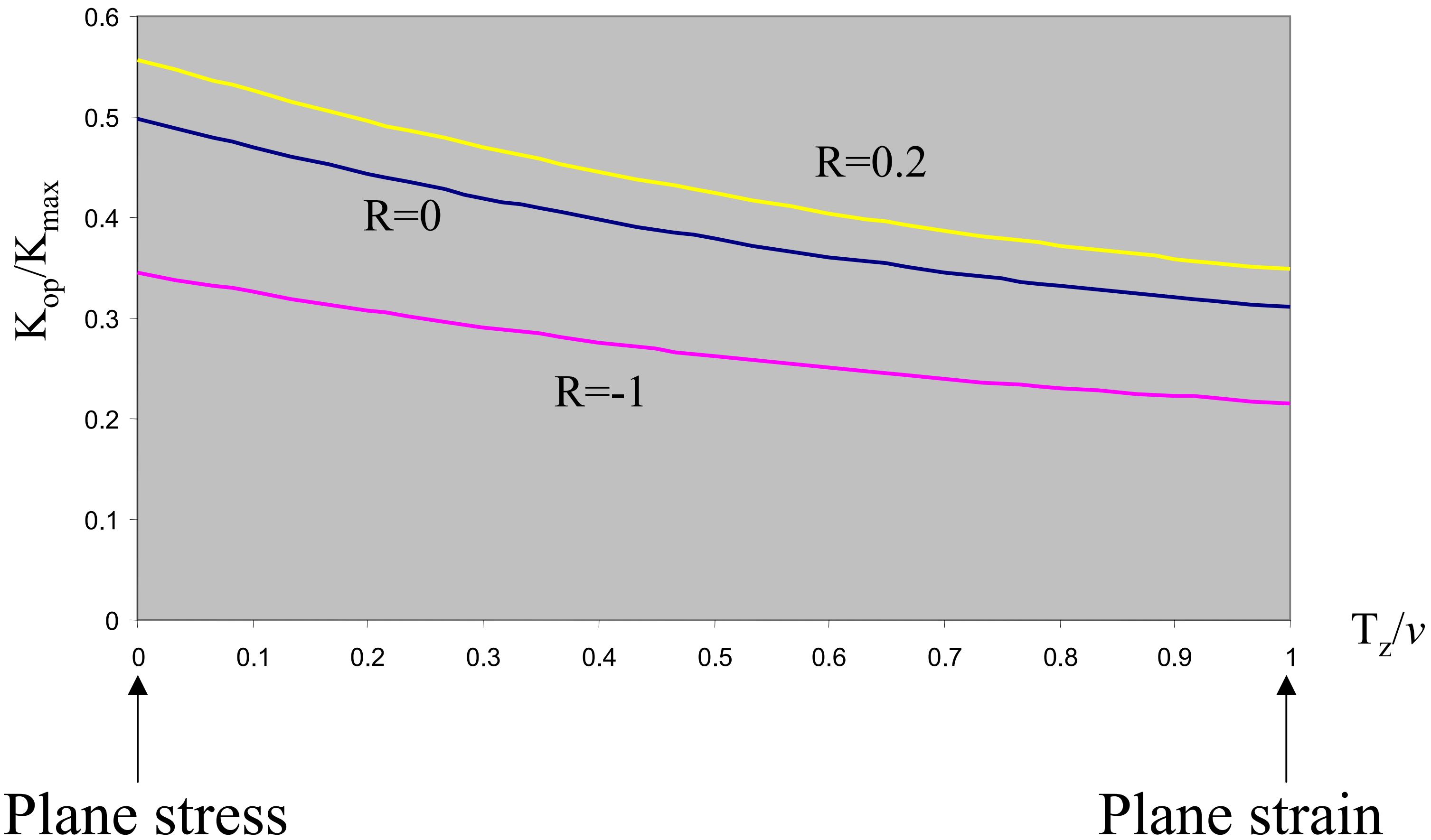

The crack propagation rate of the plane stress is less than that of the plan strain

UCI
University of California, Irvine

Plastic Zone model

Plane stress

2024-T3 AL

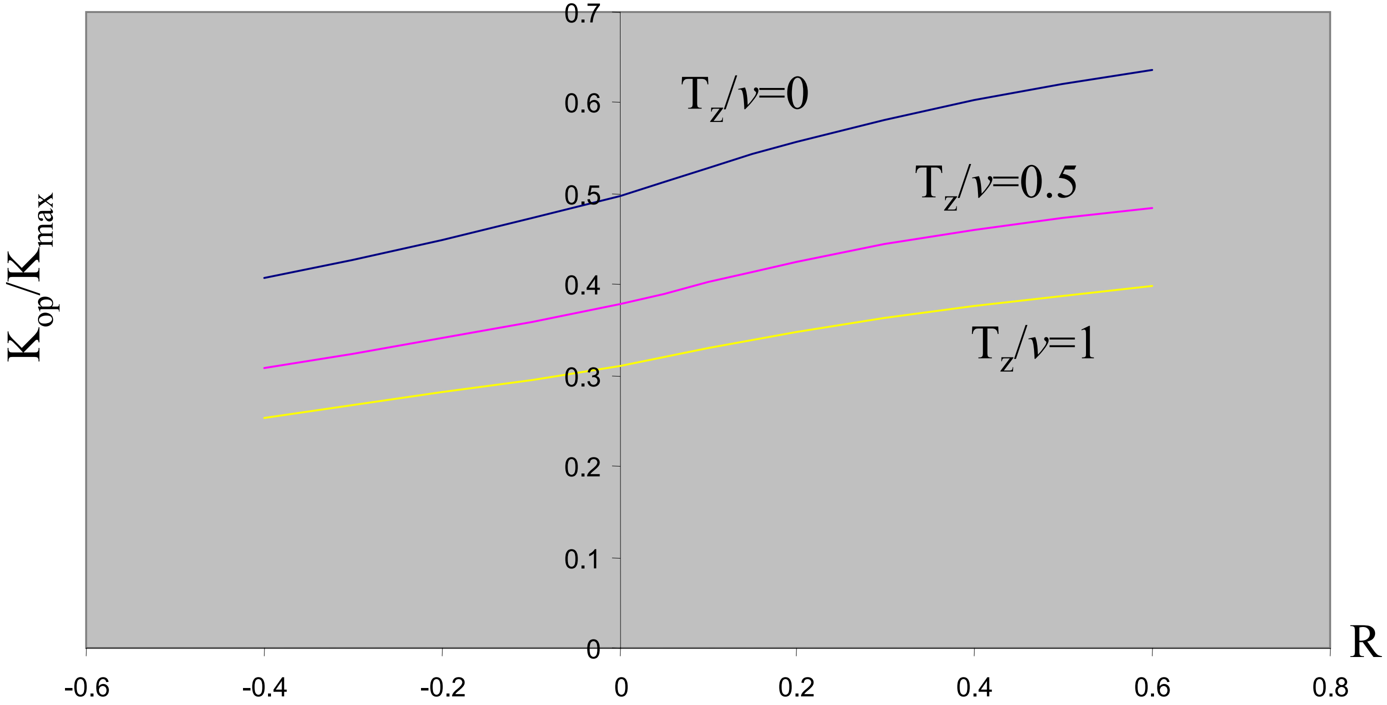

The variation of the crack opening SIF with ratio R under different 3D constraints

Plane strain

Plastic Zone model

2024-T3 AL

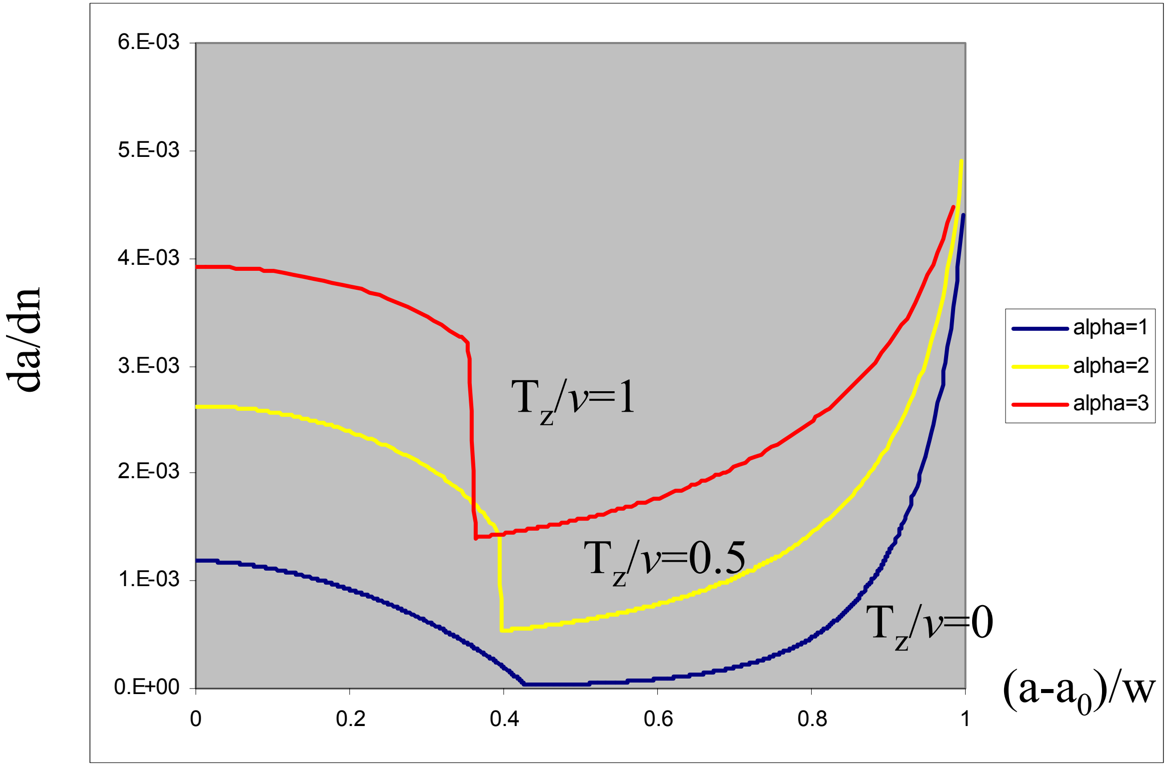

K_{1max}=869.63 MPa mm$^{1/2}$

R_m=1.5
R_1=-0.5
R=0

C=2.383E-11
n=3.2

5,219 cycles
383 cycles
126 cycles

The crack propagation rate, following an overload, under different 3D constraints

Plastic Zone model

2024-T3 AL

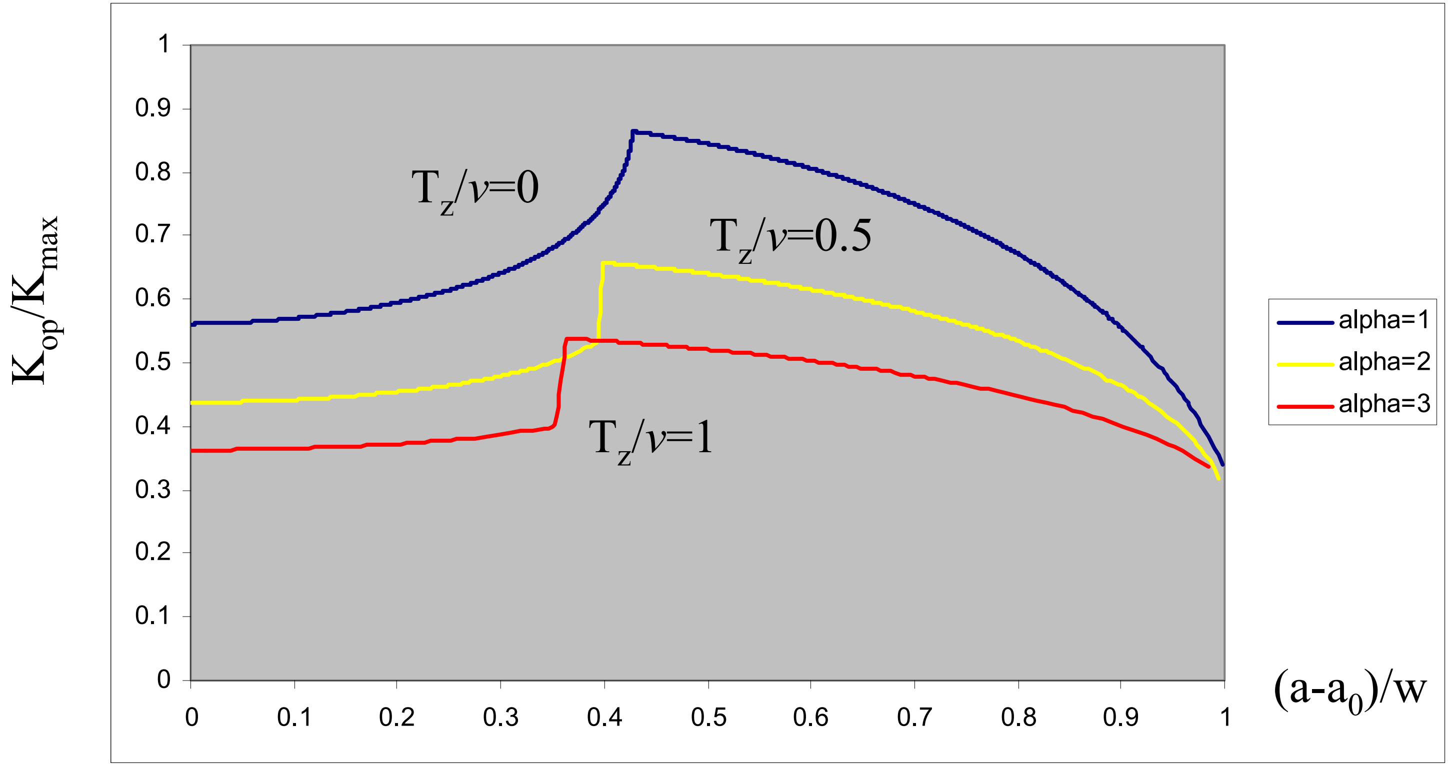

The crack opening SIF following an overload, under different 3D constraints

Plastic Zone model

2024-T3 AL

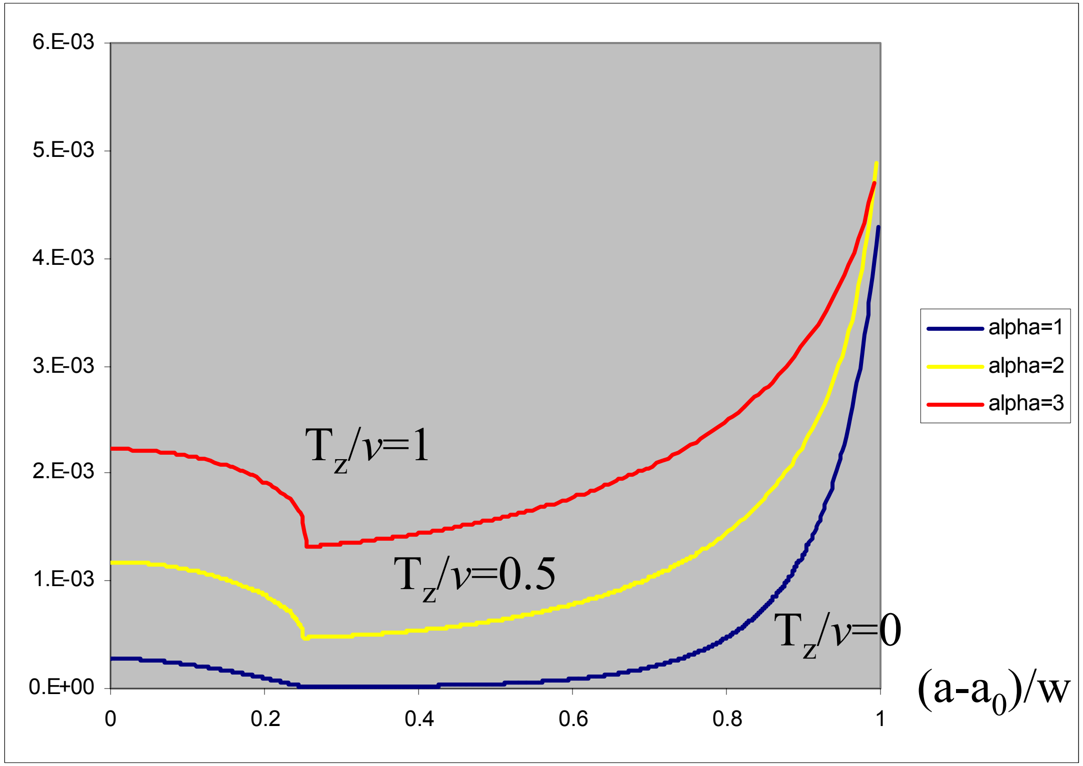

$K_{1max}=869.63$ MPa mm$^{1/2}$

$R_m=1.5$
$R_1=0$
$R=0$

$C=2.383E-11$
$n=3.2$

14,185 cycles
566 cycles
159 cycles

The crack propagation rate following an overload, under different 3D constraints

UCI
University of California, Irvine

Plastic Zone model

2024-T3 AL

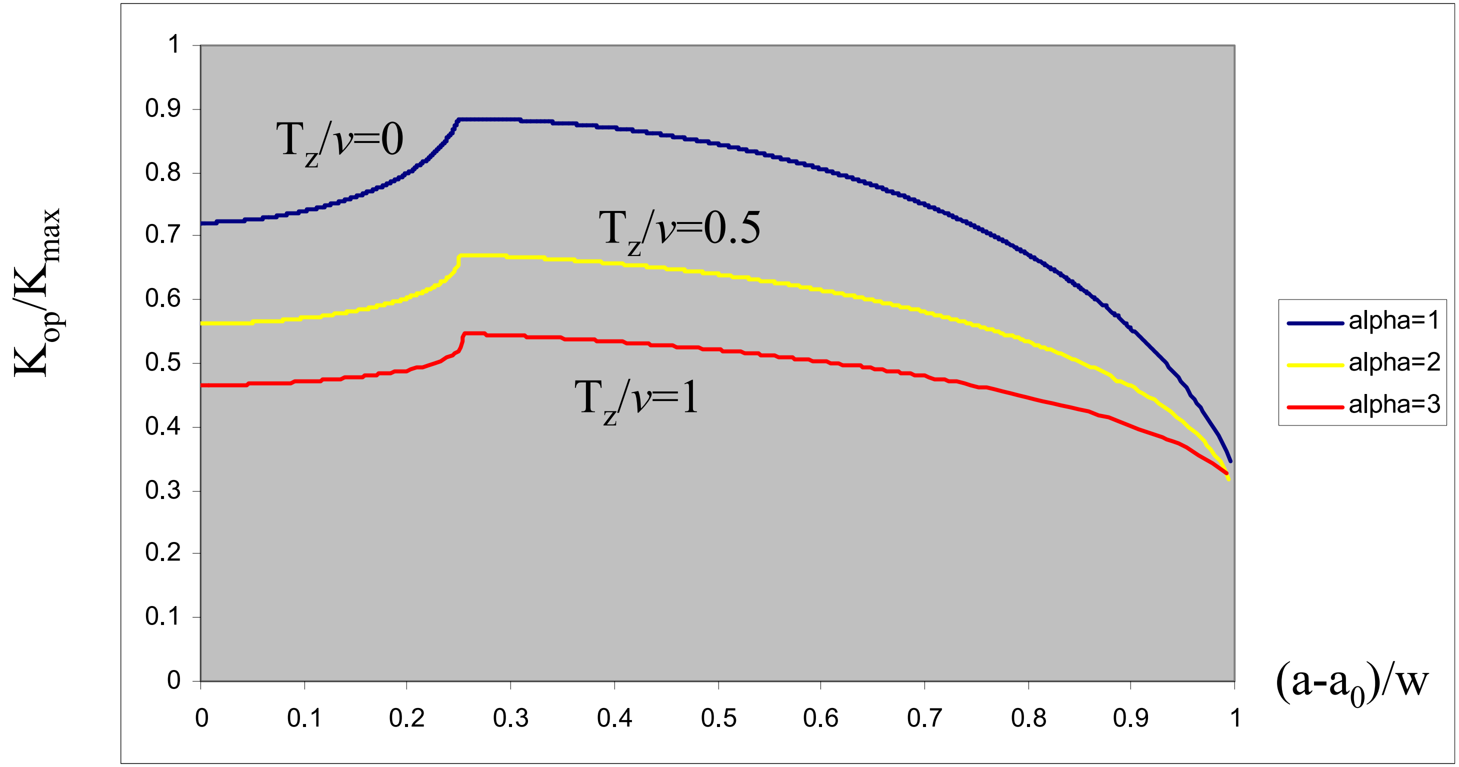

The crack opening SIF following an overload, under different 3D constraints

Plastic Zone model

2024-T3 AL

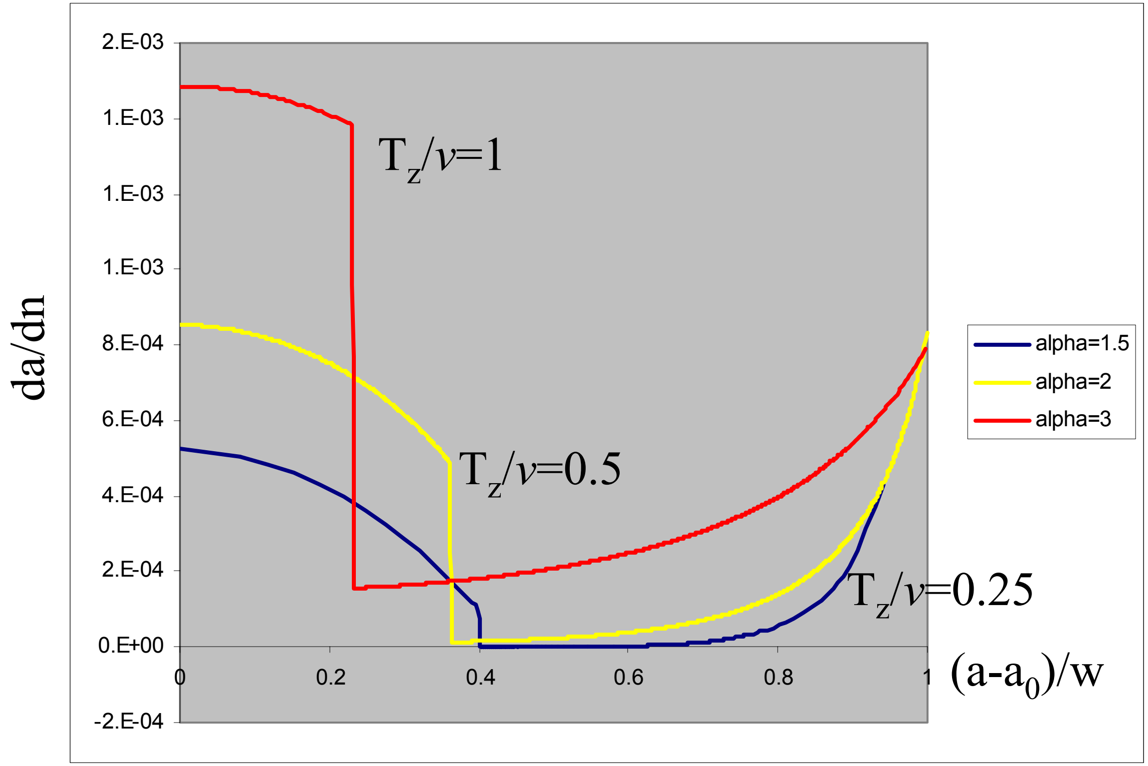

K_{1max}=869.63 MPa mm$^{1/2}$

R_m=1.8
R_1=-0.5
R=0.396

C=2.383E-11
n=3.2

1,923,201 cycles
7,489 cycles
879 cycles

The crack propagation rate following an overload under different 3D constraints

UCI
University of California, Irvine

Plastic Zone model

2024-T3 AL

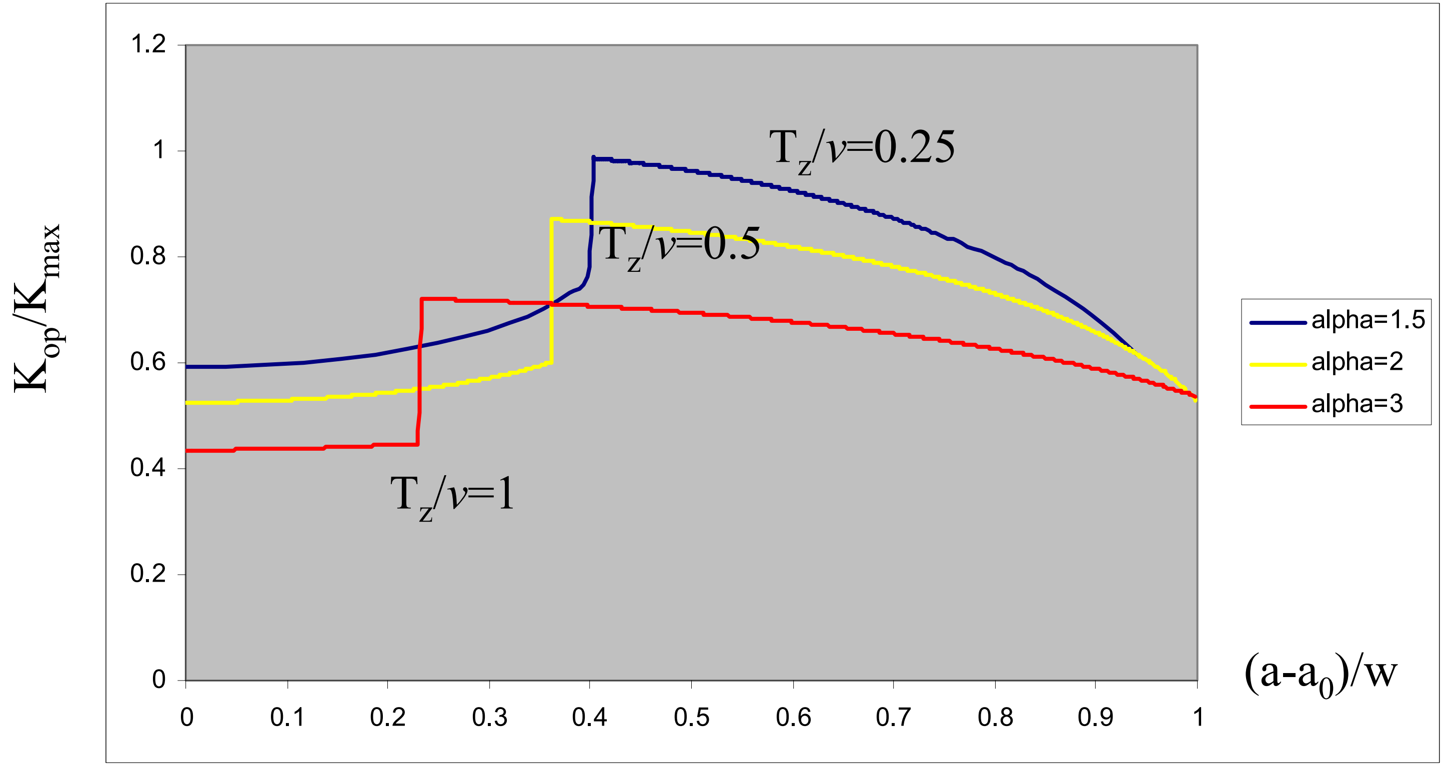

The crack opening SIF following an overload, under different 3D constraints

Plate with a center crack

2024-T3 AL

Maximum stress (S_{max})	68.94 MPa
Minimum stress (S_{min})	1.38 MPa
Stress ratio	0.02
Stress ratio of the overload	0
C	2.382 e-11
n	3.2
Yield Strength	365.42 MPa
Overload ratio (R_m)	1.5, 1.75
Initial crack length($2a_o$)	25.4 mm

Plate with a center crack

Overload spectra

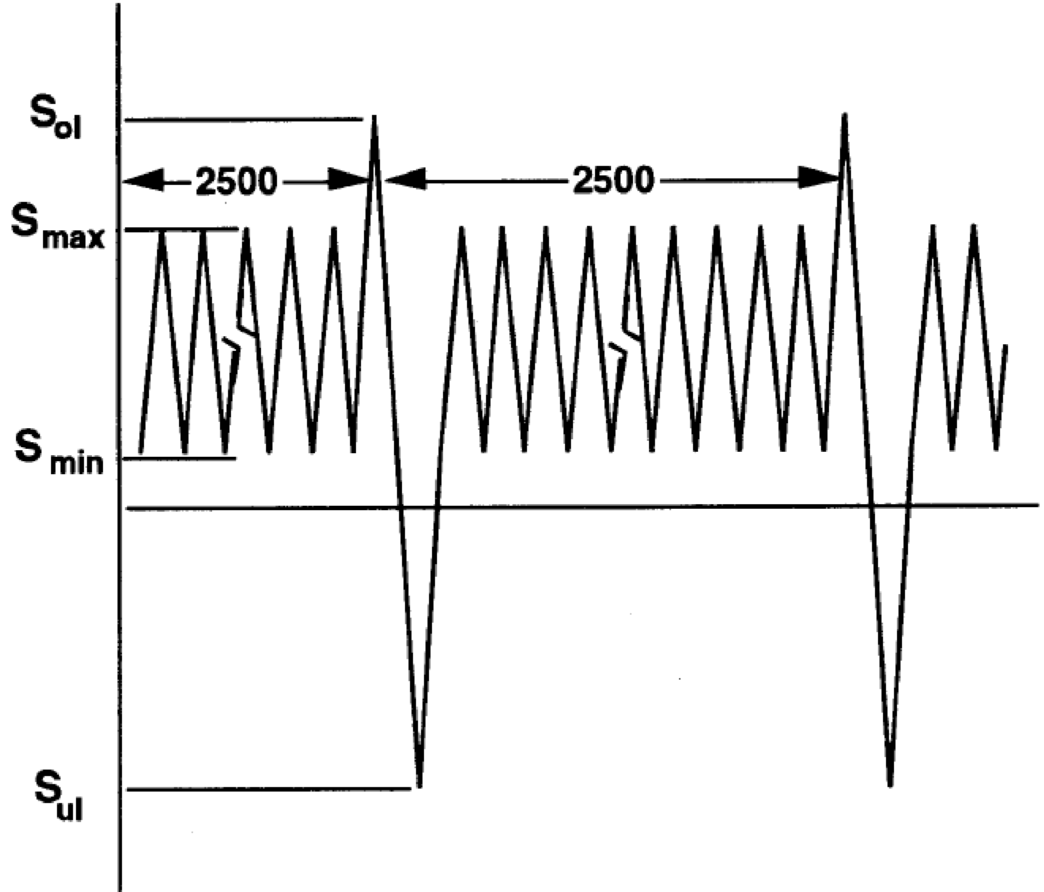

the overload repeats at every 2500 constant amplitude load cycles

The stress ratio of the overload $Ro=S_{ul}/S_{ol}$

Plate with a center crack

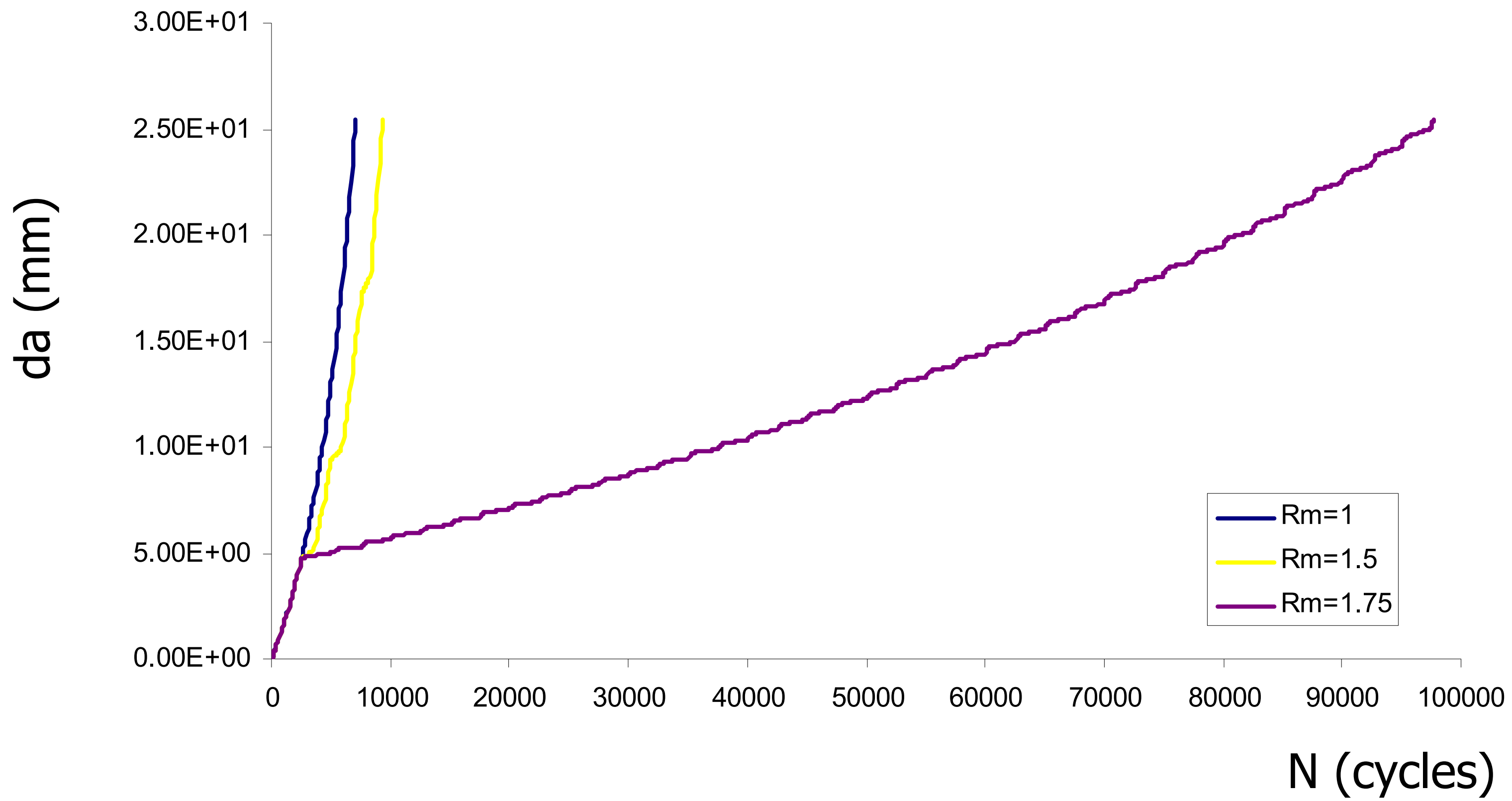

Plane stress, Tz/v=0

7,068 cycles
9,351 cycles
97,761 cycles

UCI
University of California, Irvine

Plate with a center crack

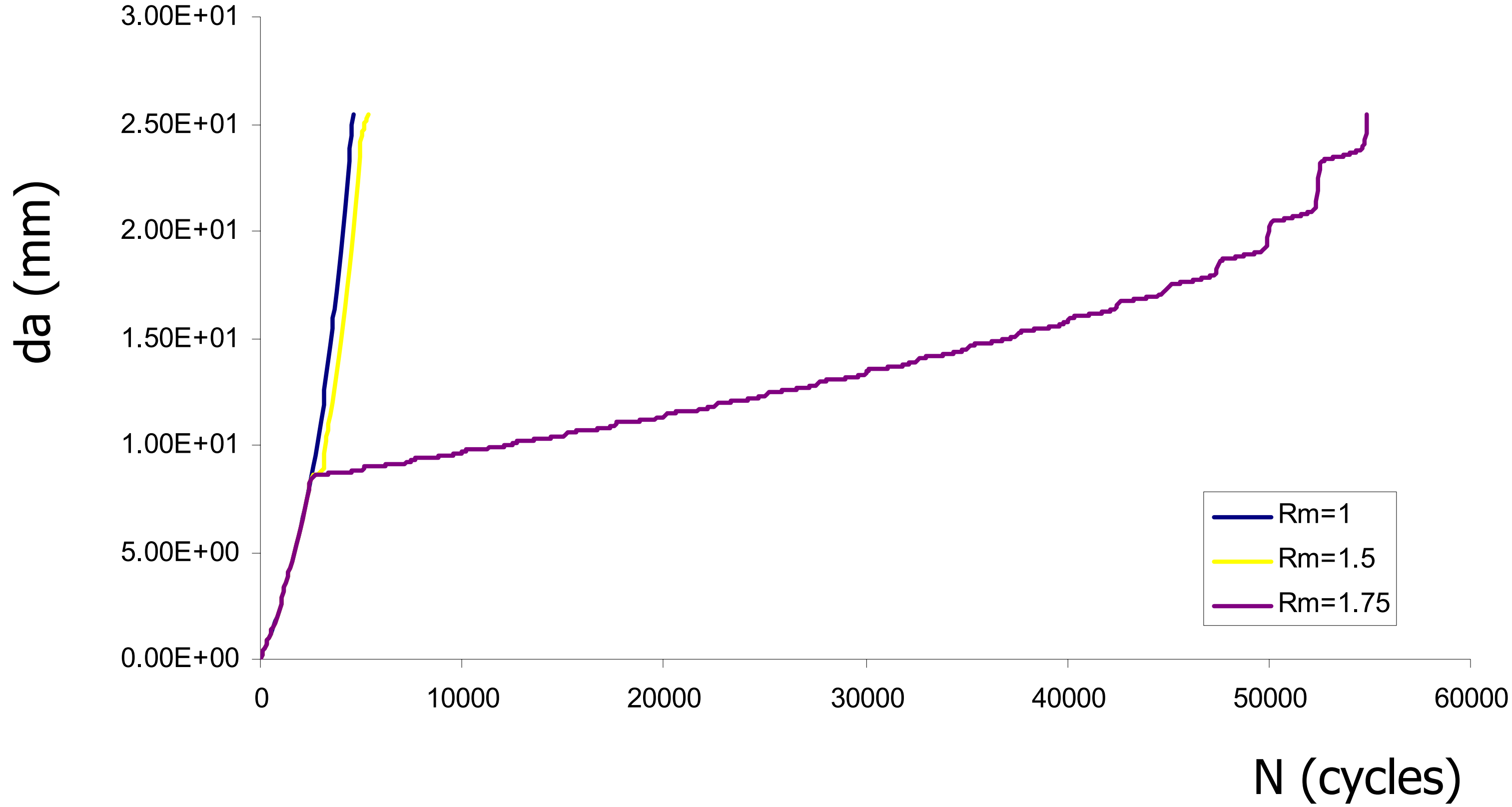

4,573 cycles
5,394 cycles
54,820 cycles

Tz/v=0.5

UCI
University of California, Irvine

Plate with a center crack

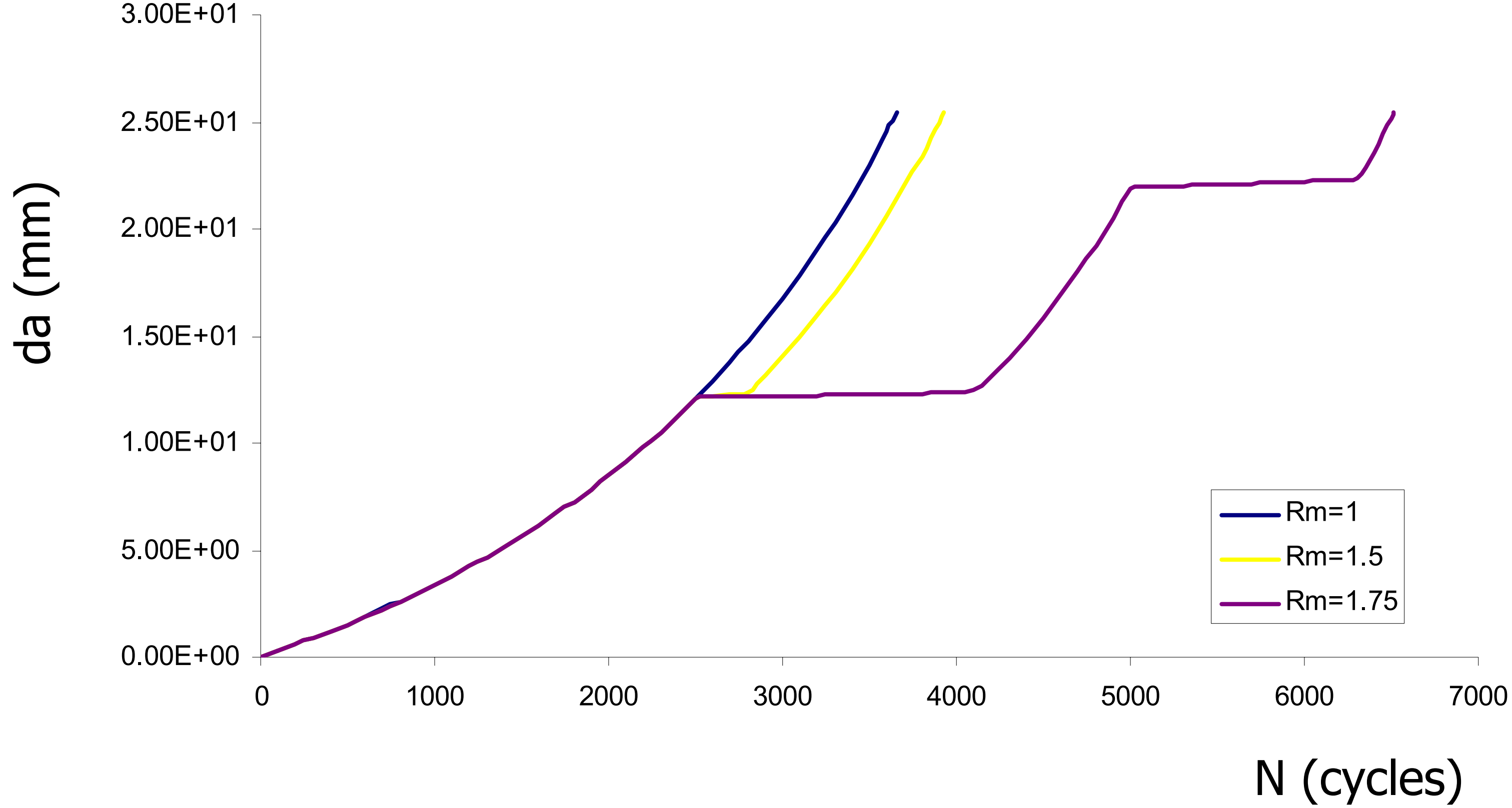

3,657 cycles
3,929 cycles
6,517 cycles

Plane strain, Tz/v=1

UCI
University of California, Irvine

Plate with a center crack

The effect of the stress status

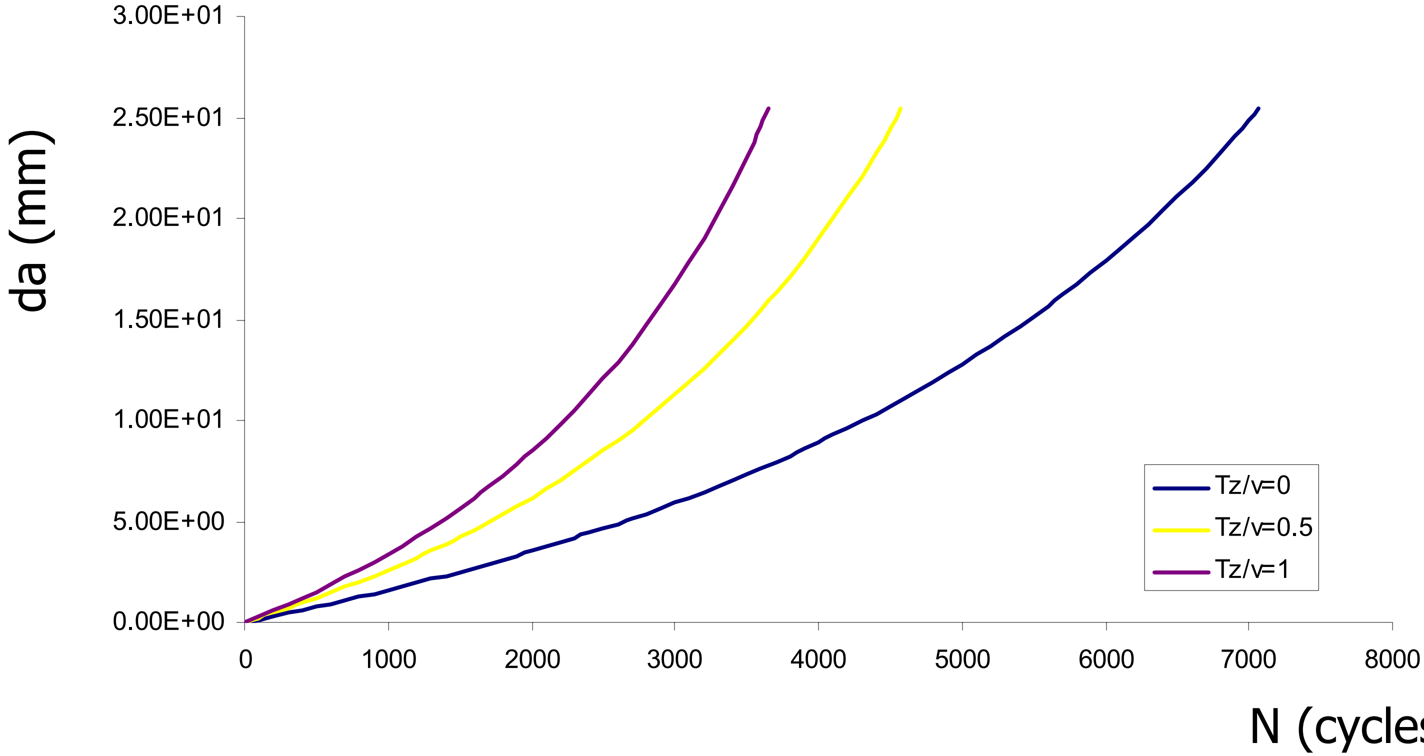

7,068 cycles
4,573 cycles
3,657 cycles

Constant amplitude load, Rm=1

UCI
University of California, Irvine

Plate with a center crack

The effect of the stress status

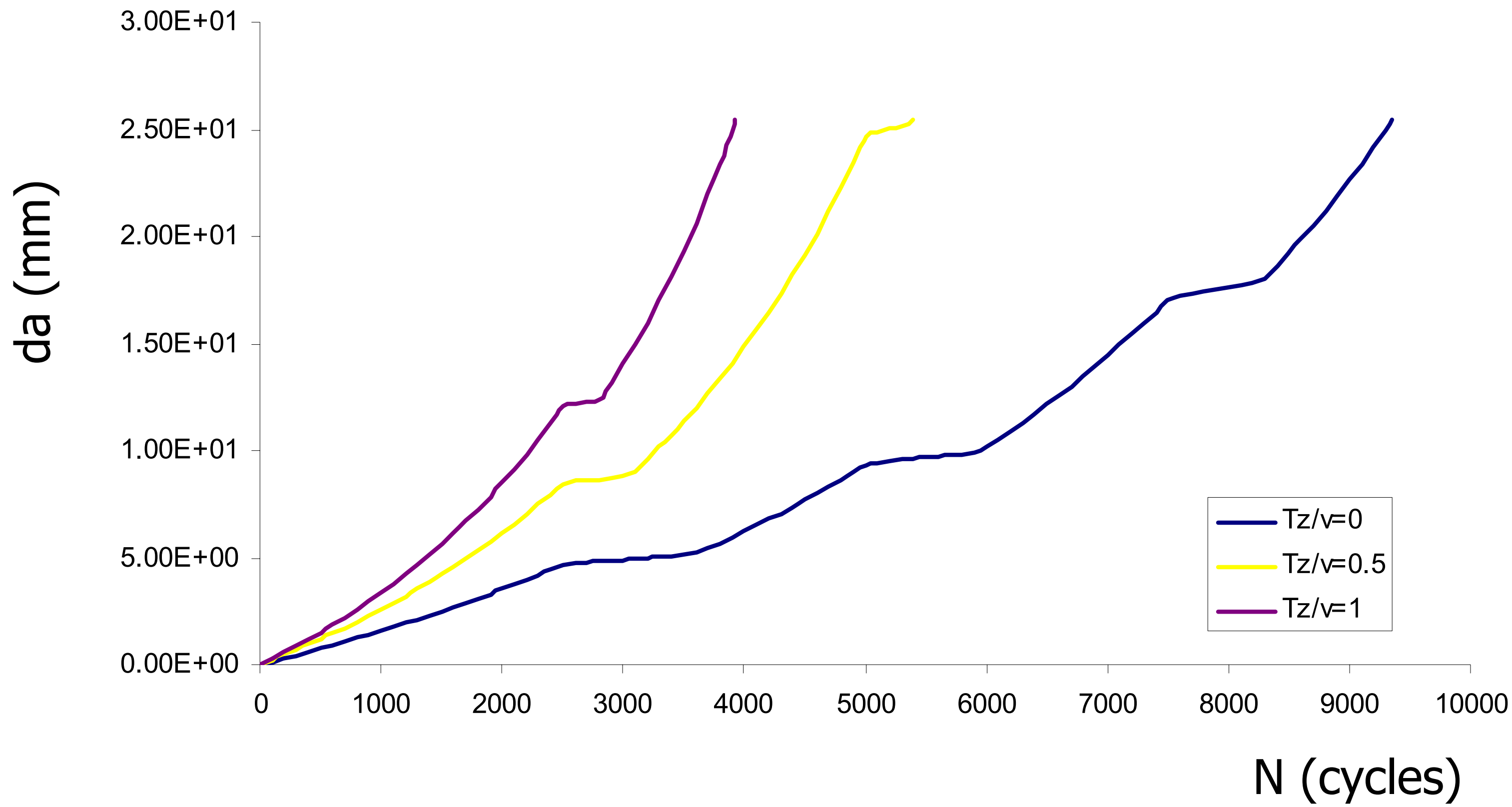

Overload spectrum, Rm=1.5

9,351 cycles
5,394 cycles
3,929 cycles

Plate with a center crack

The effect of the stress status

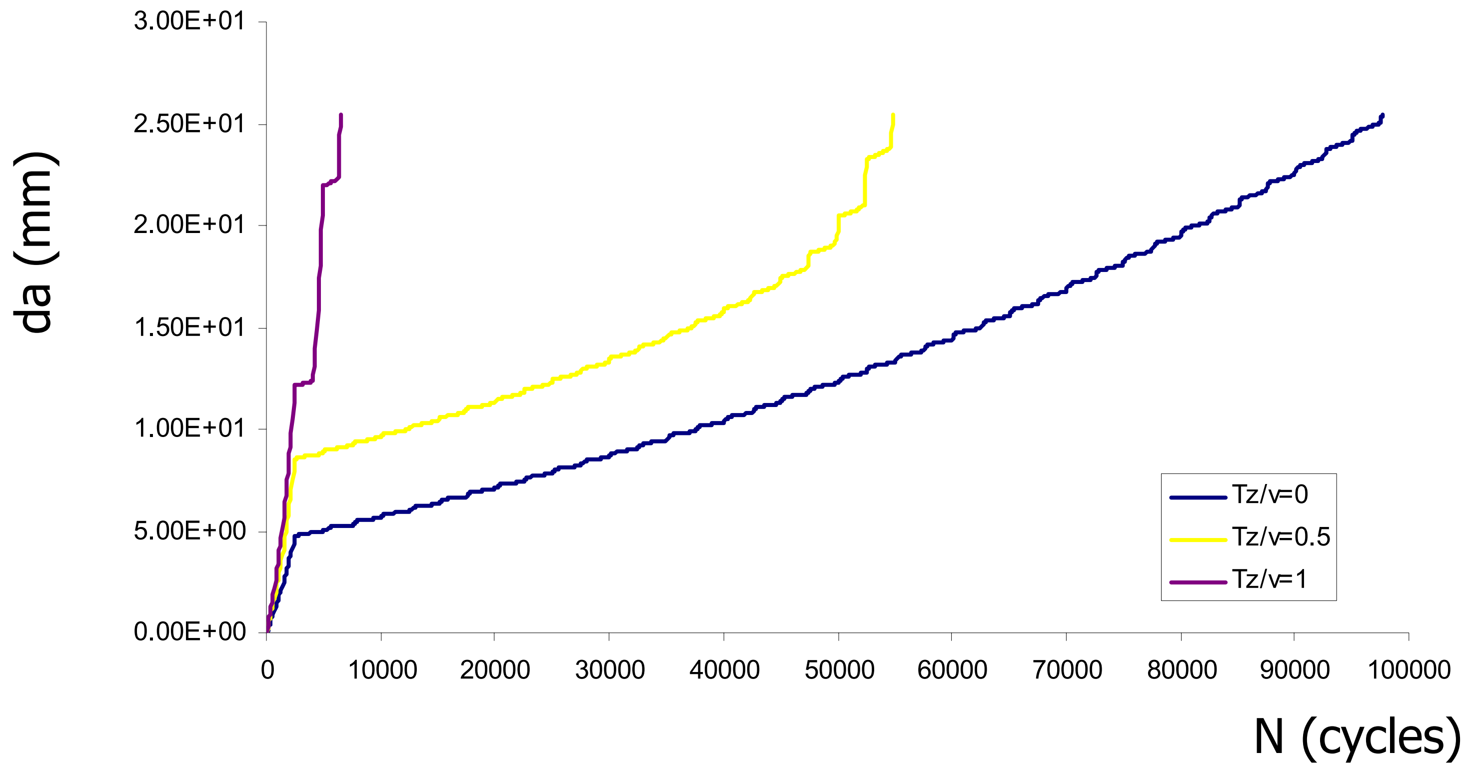

Overload spectrum, Rm=1.75

97,761 cycles
54,820 cycles
6,517 cycles

Plate with a center crack

The effect of the stress ratio of the overload

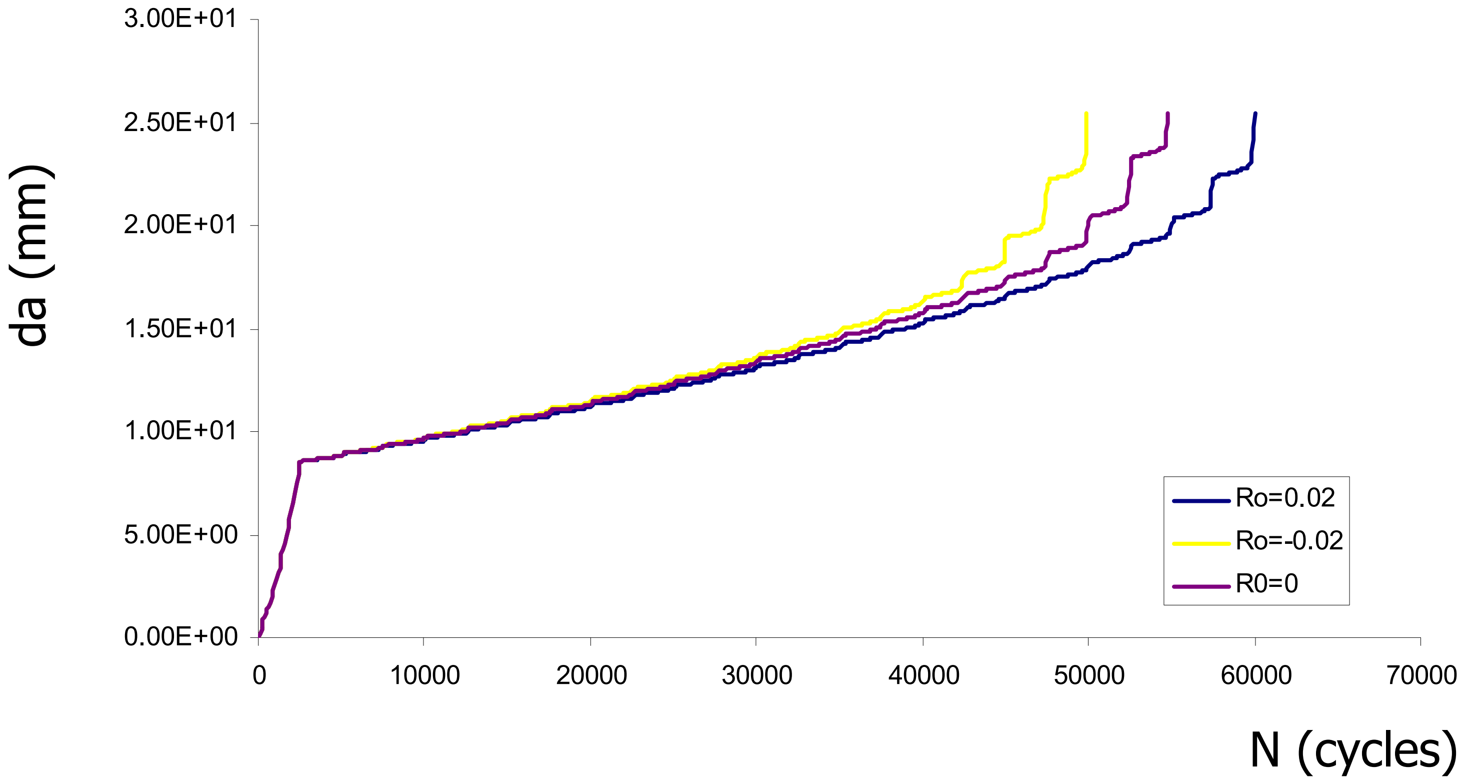

Overload spectrum, Tz/v=0.5, Rm=1.75

59,999 cycles
49,909 cycles
54,820 cycles

UCI
University of California, Irvine

Plate with a center crack

The effect of the stress ratio of the overload

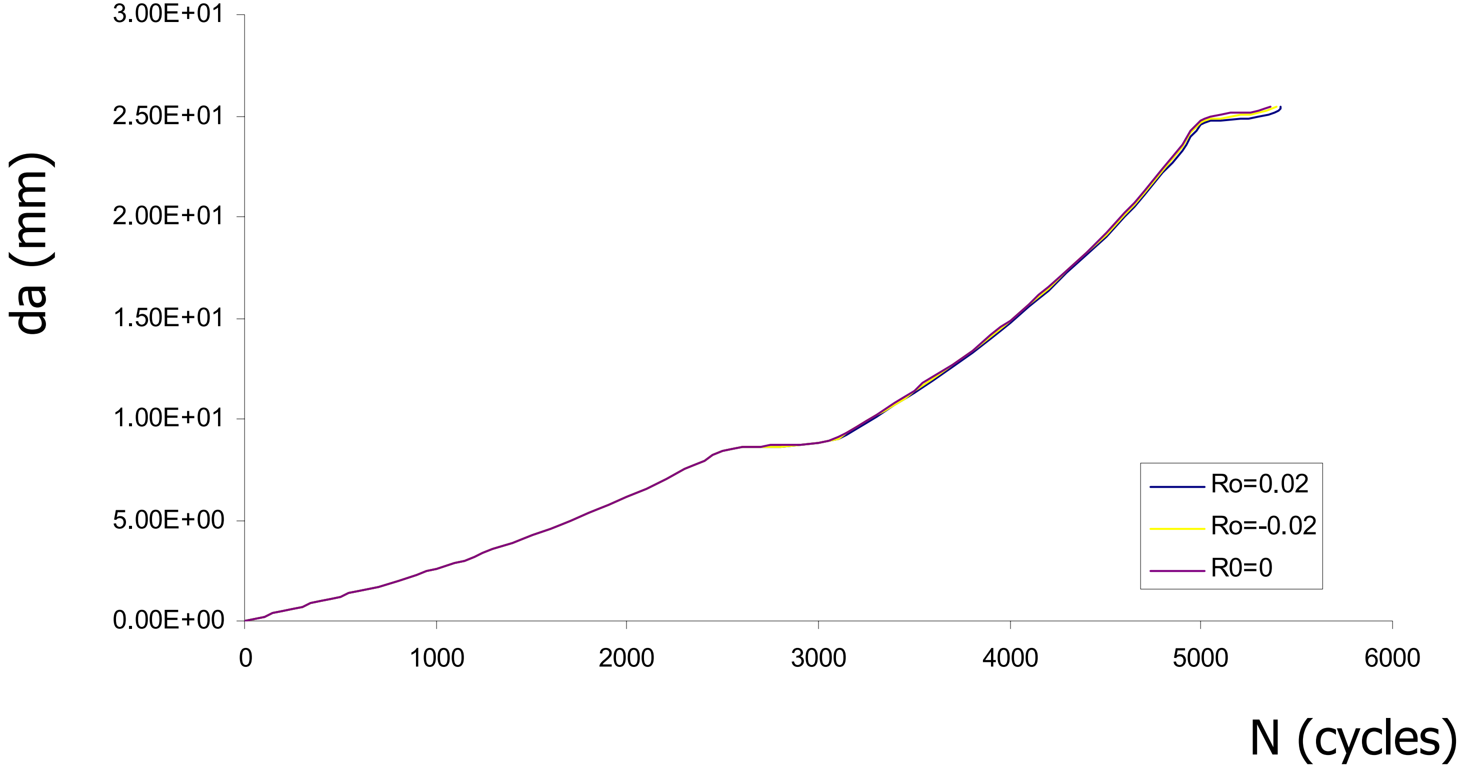

Overload spectrum, Tz/v=0.5, Rm=1.5

5,419 cycles
5,358 cycles
5,394 cycles

UCI
University of California, Irvine

Plate with an edge crack

2024-T3 AL

Maximum stress (S_{max})	68.94 MPa
Minimum stress (S_{min})	1.38 MPa
Stress ratio	0.02
Stress ratio of the overload	-0.02
C	2.382 e-11
n	3.2
Yield Strength	365.42 MPa
Overload ratio (R_m)	1.25, 1.5
Initial crack length($2a_o$)	2 mm

Plate with an edge crack

Overload spectra

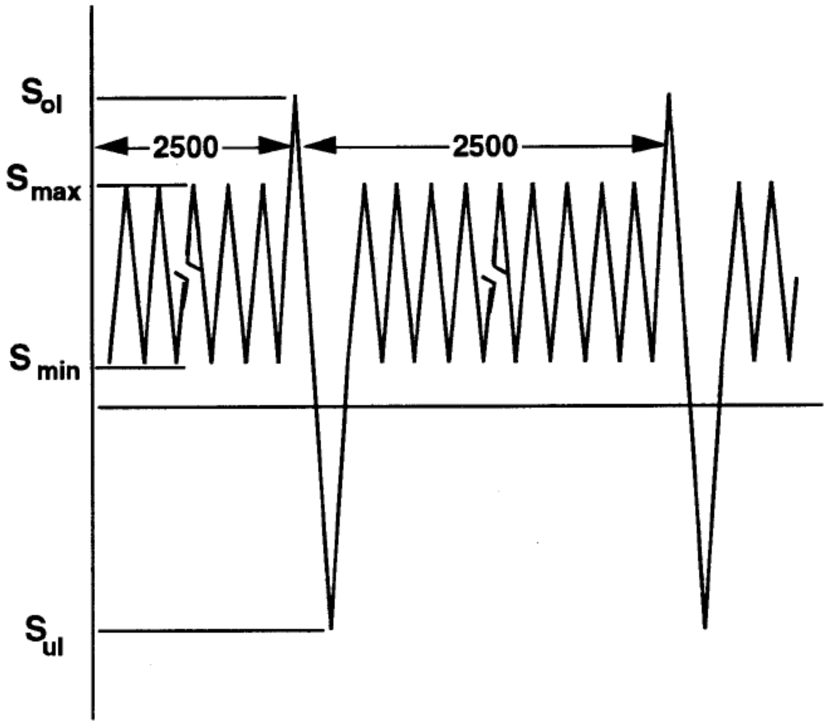

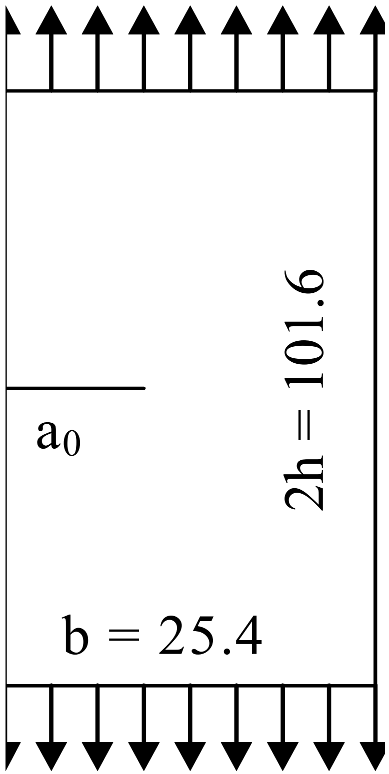

the overload repeats at every 2500 constant amplitude load cycles

The stress ratio of the overload

$Ro=S_{ul}/S_{ol}$

UCI
University of California, Irvine

Plate with an edge crack

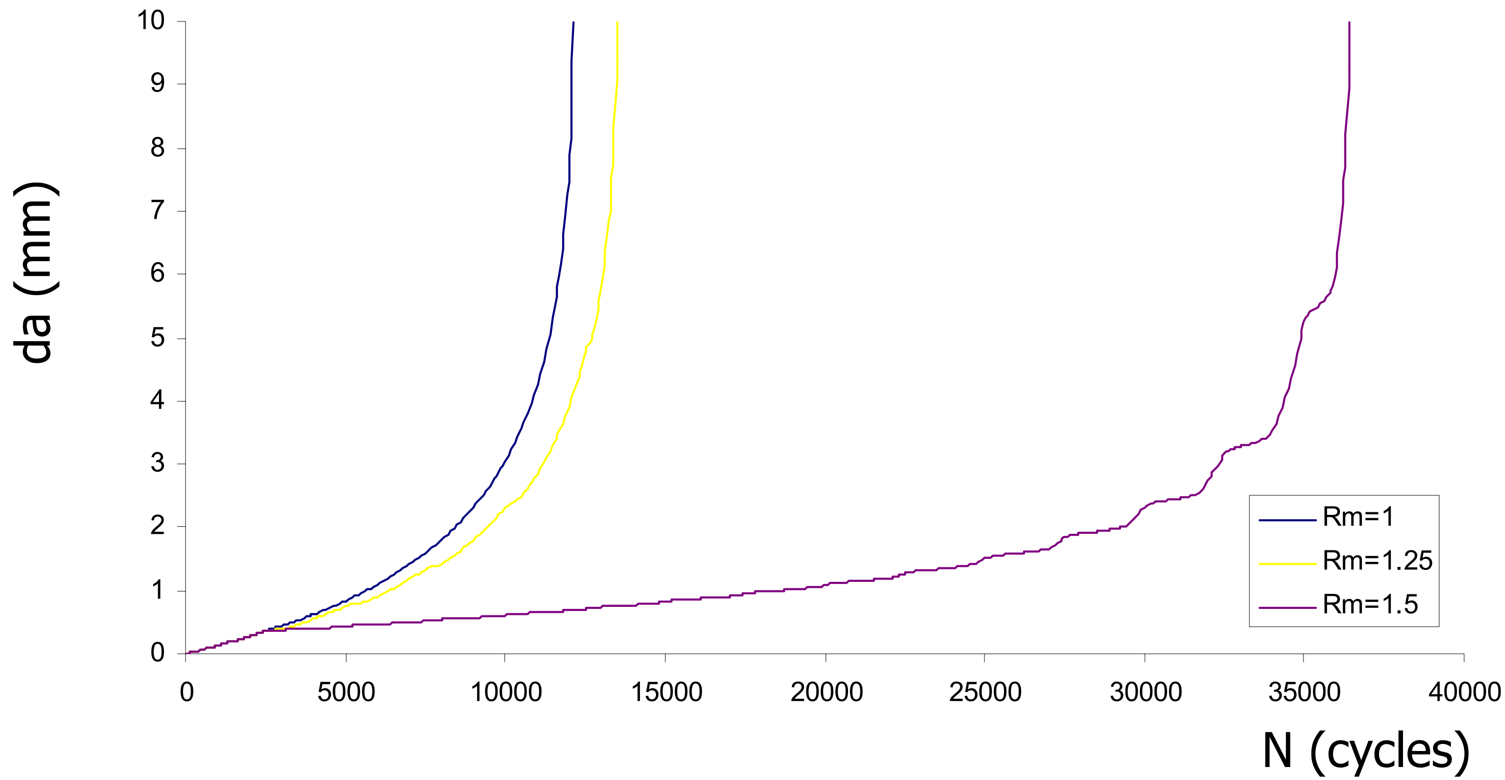

Tz/v=0

12,161 cycles
13,528 cycles
36,435 cycles

UCI
University of California, Irvine

Plate with an edge crack

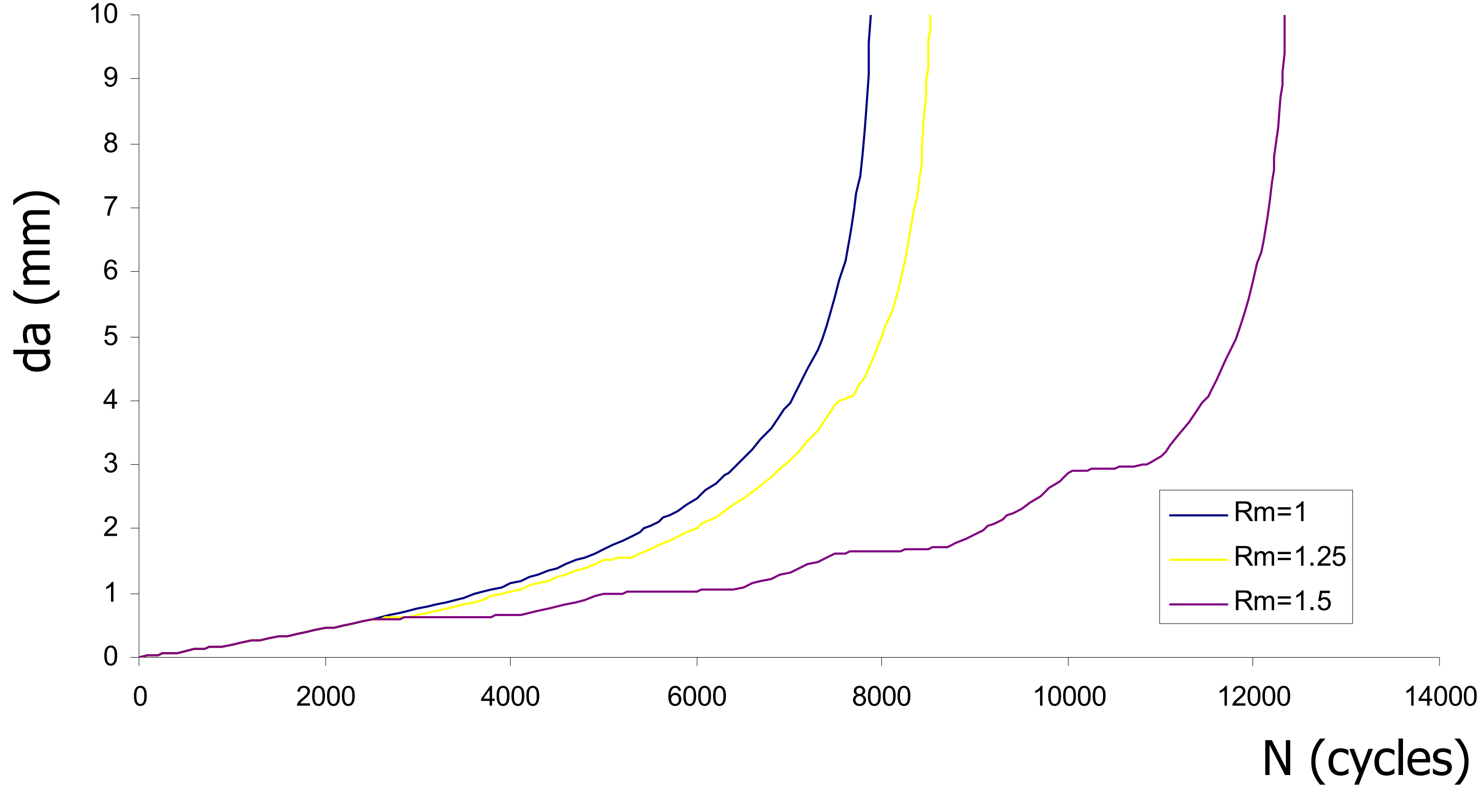

Tz/v=0.5

7,871 cycles
8,519 cycles
12,329 cycles

UCI
University of California, Irvine

Plate with an edge crack

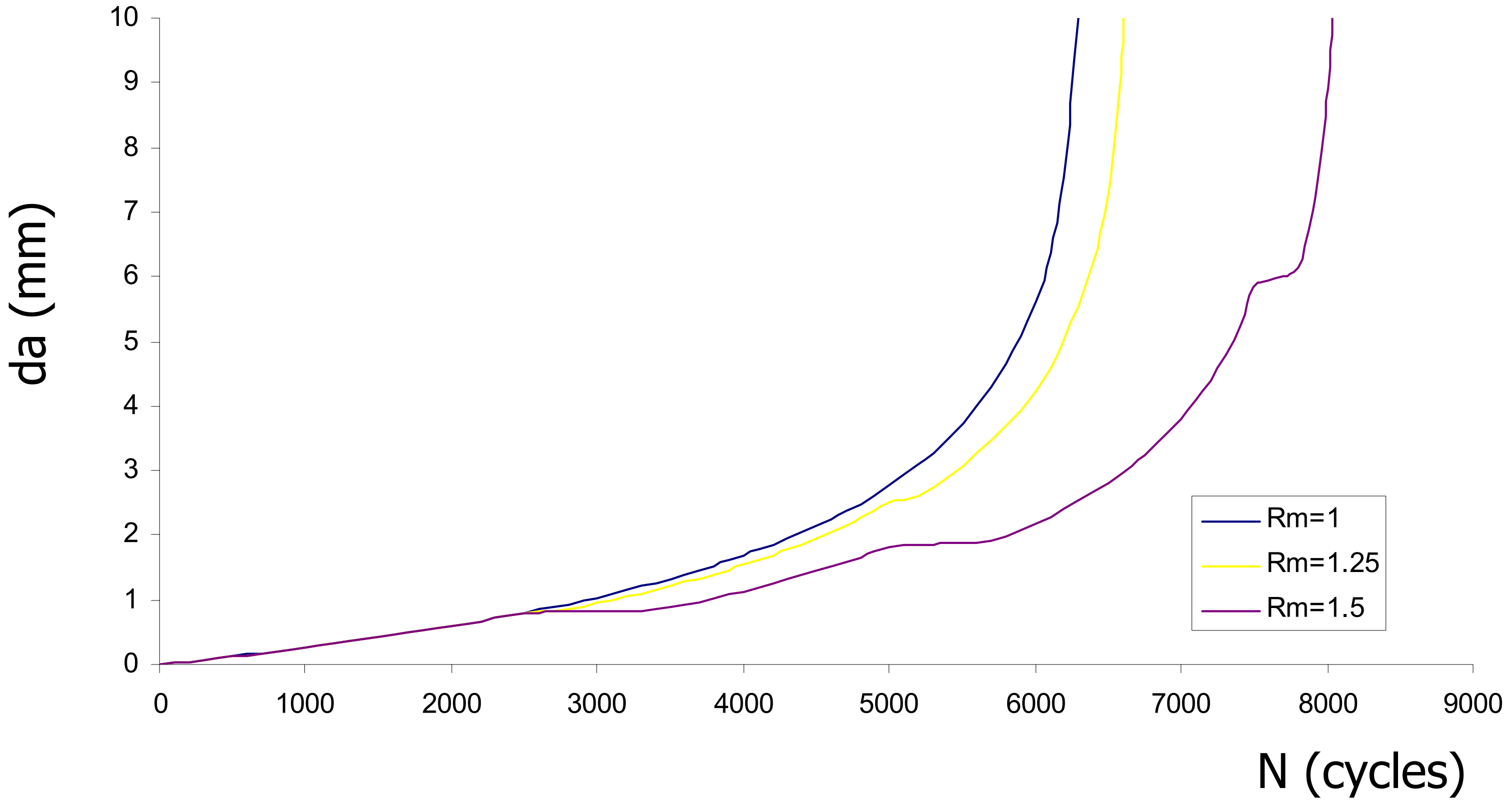

Tz/v=1

6,295 cycles
6,609 cycles
8,029 cycles

UCI
University of California, Irvine

Plate with an edge crack

The effect of the stress status

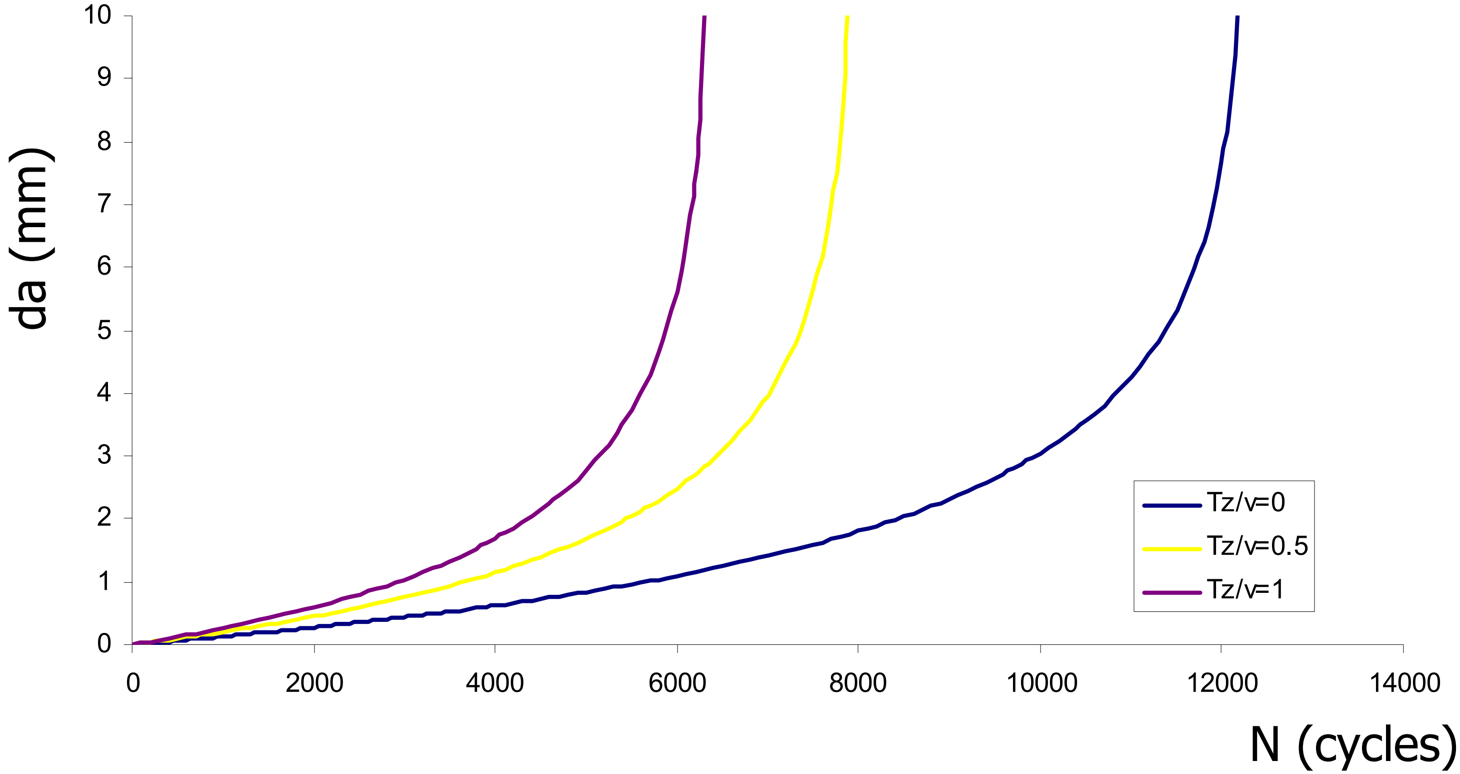

Constant amplitude load, Rm=1

12,165 cycles
7,871 cycles
6,295 cycles

UCI
University of California, Irvine

Plate with an edge crack

The effect of the stress status

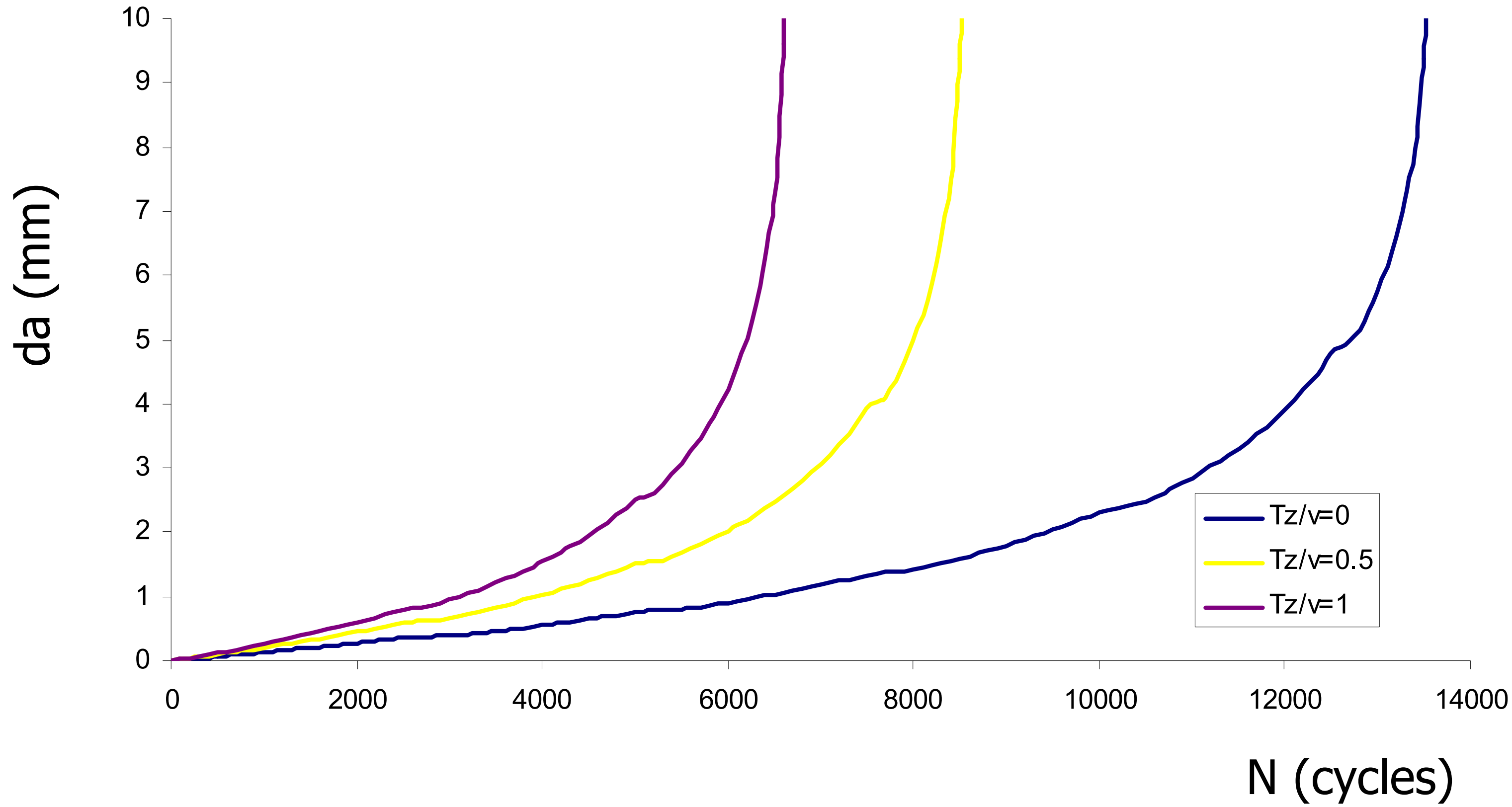

13,528 cycles
8,519 cycles
6,609 cycles

Overload spectrum, Rm=1.25

Plate with an edge crack

The effect of the stress status

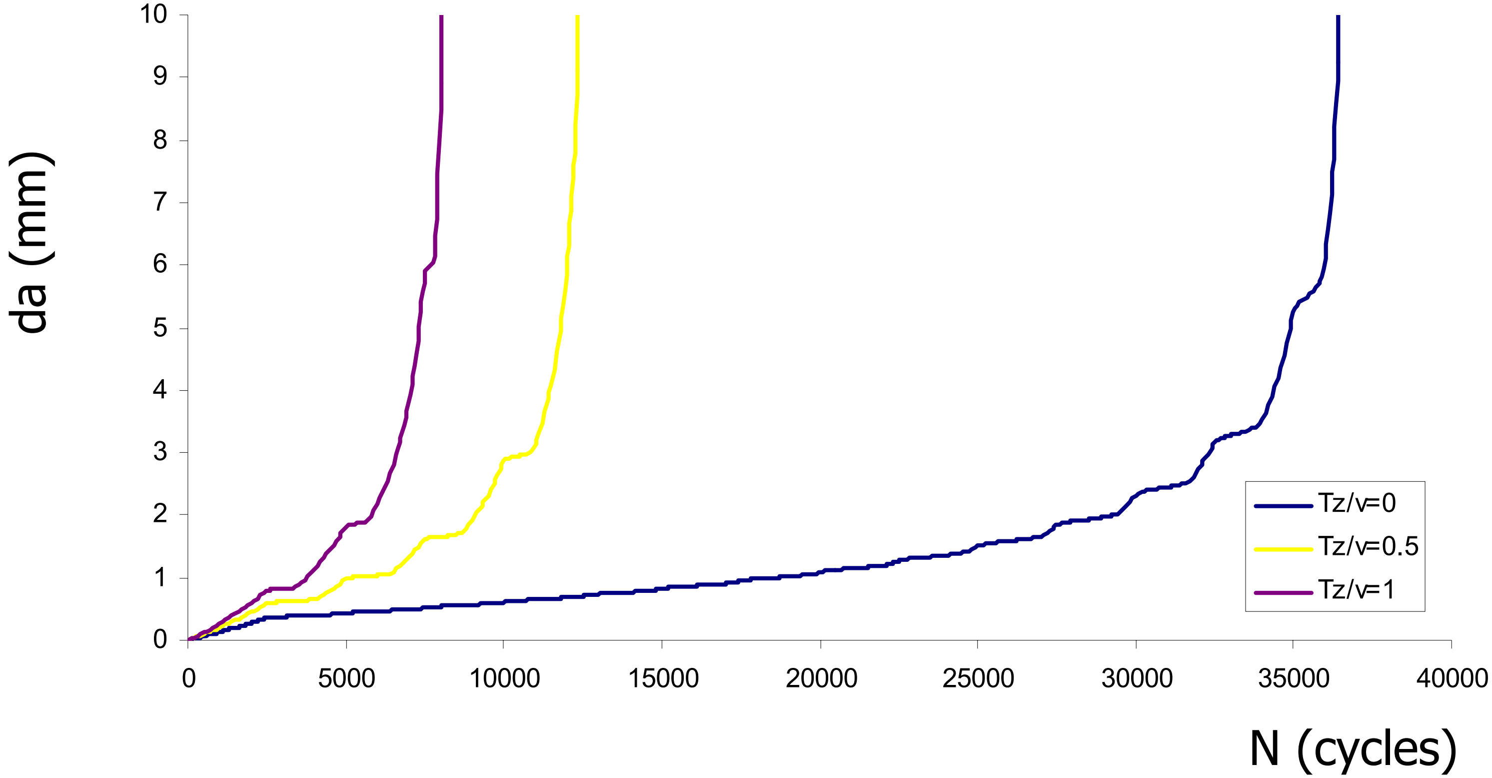

36,435 cycles

12,329 cycles

8,029 cycles

Overload spectrum, Rm=1.5

Validation of the Fatigue Model

center crack

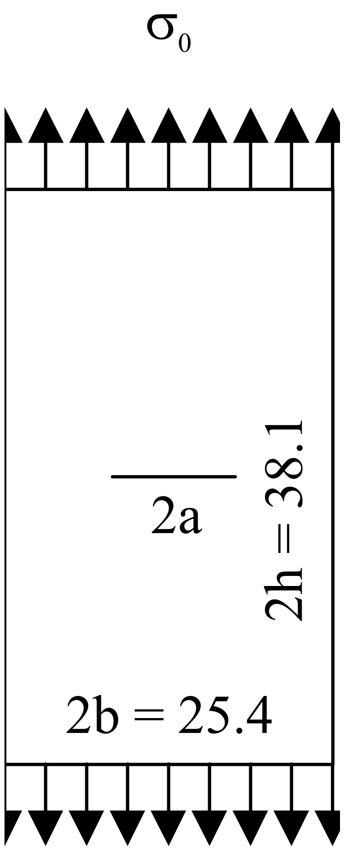

spectrum

1.9MPa of 525 cycles

2.3 MPa of 255 cycles

2.44 MPa of 95 cycles

2.7 MPa of 15 cycles

3.2 MPa of 75 cycles

R=0

Fatigue model

c=1.60E-8, n=3.59

Validation of the Fatigue Model

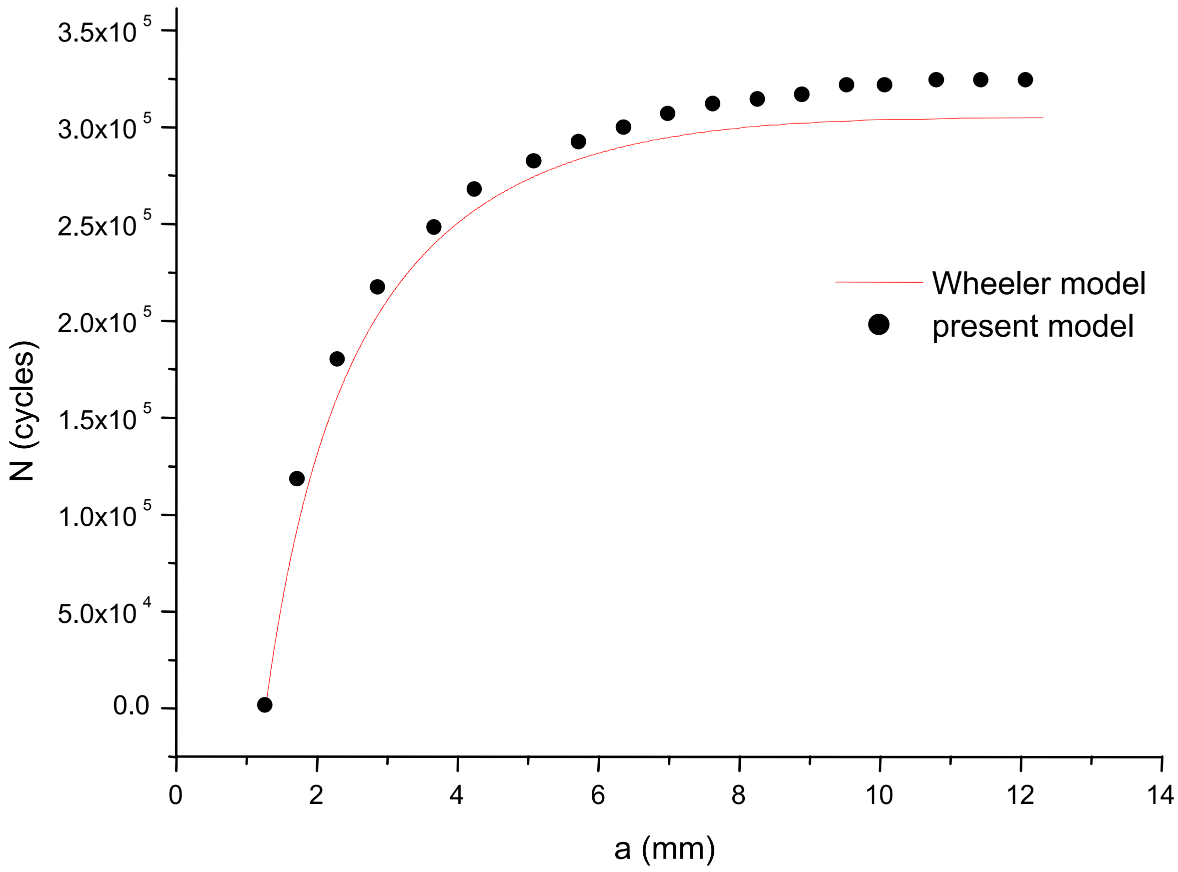

Validation of the Fatigue Model

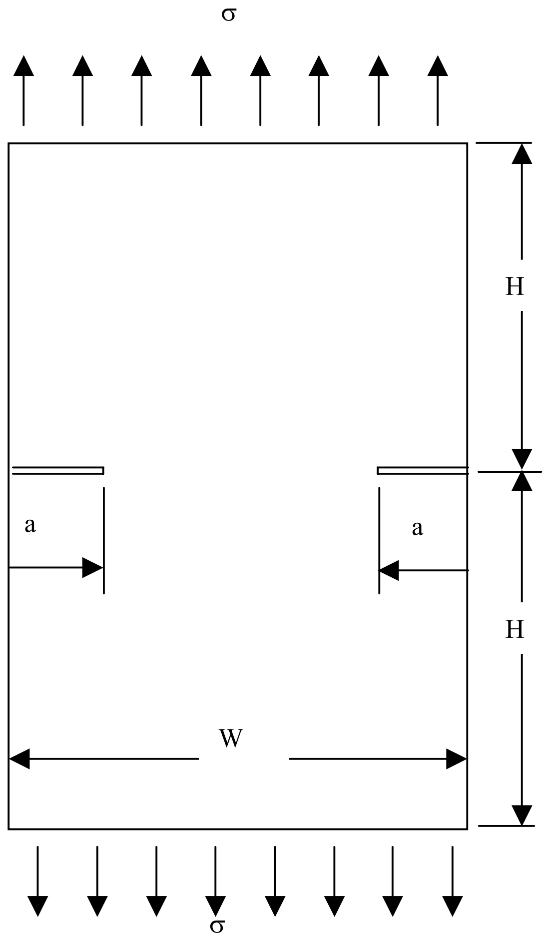

Two edge crack

spectrum
1.9psi of 525 cycles
2.3 psi of 255 cycles
2.44 psi of 95 cycles
2.7 psi of 15 cycles
3.2 psi of 75 cycles

R=0

Fatigue model
c=1.49E-8, n=3.321

Validation of the Fatigue Model

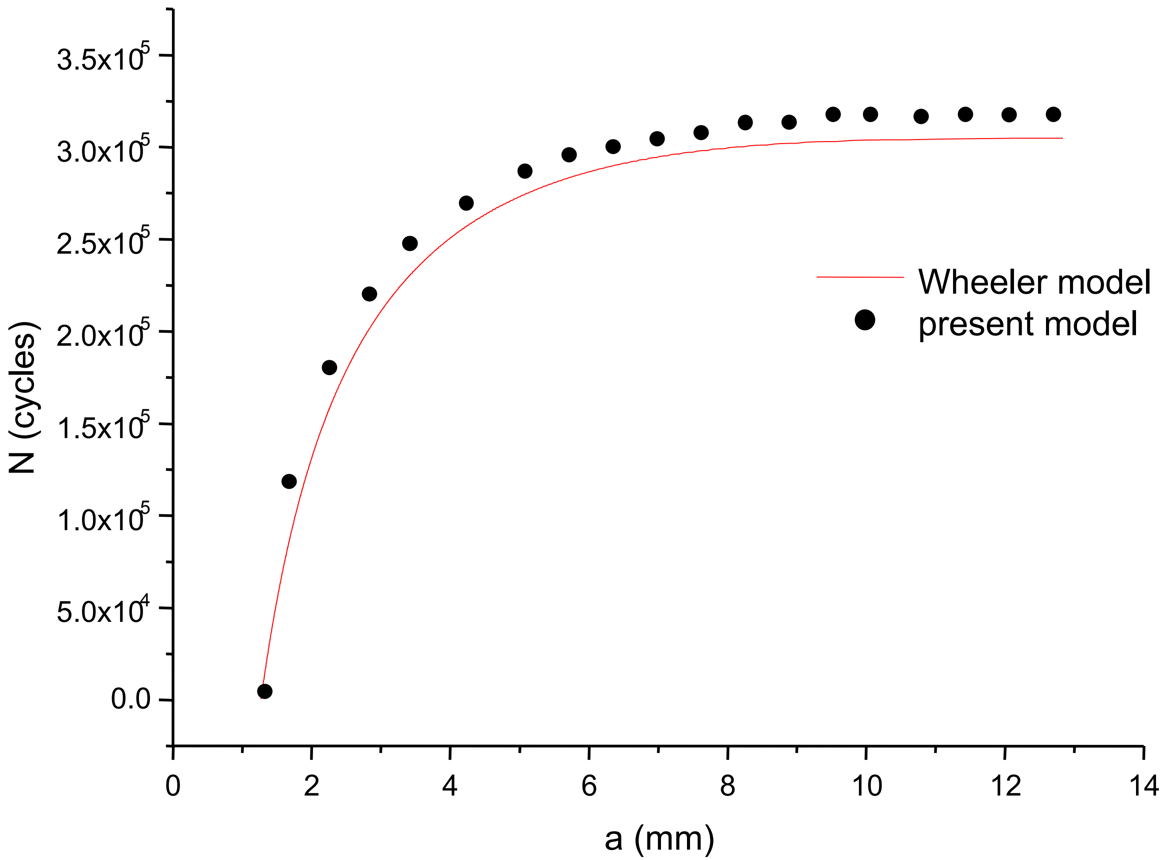

UCI
University of California, Irvine